

March 2023

# Development and Implementation of Telemetry Devices to Identify and Characterize Sources of Intraocular Pressure Variability in Rats

Christina M. Nicou  
*University of South Florida*

Follow this and additional works at: <https://digitalcommons.usf.edu/etd>



Part of the [Biomedical Engineering and Bioengineering Commons](#), [Electrical and Computer Engineering Commons](#), and the [Ophthalmology Commons](#)

---

## Scholar Commons Citation

Nicou, Christina M., "Development and Implementation of Telemetry Devices to Identify and Characterize Sources of Intraocular Pressure Variability in Rats" (2023). *USF Tampa Graduate Theses and Dissertations*.

<https://digitalcommons.usf.edu/etd/9910>

This Dissertation is brought to you for free and open access by the USF Graduate Theses and Dissertations at Digital Commons @ University of South Florida. It has been accepted for inclusion in USF Tampa Graduate Theses and Dissertations by an authorized administrator of Digital Commons @ University of South Florida. For more information, please contact [digitalcommons@usf.edu](mailto:digitalcommons@usf.edu).

Development and Implementation of Telemetry Devices to Identify and Characterize Sources of  
Intraocular Pressure Variability in Rats

by

Christina M. Nicou

A dissertation submitted in partial fulfillment  
of the requirements for the degree of  
Doctor of Philosophy  
Department of Medical Engineering  
College of Engineering  
University of South Florida

Major Professor: Christopher L. Passaglia, Ph.D.  
Robert D. Frisina, Ph.D.  
Mark J. Jaroszeski, Ph.D.  
Ismail Uysal, Ph.D.  
Manas R. Biswal, Ph.D.

Date of Approval:  
March 20, 2023

Keywords: Glaucoma, Anesthetics, Stress, Tonometry, Body Temperature, Locomotor Activity

Copyright © 2023, Christina M. Nicou

## **Dedication**

First and foremost, I would like to humbly dedicate this dissertation to my brother, Nicholas Nicou. You have been my source of inspiration from the very beginning. From a young age, I looked up to you as my role model and as the younger sibling, I had big shoes to fill. I am truly thankful and honored to have you as my brother. I would also like to dedicate this manuscript to my loving father, Christos Nicou. You taught me the importance of education and gave me the confidence to reach for the stars. You have provided endless support, guidance, and wisdom throughout my pursuit of this degree. If it weren't for you, I would not be where I am today. We did it, daddy, we finished our PhD. Finally, I would like to dedicate this dissertation to the love of my life, my forever partner, Stuart Popenoe. You have stood by me since the very first semester I began this journey. I want to sincerely thank you for your continual support of my career goals.

## **Acknowledgments**

I would like to acknowledge my major professor, Dr. Chris Passaglia, for his consistent guidance and support during my academic and research endeavors. I would like to express my sincerest gratitude towards my committee members, Dr. Robert Frisina, Dr. Mark Jaroszeski, Dr. Manas Biswal, and Dr. Ismail Uysal, for their advice and time spent on my research aims. This journey would have also been impossible without the mentorship and support of fellow lab mates Youssef Mohamed, Nicholas Johnson, Aditi Pillai, Aman Chawla, Cesar Hernandez, and Alexandra Zamitalo. Furthermore, I would like to mention former undergraduate volunteers Jacob Yarinsky, Lan Tran, and Abdal Alogaidi, for their assistance in data collection. Finally, I would like to thank Alex Otten and Molly Skinner for their input on research related topics as well as their friendship over the years.

## Table of Contents

List of Figures .....	iii
Abstract .....	v
Chapter 1: Background .....	1
1.1 Importance of Intraocular Pressure .....	1
1.2 Glaucoma and Common Treatments .....	2
1.3 Measurement of Intraocular Pressure .....	4
1.4 Specific Aims .....	4
Chapter 2: Effects of Acute Stress, General Anesthetics, Tonometry, and Temperature on Intraocular Pressure in Rats .....	6
2.1 Note to Reader .....	6
2.2 Introduction .....	6
2.3 Materials and Methods .....	7
2.3.1 Animal Preparation .....	7
2.3.2 Experimental Design .....	9
2.3.3 Data Analysis .....	10
2.4 Results .....	10
2.4.1 Effect of Stress on IOP .....	12
2.4.2 Effect of Anesthesia on IOP .....	13
2.4.3 Effect of Tonometry on IOP .....	15
2.4.4 Effect of Temperature on IOP .....	16
2.5 Discussion .....	19
2.5.1 Relation to Prior Work .....	20
2.5.2 Limitations .....	22
2.6 Conclusion .....	23
Chapter 3: Characterization of Intraocular Pressure Variability in Rats .....	24
3.1 Introduction .....	24
3.2 Materials and Methods .....	25
3.2.1 Animal Preparation .....	25
3.2.2 Data Analysis .....	25
3.2.3 Daily IOP Mean and Variance Analysis .....	26
3.2.4 Transient and Sustained IOP Fluctuation Analysis .....	26
3.2.5 IOP-Related Mechanical Energy Calculation .....	29
3.3 Results .....	29
3.4 Discussion .....	36
3.4.1 Relation to Prior Work .....	37

3.4.2 Limitations .....	38
3.5 Conclusion .....	39
Chapter 4: Effects of Ambient Lighting on Intraocular Pressure Variability in Rats.....	40
4.1 Introduction.....	40
4.2 Materials and Methods.....	41
4.2.1 Animal Preparation .....	42
4.2.2 Manipulation of Ambient Lighting .....	42
4.2.3 Data Analysis .....	42
4.3 Results.....	43
4.4 Discussion .....	50
4.4.1 Relation to Prior Work.....	50
4.4.2 Limitations .....	54
4.5 Conclusion .....	54
Chapter 5: A Wearable Device for Continuous Monitoring of Intraocular Pressure, Body Temperature, and Locomotor Activity in Conscious Rats.....	56
5.1 Introduction.....	56
5.2 Materials and Methods.....	57
5.2.1 System Design and Data Acquisition .....	57
5.2.2 Benchtop Testing of System .....	59
5.2.3 Animal Preparation .....	60
5.2.4 Data Analysis .....	61
5.3 Results.....	62
5.4 Discussion.....	67
5.4.1 Relation to Prior Work.....	67
5.4.2 Limitations .....	70
5.5 Conclusion .....	71
Chapter 6: Conclusions and Future Works .....	72
6.1 Summary of Major Findings.....	72
6.2 Technological Advancement .....	74
6.3 IOP and the Autonomic Nervous System .....	76
6.4 Future Works .....	77
References.....	80
Appendix A: Microbead Occlusion Model.....	94
Appendix B: Effect of Pharmacological Agents on IOP .....	98
Appendix C: Continuous Intracranial Pressure Monitoring .....	102
Appendix D: Copyright Permissions .....	104

## List of Figures

Figure 1.1:	Anatomical diagrams of the eye .....	2
Figure 1.2:	Effect of glaucoma on vision .....	3
Figure 2.1:	Wireless telemetry system for continuous IOP recording in rats .....	8
Figure 2.2:	IOP variability in conscious free-moving rats .....	11
Figure 2.3:	Effect of acute stress on IOP.....	12
Figure 2.4:	Blocking IOP stress response with anesthesia.....	13
Figure 2.5:	Effect of common anesthetics on IOP .....	14
Figure 2.6:	Effect of different tonometers on IOP .....	16
Figure 2.7:	Effect of temperature on IOP.....	17
Figure 2.8:	Control experiments for temperature effects on IOP.....	18
Figure 3.1:	Determination of peak detection parameters .....	27
Figure 3.2:	Detection of transient and sustained IOP fluctuations.....	27
Figure 3.3:	IOP mean and variance statistics .....	30
Figure 3.4:	Transient IOP fluctuation statistics.....	31
Figure 3.5:	Sustained IOP fluctuation statistics .....	32
Figure 3.6:	Daily IOP-related mechanical energy expenditure.....	33
Figure 3.7:	Analysis of cut tube data and effect of isoflurane on IOP variability.....	34
Figure 3.8:	Cross-correlation of IOP fluctuations between simultaneously recording rats .....	36
Figure 4.1:	Effect of reversed light cycle on IOP rhythm .....	43
Figure 4.2:	Effect of constant darkness on IOP rhythm .....	44

Figure 4.3:	Effect of constant light on IOP rhythm.....	45
Figure 4.4:	Inter-animal variability of constant light effects on IOP rhythm.....	46
Figure 4.5:	Effect of anti-phasic lighting conditions on IOP rhythm.....	47
Figure 4.6:	IOP phase response to a single light pulse.....	48
Figure 5.1:	Telemetry system design and experimental setup .....	57
Figure 5.2:	Calibration of telemetry system .....	59
Figure 5.3:	Continuous recording of IOP, BT, and LMA .....	63
Figure 5.4:	Cross-correlations of IOP, BT, and LMA data.....	64
Figure 5.5:	Transient and sustained IOP event triggered average of BT and LMA.....	65
Figure 5.6:	Telemetry system functionality.....	66
Figure A1:	Effect of microbeads on IOP.....	95
Figure A2:	Effect of microbead material and diameter on IOP .....	96
Figure B1:	Effect of cyclopentolate on IOP.....	99
Figure C1:	Continuous ICP recording using wireless telemetry.....	102



## **Abstract**

Eye health depends partially on intraocular pressure (IOP) as abnormal levels can lead to ocular tissue damage. Glaucoma is a neurodegenerative disease that affects nearly 80 million people worldwide [1]. It is associated with elevated IOP, which can lead to irreversible blindness. Relatively little is known about IOP dynamics and the physiological factors that affect it as IOP is typically monitored using tonometry. Tonometry is a common tool used by clinicians and researchers to measure IOP noninvasively. It provides a good estimate of IOP mean but not variance because data collection takes time. Readings can also be influenced by subject stress and tonometer operation. To resolve this issue, our lab has developed a novel telemetry system to monitor IOP continuously in conscious freely moving rats. The device works by conducting pressure from a microcannula implanted in the anterior chamber to a transducer worn as a backpack. To improve our understanding of IOP as a risk factor for glaucoma, we used this system to test the effects of various internal and external factors including stress, anesthetics, temperature, tonometry, light cycle, and locomotor activity. Our results indicate that IOP varies continuously over fast and slow time scales. IOP fluctuations can naturally range over 5 - 10 mmHg, which is quite large considering the resting level is 10 - 15 mmHg and chronic elevation by this amount can cause glaucomatous nerve damage. Physiological mechanisms must therefore exist to slowly and rapidly modulate IOP. Autoregulatory processes that control ocular hemodynamics are one known mechanism, and efferent nerve signals from the brain are another. We conclude that IOP in rats, much like in higher mammals, is a complex time-dependent variable due to internal and external perturbing forces and homeostatic feedback mechanisms.

## Chapter 1: Background

### 1.1 Importance of Intraocular Pressure

Intraocular pressure (IOP) is the fluid pressure inside the eye that provides biomechanical support to ocular tissues. This pressure is controlled by the secretion and excretion of aqueous humor. The left diagram in Figure 1.1 highlights the different compartments of the eye. The anterior chamber is the front most compartment of the eye (red), which is filled with aqueous humor. Aqueous humor supplies nutrients and oxygen to the avascular tissues of this space including the cornea and lens [2]. The right diagram in Figure 1.1 shows a zoomed in section of the anterior chamber with arrows marking the flow of aqueous humor from the posterior chamber (green), where it is produced by the ciliary body, through the opening of the pupil, and into the anterior chamber. The principal locations that aqueous humor exits the eye are the trabecular meshwork via the conventional outflow pathway, and the supraciliary space via the uveoscleral pathway (not marked in Figure 1.1).

Drastic changes in aqueous humor dynamics may result in an array of pressure-related ocular disorders. Hypotony is characterized as lower than normal IOP and increases the risk of retinal detachment, corneal edema, and cataract formation [3]. Alternatively, ocular hypertension, or elevated IOP, leads to glaucomatous damage including optic nerve cupping and retinal ganglion cell (RGC) degeneration [4]. It is therefore clinically important to identify and understand sources of IOP variation and physiological mechanisms of IOP regulation.

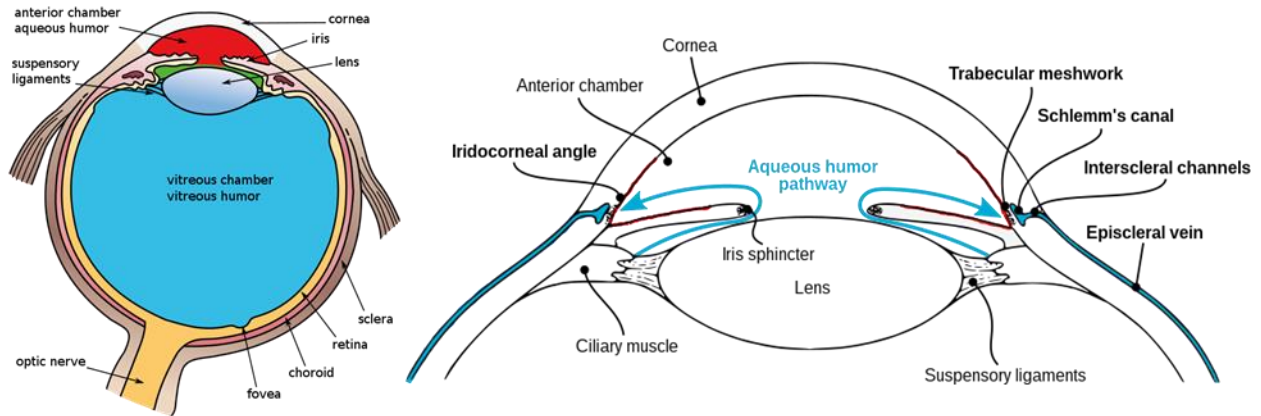


Figure 1.1: Anatomical diagrams of the eye. The illustration on the left is a cross-section of the human eye that highlights the major components necessary for vision. Artwork done by Holly Fischer and licensed under CC BY 3.0.

[https://commons.wikimedia.org/wiki/File:Three\\_Internal\\_chambers\\_of\\_the\\_Eye.svg#file](https://commons.wikimedia.org/wiki/File:Three_Internal_chambers_of_the_Eye.svg#file)

The illustration on the right is a zoomed in diagram of the pathway aqueous humor takes following secretion from the ciliary body and exits the eye through the conventional outflow pathway. Artwork done by José Ignacio Orlando and made available under CC0 1.0.

[https://commons.wikimedia.org/wiki/File:Aqueous\\_humor\\_pathway.svg](https://commons.wikimedia.org/wiki/File:Aqueous_humor_pathway.svg)

## 1.2 Glaucoma and Common Treatments

According to the 2020 Global Burden of Disease Study, glaucoma is one of the leading causes of irreversible blindness worldwide and it is therefore important to study factors that contribute to its onset and progression [5]. Glaucoma is a set of neurodegenerative ocular disorders characterized by RGC dysfunction [6]. RGCs are neurons that comprise the inner most layer of the retina and are responsible for transmitting visual information to the brain. These cells are sensitive to mechanical insult and damage can lead to visual field loss. Figure 1.2 compares the visual field of a healthy person to a person with glaucoma. The illustration correlates a noticeable loss in vision to pressure-induced optic nerve damage. In glaucoma, elevated pressure is typically caused by blockage of the fluid pathway leaving the eye. The trabecular meshwork, a major component of the conventional outflow pathway, is located within the iridocorneal angle. It is analogous to a sponge that has canals for fluid to pass through. In the case of glaucoma, the tissue

of the trabecular meshwork stiffens and the canals become compromised [7]. The most prominent forms of glaucoma are the primary open-angle glaucoma (POAG) and primary angle-closure glaucoma (PACG), both of which involve elevated IOP [1]. The severity of a glaucoma diagnosis is termed secondary if there is an identifiable cause for the elevated IOP. Thus, elevated IOP is the most significant risk factor for the development and progression of glaucoma.

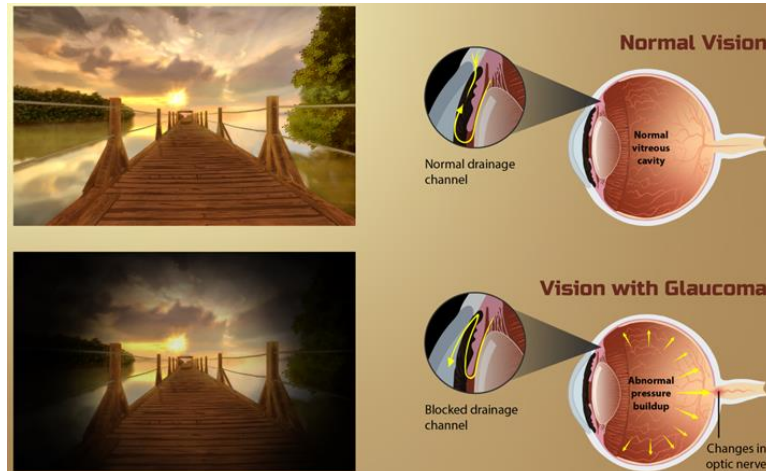


Figure 1.2: Effect of glaucoma on vision. A depiction of vision differences between healthy and glaucomatous subjects. Glaucoma patients tend to have significant visual field loss brought on by elevated intraocular pressure that presses on the optic nerve head leading to RGC death. Illustration created by MyUpchar and licensed under CC BY-SA 4.0.

[https://commons.wikimedia.org/wiki/File:Depiction\\_of\\_vision\\_for\\_a\\_Glaucoma\\_patient.png](https://commons.wikimedia.org/wiki/File:Depiction_of_vision_for_a_Glaucoma_patient.png)

Treatment of glaucoma usually begins with prescription eye drops that target IOP levels. These treatments work to lower IOP by altering either production and/or outflow of aqueous humor. More severe cases of glaucoma may require invasive treatments such as laser surgery or shunt implantation. Other remedies for glaucoma that are important but not commonly studied are regular meditation, exercise, and a healthy diet. However, it is unclear whether these remedies directly or indirectly affect IOP. Thus, consideration of various physiological factors including stress level, body temperature, respiration, and blood pressure may be necessary to understand the effects of various treatments on IOP.

### **1.3 Measurement of Intraocular Pressure**

Research to improve the understanding of glaucoma onset and progression is inhibited by challenges in accurately monitoring IOP. Tonometry is a common technique used by clinicians and researchers to estimate IOP. There are various forms of tonometry including but not limited to rebound tonometry, applanation tonometry, and non-contact air puff tonometry. All methods provide an indirect measure of IOP based on the force needed to temporarily flatten the cornea. Although this technique is preferred for its noninvasiveness, it is prone to operator error and fails to adjust for patient-specific corneal thickness and curvature. The tonometer is unable to capture moment-to-moment IOP fluctuations as collection is laborious and provides only snap-shot estimates. As a result, previous tonometric studies are unable to fully characterize IOP variability. IOP telemetry offers a solution to this problem. We have developed a novel telemetry system for continuous IOP recording in free-moving conscious rats. Although this system requires an invasive procedure, it has shown to accurately measure IOP for extended durations without altering ocular physiology [8]. Others have used similar commercially available implantable systems to monitor IOP continuously in rabbits and monkeys [9-11]. There are also contact lens sensors that have been used in humans to estimate changes in pressure based on changes in corneal curvature [12, 13]. Although this technology is still under development, it represents a major step forward in glaucoma research.

### **1.4 Specific Aims**

The studies discussed in the following chapters will address limitations in research pertaining to the evaluation of IOP as a risk factor for glaucoma. Evidence will be provided to clarify ambiguities in previous literature and offer a new perspective on current glaucoma related research. Biomedical engineering skills including circuit design, device programming, and data

processing will be used to develop and implement a wearable telemetry system that continuously monitors IOP in addition to other physiological signals. This technology will be used to test effects of various internal and external factors on IOP dynamics in an animal model. Rats will serve as the animal model for IOP telemetry in this study as they have similar anatomy and genetics to humans, and they are more economical for use in research than larger mammals.

## **Chapter 2: Effects of Acute Stress, General Anesthetics, Tonometry, and Temperature on Intraocular Pressure in Rats**

### **2.1 Note to Reader**

Elsevier publishing company granted copyright permission for use of the following previously published work as part of this Ph.D. dissertation. The study, “Effects of acute stress, general anesthetics, tonometry, and temperature on intraocular pressure in rats,” is published in *Experimental Eye Research* (volume 210, pages 1-8) by authors: Christina M. Nicou, Aditi Pillai, and Christopher L. Passaglia under Elsevier Copyright (2021). Aditi Pillai, a former student, collected preliminary data for anesthesia, tonometry, and temperature experiments. Minor modifications were made to the text.

### **2.2 Introduction**

Intraocular pressure (IOP) is necessary for maintaining the optical properties of the eye and for providing biomechanical support to internal tissues. Deviations from baseline can induce an assortment of vision problems depending on the magnitude, direction, and duration of IOP change. Ocular hypotension can cause retinal detachments [3], while ocular hypertension can lead to glaucomatous degeneration of the retina and optic nerve [14]. It is therefore important to identify and understand sources of IOP variation and physiological mechanisms of IOP regulation.

Determining baseline IOP and the impact of IOP deviations is not trivial. For one, many external and internal factors are reported to alter IOP on time scales of seconds to days. External sources of variation include posture [15-17], altitude [18, 19], ambient temperature [19, 20], and

psychoactive agents like caffeine [21], cannabis [22], and anesthetics [23-26]. Internal sources include saccades and blinks [9, 27], body temperature [28], respiration [27, 29], blood pressure [30], cerebrospinal fluid pressure [31-33], circadian rhythms [12, 34], and mental stress [35-37]. Baseline IOP varies continuously as a result. For another, the precise effect of some factors is not certain because results are contradictory or confounded by the other factors. The method of measurement may be partially to blame since most studies used tonometry, which only gives a snapshot of IOP. Moreover, the snapshot may be influenced by psychosomatic responses to the act [38]. Baseline IOP is thus implicitly unknown and inferred from collected data. Tonometry also provides limited information about IOP fluctuations and the time course over which diverse sources of IOP variation exert their modulatory effects.

We have developed a wireless telemetry system for continually recording IOP in free-moving conscious rats. Similar systems are commercially available for larger animals and have been adapted to monitor IOP in rabbits and non-human primates [9-11]. The aim of this study was to use the rat telemetry system to examine internal sources of IOP variation with minimal experimental bias and greater temporal detail than tonometry permits. Of particular interest are putative effects of acute stress, general anesthetics, tonometry, and temperature.

## **2.3 Materials and Methods**

All experiments were conducted in accordance with the National Institutes of Health guide for the care and use of laboratory animals and compliance with a protocol approved by the Institutional Animal Care and Use Committee (IACUC) at the University of South Florida.

### **2.3.1 Animal Preparation**

Male retired-breeder Brown-Norway rats (300-400 g) were housed in a temperature-controlled room (22 °C) under a 12-h light (6 AM):12-h dark (6 PM) cycle with food and water



available ad libitum. On the day of surgery, animals were anesthetized with an intraperitoneal bolus of ketamine hydrochloride (75 mg/kg) and xylazine (7.5 mg/kg) that was supplemented as needed. Animals were rested on an isothermal (37-38 °C) heat pad (T/Pump Pro, Stryker, Portage, MI) to maintain body temperature (BT). A polyimide microcannula (MicroLumen, Oldsmar, FL) was inserted in one eye and connected to the telemetry system, details of which have been described [8, 39]. In short, the cannula (100  $\mu$ m inner diameter, 20 mm length) was guided

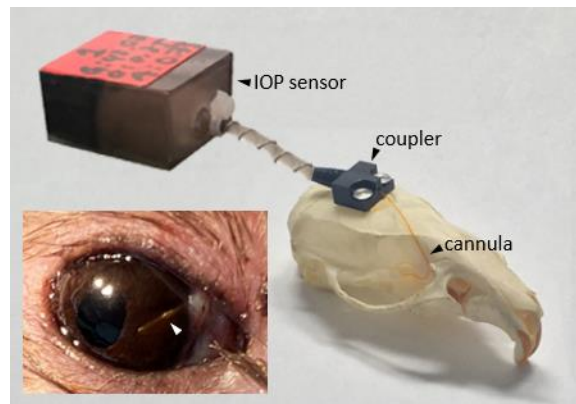


Figure 2.1: Wireless telemetry system for continuous IOP recording in rats. The IOP sensor is worn on the back and connects to a fine cannula that is implanted in the eye via a coupler affixed atop the skull with bone screws. Inset shows a rat eye implanted with a cannula.

subdermally through an incision on the skull to a translimbal hole in the eye and the tip was inserted in the anterior chamber. The cannula was sutured to the sclera and connected to a plastic coupler affixed to the skull with bone screws and cement. The coupler was connected with a 16G PTFE tubing to the IOP sensor, which was fastened to the back of a custom-fit vest worn by the animal. The pressure line was filled with a balanced salt solution, 3 mM moxifloxacin hydrochloride (Vigamox®, Alcon, Fort Worth, TX), 1.3 mM enoxaparin sodium (Lovenox®, Henry Schein, Melville, NY) and 2.2 mM triamcinolone acetonide (Triessence®, Alcon, Fort Worth, TX) to prevent microbial and fibrin buildup that can clog the cannula over time. After surgery, animals received an intramuscular bolus of carprofen analgesic (5 mg/kg) every 12 hours for 3 days and

the status was monitored with a cage-mounted webcam. Figure 2.1 illustrates the IOP telemetry system, which wirelessly transmitted data round-the-clock at 0.25 Hz. Sensor calibration was checked by mercury manometry at placement and removal.

### 2.3.2 Experimental Design

Implanted rats were transported during daytime hours (9AM - 4PM) from housing to a test room in the animal care facility. For sake of quantification, resting IOP, transport IOP, and baseline IOP were respectively defined as the 5-min average IOP immediately before the researcher entered housing, the 5-min average of peak IOP after exiting housing, and the 5-min average immediately before each experiment in the test room. To assess stress effects, animals were placed for 10 min in an anesthesia chamber perfused with oxygen at 2 L/min. The chamber (9 cm x 9 cm x 23 cm) was considered stress-inducing because it greatly constrained animal movement. Chamber temperature (CT) was monitored with a digital thermometer and pre-heated in some experiments by a warm gel pack (34 °C). IOP and CT readings were averaged in sequential 2-min intervals before, during, and after constraint. To assess anesthetic effects, animals were sedated in the chamber with 3% isoflurane in oxygen at the same flow rate. Upon sedation animals were placed belly down on the heat pad and anesthesia was maintained via isoflurane inhalation through a nose cone or an intraperitoneal injection of ketamine (75 mg/kg). BT was recorded every 60 s with a rectal thermometer until the animal waked. Saline drops were periodically instilled to keep corneas moist. In isoflurane experiments, anesthetic concentration was varied in 10-min intervals between 1, 3, and 5% and IOP and BT readings were averaged over the last 5-min of each interval. In ketamine experiments, IOP and BT readings were averaged in sequential 10-min intervals until the anesthesia wore off. To assess tonometry effects, isoflurane-anesthetized animals were placed belly down on the heat pad and IOP was measured via applanation (TonoPen XL, Medtronic,

Sarasota, FL) and rebound (TonoVet, Icare USA, Raleigh, NC) tonometry. Ten tonometry readings were taken by hand and averaged. To assess temperature effects, isoflurane-anesthetized animals were placed belly down on a heat pad or cool (20 °C) metal table. IOP and BT readings were averaged in sequential 2-min intervals as the animal was slid every 10 min between the two surfaces. Animals were returned to housing after experiments for testing on another day.

### 2.3.3 Data Analysis

Raw IOP records were processed with MATLAB software (The MathWorks, Natick, MA) using a running median filter and lowpass filter with 80-s windows to remove spurious data. Filtered IOP records were subjected to statistical analysis using SigmaPlot software (Systat, San Jose, CA), with significance assessed at  $\alpha$  of 0.05. Resting IOP was log-normal distributed across animals [40], so data of each experiment were referenced to baseline IOP and expressed as  $\Delta$ IOP. IOP changes were evaluated with paired t-tests if normally distributed and reported as mean  $\pm$  standard deviation. Otherwise, they were log transformed before t-test evaluation and reported as median with confidence intervals in brackets. Anesthetic concentration and time dependence were evaluated with a one-way repeated-measure ANOVA followed by a Holm-Sidak multiple-pairwise comparison. Animals were implanted for weeks so some were tested on different experiments and multiple times on the same experiment. No bias was noted of a particular rat dataset on the group for any experiment.

## 2.4 Results

Continuous IOP recordings were performed on 32 rats. Median resting IOP was 12.7 [11.1, 14.2] mmHg. Figure 2.2A shows that IOP was rarely constant, varying even when animals were idle. Spontaneous fluctuations of  $> 2$  mmHg were observed in 34 of 51 video clips of animal inactivity, which implies that IOP is dynamically modulated by internal physiological processes.

Figure 2.2B shows that these processes respond to environmental disturbances. Opening the animal housing door led to a transient IOP bump, which was prolonged if a person entered the room. Moreover, IOP bumps were synchronous across implanted rats. Figure 2.2C shows that transporting animals to the test room produced an even longer IOP perturbation in most instances (23 of 33 room transfers across 17 animals). IOP in the test room was therefore slightly higher than resting IOP in housing (peak  $\Delta$ IOP =  $3.7 \pm 2.0$  mmHg,  $p < 0.001$ ,  $n = 23$ ) for up to 50 mins.

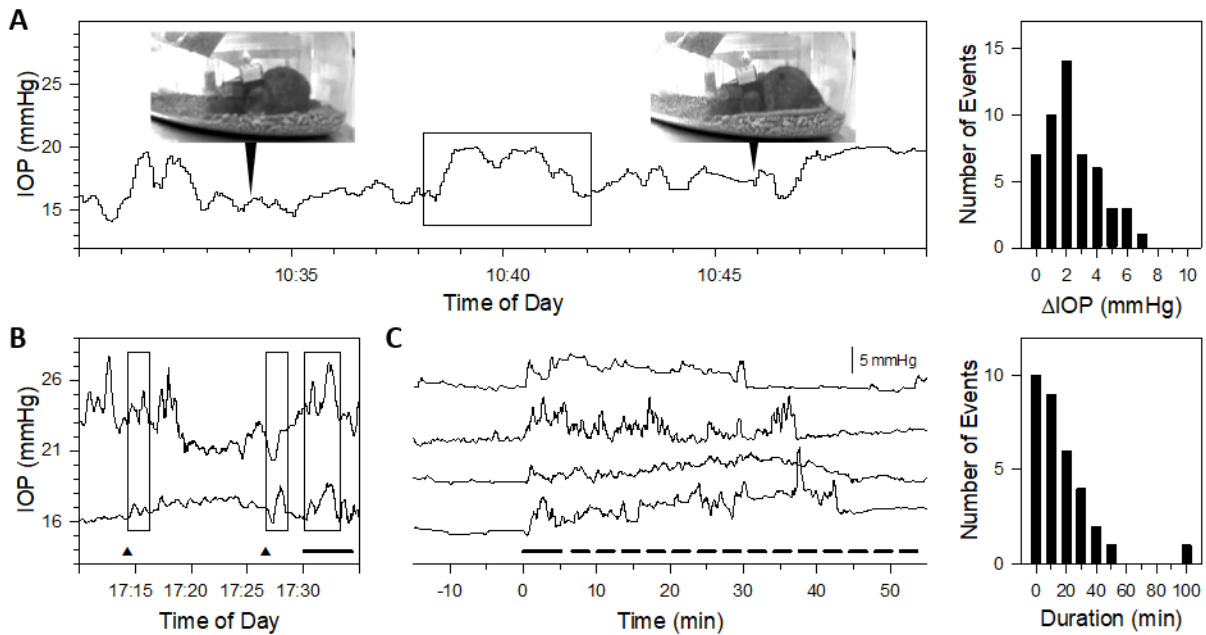


Figure 2.2: IOP variability in conscious free-moving rats. (A) Left, IOP recorded from a conscious rat during a period of animal inactivity. Inset images were acquired at times marked by arrowheads and show that the animal had not moved during a spontaneous bump in IOP (box). Right, histogram of spontaneous IOP bump amplitudes across 51 video clips of animal inactivity. (B) IOP recorded simultaneously from two conscious rats exhibited synchronous bumps (boxes) when the animal housing room door was momentarily opened (arrowheads) and when the investigator was in the room (bar). (C) Left, IOP recorded from conscious rats transferred on four instances from housing to the test room. Bars mark the period of housing room entry and cage transport (solid) and undisturbed waiting in the test room (dashes). Traces are shifted vertically for ease of comparison. Resting IOPs are 9.6, 13.6, 11.9, and 15.8 mmHg (top to bottom). Right, histogram of the duration of IOP elevation following 33 room transfers.

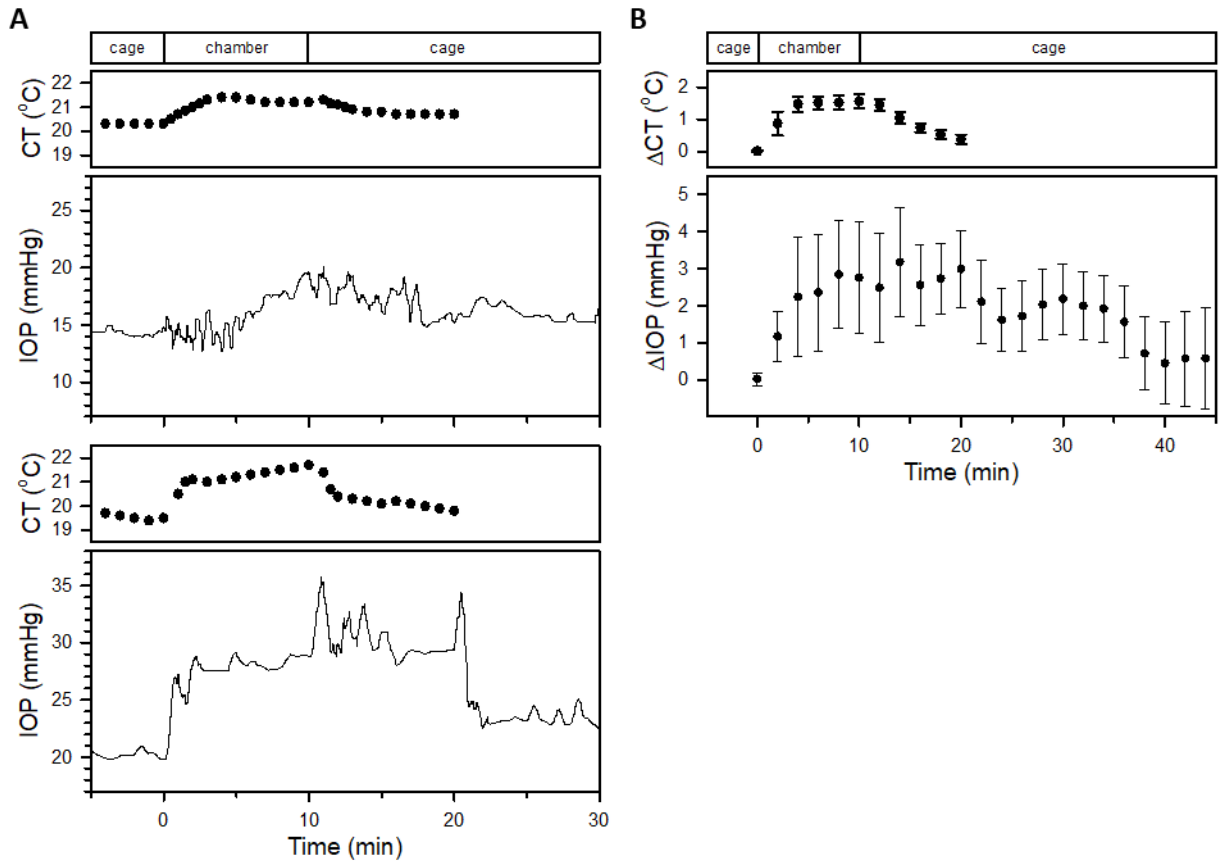


Figure 2.3: Effect of acute stress on IOP. (A) IOP of two conscious rats before, during, and after animal immobilization in a clear chamber, the ambient temperature of which (CT) was concurrently monitored. Selected records illustrate the range in IOP stress response amplitude and waveform. (B) Time-average change in IOP and CT across immobilization experiments relative to their baseline levels before chamber placement. Error bars give standard errors.

#### 2.4.1 Effect of Stress on IOP

The nature of the environmental disturbance suggests that IOP bumps may reflect a startle or stress response. However, disturbances often evoked a burst of motor activity as well. To exclude hyperactivity as an explanation, animals were put in a clear restrictive chamber. Figure 2.3A shows that the bumps cannot be attributed to animal motion since IOP still increased by varying amounts and time course during chamber confinement. CT rose concurrently by  $\sim 1.5$  °C due to animal body heat. Figure 2.3B plots the average time course of IOP and CT changes across

11 experiments on 4 animals. IOP went up  $2.7 \pm 1.3$  mmHg ( $p = 0.01$ ) in the chamber and took around 40 min to return to near-baseline level. Since IOP remained high long after chamber removal, it cannot be attributed to ambient heating of sensor fluids or electronics. Figure 2.4 provides further confirmation of the stress response. IOP increased when conscious but not when anesthetized animals were placed in a pre-heated chamber of roughly constant CT ( $n = 2$ ).

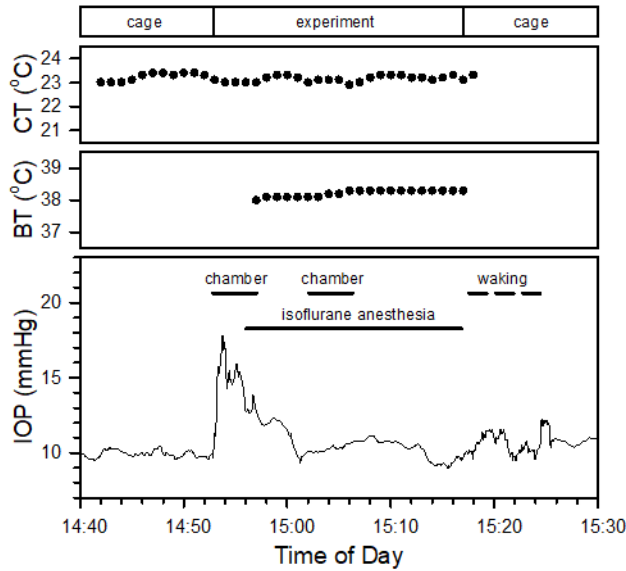


Figure 2.4: Blocking IOP stress response with anesthesia. IOP and BT of a rat that was first placed conscious in the immobilization chamber and then put back in the chamber unconscious under isoflurane anesthesia. CT was concurrently monitored.

### 2.4.2 Effect of Anesthesia on IOP

Effects of two commonly used anesthetics on IOP were examined. Figure 2.5A shows the IOP record of a rat before, during, and after isoflurane anesthesia. Heat support was provided throughout the experiment to counter any anesthetic effect on BT. An IOP stress response can be seen upon animal placement in the isoflurane chamber, which subsides as anesthesia is induced and IOP returns to near-baseline level. Subsequent alterations in isoflurane concentration had no discernable effect on IOP or BT. Spontaneous IOP bumps were also seen in anesthetized animals

on occasion. Figure 2.5B summarizes the results of 15 isoflurane experiments on 7 animals in which BT was held constant with heat support ( $BT = 37.5 \pm 0.9 \text{ }^\circ\text{C}$  across concentrations,  $F = 2.39$ ,  $p = 0.11$ ). Mean IOP change was not significantly different from zero ( $F = 1.50$ ,  $p = 0.23$ ) under 1% ( $-0.3 \pm 1.8 \text{ mmHg}$ ), 3% ( $0.2 \pm 1.8 \text{ mmHg}$ ), or 5% ( $-0.6 \pm 1.6 \text{ mmHg}$ ) isoflurane.

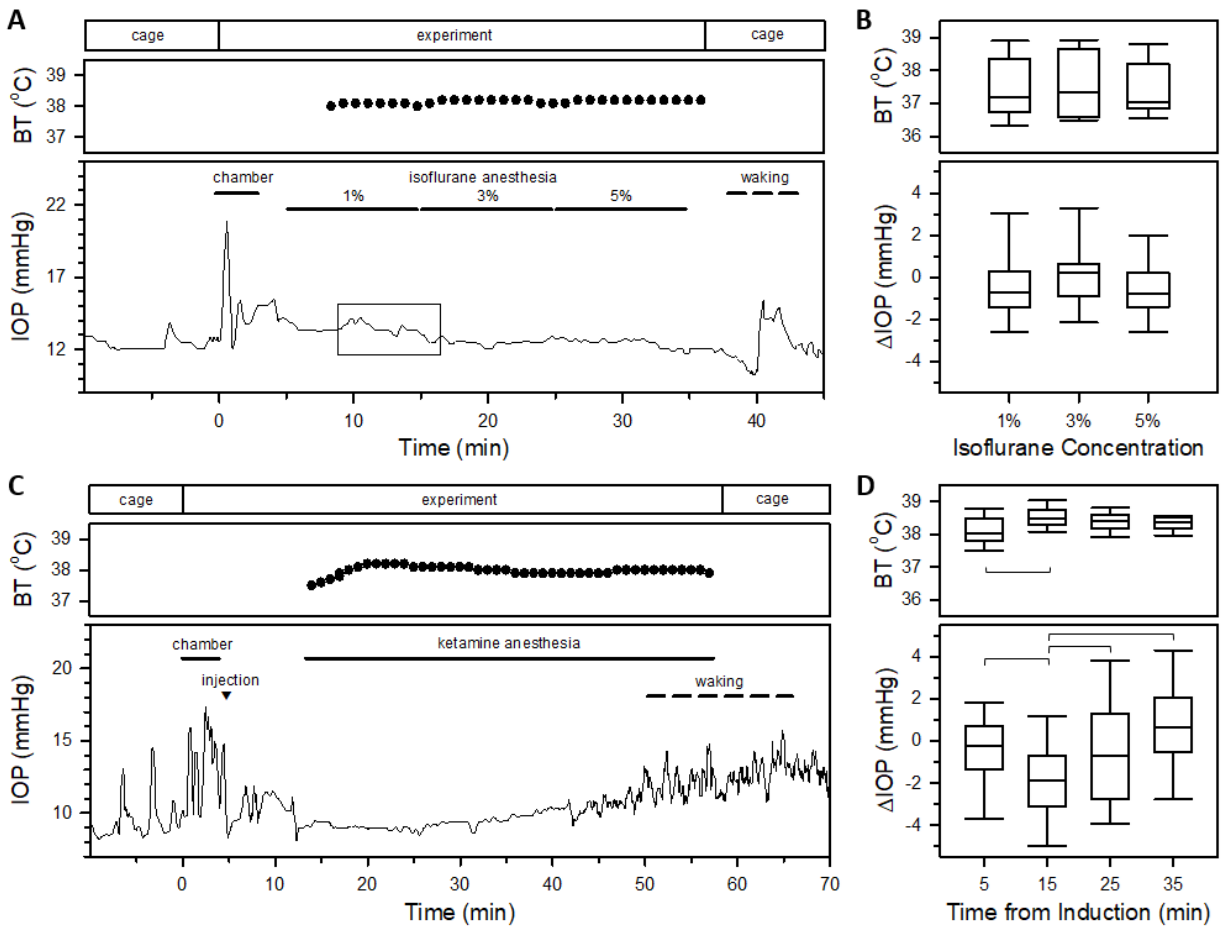


Figure 2.5: Effect of common anesthetics on IOP. (A) IOP and BT of a rat before, during, and after isoflurane anesthesia. Animal was sedated in the isoflurane chamber, placed on a heat pad, and anesthetic concentration was then varied via a nose cone. Spontaneous IOP fluctuations (box) still occurred in anesthetized animals. (B) Cumulative analysis of IOP and BT data across isoflurane concentration. (C) IOP and BT of a rat before, during, and after ketamine anesthesia. Animal was briefly sedated with isoflurane in the chamber, injected with ketamine just before waking, and placed on a heat pad when unconscious. (D) Cumulative analysis of IOP and BT time course across ketamine experiments. Brackets indicate time points that differ significantly. All IOP changes are relative to experimental baseline, and whiskers in box plots indicate minima and maxima.

Figure 2.5C shows the IOP record of a rat before, during, and after ketamine anesthesia. An IOP stress response can again be seen upon sedation and ketamine injection. IOP returned erratically to near-baseline level as anesthesia was induced and remained there for 30 min until the bolus wore off and the animal began waking. BT rose slightly after initiating heat support and held steady thereafter. Figure 2.5D summarizes the results of 16 ketamine experiments on 6 animals. BT was constant for the most part during ketamine anesthesia ( $BT = 38.3 \pm 0.4$  °C,  $p > 0.05$  for all comparisons except 5 versus 15 min). Mean IOP change was not significantly different from zero for the 5 min ( $-0.5 \pm 1.9$  mmHg,  $p = 0.31$ ), 25 min ( $-0.5 \pm 2.6$  mmHg,  $p = 0.44$ ), and 35 min ( $0.7 \pm 2.8$  mmHg,  $p = 0.27$ ) post-induction intervals but was slightly lower for the 15 min interval ( $-1.9 \pm 1.9$  mmHg,  $p < 0.01$ ).

#### 2.4.3 Effect of Tonometry on IOP

Possible effects of tonometry on IOP were also examined. Figure 2.6A shows the IOP record of an anesthetized rat while collecting applanation tonometry (AT) and rebound tonometry (RT) data. IOP continually crept higher during AT and was fairly steady during RT. Individual AT readings were highly variable and the average exceeded baseline. RT readings, on the other hand, scattered closely around baseline. Figure 2.6B summarizes the results of 9 experiments with each tonometer across 5 animals. IOP measured by AT and the system after AT differed significantly from baseline (median  $\Delta IOP = 3.1$  [1.0, 4.7] mmHg and  $2.7$  [1.4, 3.2] mmHg, respectively;  $p < 0.01$  for both), while there was no measurable difference for RT or the system after RT ( $p = 0.44$  and  $0.97$ , respectively). IOP likely increased during AT because of repeated tapping of its much larger tip on the small rat cornea. Figure 2.6C shows the IOP record of a conscious rat placed in a large plexiglass enclosure with an open wall to perform RT when the animal was idle. Transient bumps can be seen when the experimenter entered housing and when the animal was placed in the



enclosure. The latter bump was prolonged though the animal was not further handled. Individual RT readings were more variable in conscious animals and averaging does not capture the dynamic nature of IOP. Across 5 awake tonometry experiments, IOP was significantly higher than the resting level for both the system and RT (median  $\Delta$ IOP = 3.0 [2.7, 5.8] mmHg and 4.9 [1.8, 7.2] mmHg, respectively;  $p < 0.05$  for both). Again, no difference was detected between system and RT ( $p = 0.48$ ).

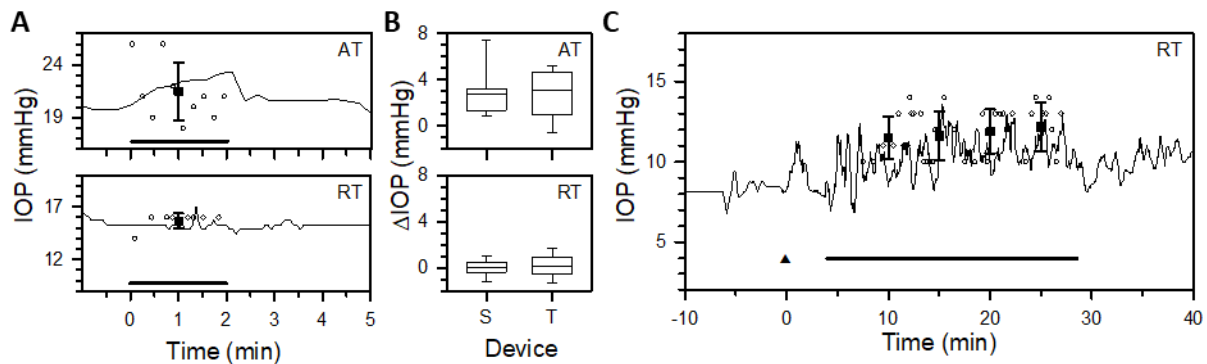


Figure 2.6: Effect of different tonometers on IOP. (A) IOP of an anesthetized rat before, during, and after applanation tonometry (AT, top) and rebound tonometry (RT, bottom). Bars indicate period when tonometer readings were made, circles indicate individual tonometer readings, and squares give the mean and standard deviation of those readings. (B) Cumulative analysis of IOP data measured with the telemetry system (S) and tonometers (T) for AT (top) and RT (bottom) experiments. IOP changes are relative experimental baseline, and whiskers indicate minima and maxima. (C) IOP of a free-moving conscious animal before, during, and after RT. Arrowhead marks the experimenter entering the housing room. Bar indicates period when animal was placed in a tabletop three-walled enclosure in the room and tonometer readings were made when the animal was idle. Circles indicate individual tonometer readings, and squares give the mean and standard deviation of 10 sequential readings.

#### 2.4.4 Effect of Temperature on IOP

It was noted during anesthesia experiments that BT influenced IOP. Figure 2.7A shows the IOP record of an anesthetized rat without heat support. IOP decreased steadily after anesthetic induction at  $-0.5$  mmHg/min and returned to near-baseline level as the animal waked. The IOP decline was confirmed by RT and mirrored by a BT decline of  $-0.2$  °C/min. Figure 2.7B shows the

IOP and BT records of an anesthetized rat before, during, and after sliding the animal between a heat pad and cool table. Both initially crept higher on the heat pad, which was presumably warmer than resting BT, and steadily decreased on the cool table. Sliding the animal back on the heat pad incompletely reversed the decline, so IOP and BT declined further upon return to the cool table. The IOP changes were again confirmed by RT. Figure 2.7C summarizes the results of 11 temperature experiments on 5 animals. IOP and BT were highly correlated ( $R^2 = 0.73$ ).

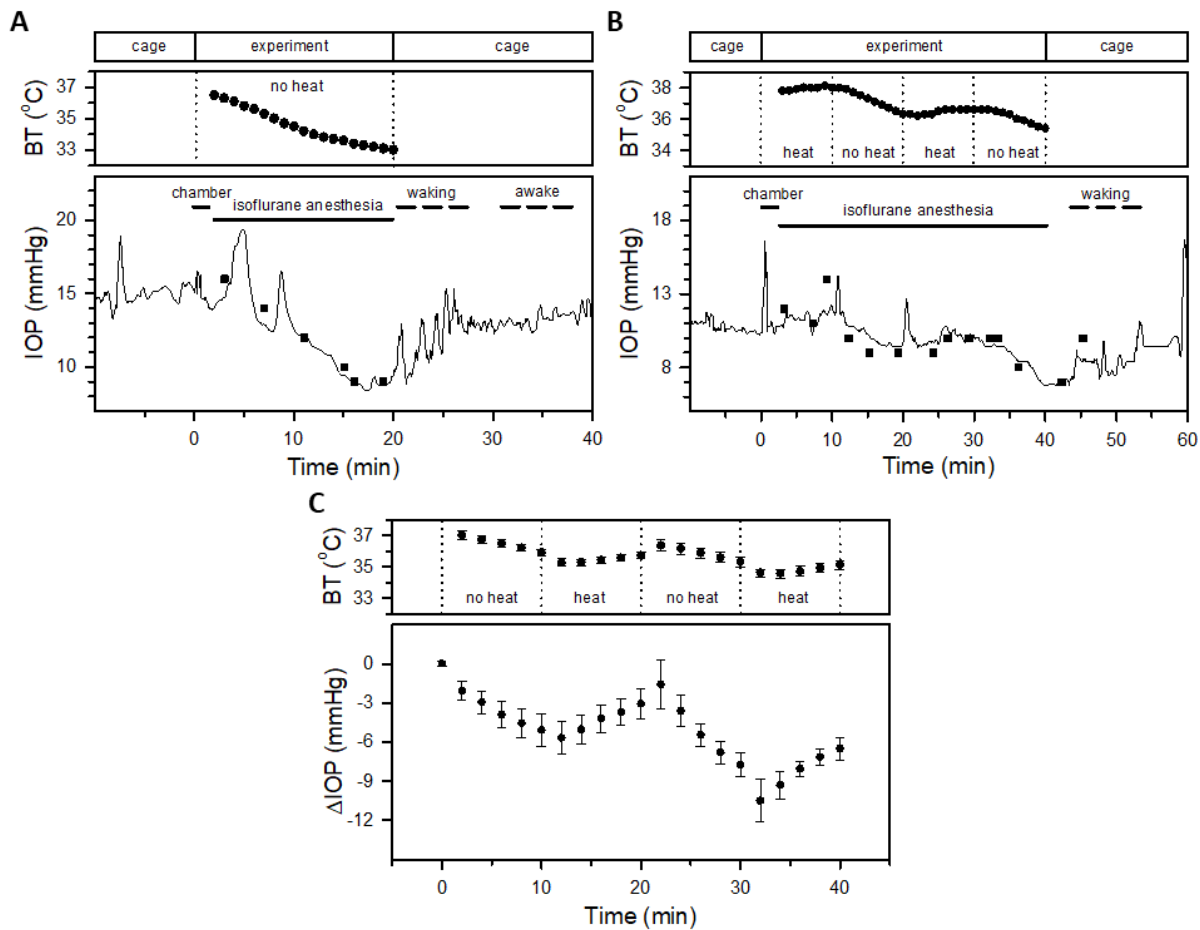


Figure 2.7: Effect of temperature on IOP. (A) IOP and BT of a rat before, during, and after isoflurane anesthesia with the animal resting on a cool table without heat support. Square symbols give mean IOP via RT. (B) IOP and BT of a rat before, during, and after isoflurane anesthesia with the animal moved between a heat pad and cool table. Square symbols give mean IOP via RT. (C) Time-averaging IOP and BT data across temperature manipulation experiments. IOP changes are relative to experimental baseline. Error bars give standard error.

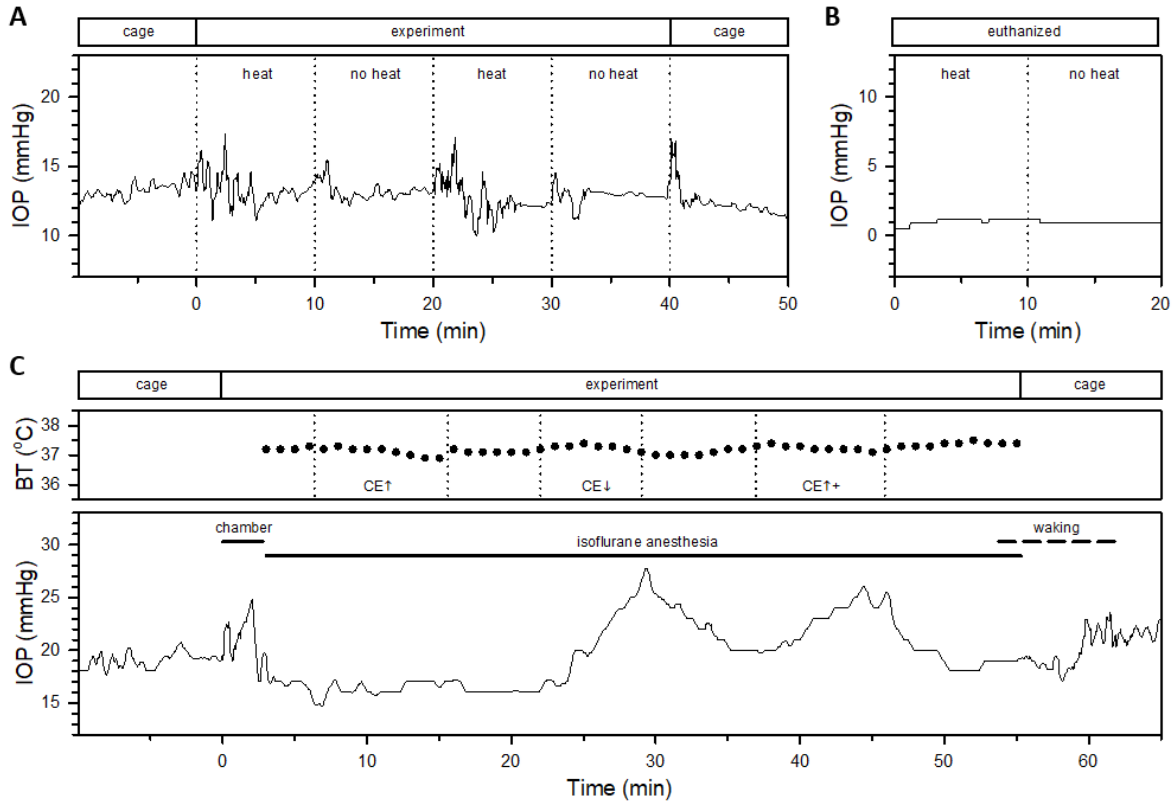


Figure 2.8: Control experiments for temperature effects on IOP. (A) IOP of a conscious rat moving between warm and cool surfaces. Animal was gently steered onto a heat pad and cool table using a large clear enclosure. (B) IOP of a euthanized rat laid on the warm and cool surfaces. (C) IOP and BT of an anesthetized rat in different recumbent positions. Animal rested either belly down or on its side with the cannulated eye up (CE↑) or down (CE↓). A warm gel pack was brought near the cannulated eye over the period indicated by the + symbol.

Additional experiments were conducted to corroborate the temperature results. Figure 2.8A shows the IOP record of a conscious rat steered between the heat pad and cool table. IOP bumps can be seen when the animal was removed and returned to its cage, as well as during each surface transition when it was not directly handled. More importantly, IOP fluctuated about a baseline that was comparable to the resting level. Figure 2.8B shows that IOP readings from a euthanized rat were similarly unaffected by warm and cool surfaces. Temperature effects in anesthetized animals thus reflect inhibition of thermoregulation. Figure 2.8C shows IOP and BT records of an anesthetized rat in different recumbent positions. BT was steady except for slight dips on rotation

from sternal to lateral recumbency. IOP was unchanged when the cannulated eye was rotated away from the heating pad and rose several mmHg when rotated toward the pad. IOP also increased when a warm gel pack was positioned near the cannulated eye while BT was unchanged. Effect of BT on IOP is thereby mediated in part or whole through changes in eye temperature.

## **2.5 Discussion**

In this study, IOP was found to spontaneously vary by several mmHg in conscious free-moving rats. The fluctuations persisted in idle and anesthetized animals and thereby reflect internal physiological processes that directly or indirectly modulate IOP. Some of these processes are keenly sensitive to environmental disturbances. Their sensory trigger was not investigated but auditory, tactile, and perhaps visual cues are certainly involved. Activation of these processes was generally associated with transient IOP increases but transient decreases were sometimes observed. IOP bumps lasted a few minutes if the disturbance was startling in nature or tens of minutes if more stressful. The fast dynamics cannot be captured by averaging AT or RT readings because data are too sparse and variable. Tonometry measurements were found to overestimate resting IOP by a few mmHg in conscious rats, and better estimates were obtained by attenuating the stress response with anesthetics. Tonometry measurements on anesthetized animals also had less variance, implying that the variability seen in conscious animals reflects spontaneous IOP fluctuations in addition to operator skill. Isoflurane and ketamine anesthetics both maintained IOP at near-baseline level if BT was regulated. Changes in BT, or specifically eye temperature, due to anesthetics or ambient environment had a rapid and pronounced impact on IOP. Care should be exercised during tonometry to ensure operator body heat does not artificially elevate readings.

### 2.5.1 Relation to Prior Work

Our results support and extend prior work and clarify contradictory reports on effects of stress, anesthetics, and temperature on IOP. Psychophysiological stress has long been associated with IOP elevation and glaucoma precipitation [41]. Mental relaxation techniques that aim to reduce stress were recently shown to lower IOP, reduce stress biomarkers, promote anti-inflammatory gene expression, and improve the quality-of-life of glaucoma patients [42]. Like this study, stress effects on IOP have been investigated experimentally by forcibly immobilizing animals. Rabbits immobilized for 1 h in a clear plastic tube had elevated cortisol, adrenaline, and noradrenaline levels and tonometry readings were 2-3 mmHg higher compared to non-immobilized animals [36]. The rise time was not examined but the duration lasted over an hour after immobilization. An IOP elevation of comparable magnitude was also observed via wireless telemetry in immobilized monkeys [37] and here in immobilized rats. The duration of elevation is unknown for the monkey study because anesthetic was injected during immobilization, which terminates the stress effect. It was similarly long-lasting in rats although the rabbit immobilization period was much longer. Prolonged effects on IOP do not, however, require forced immobilization since a rabbit telemetry study saw a 1-hr IOP bump after cage change [35]. Anticipation of immobilization appears sufficient because IOP jumped simultaneously in implanted rats upon opening the housing room door and remained elevated following room transfers. An anticipatory bump was also observed in monkeys when someone was in the housing room even if the animal was not handled [37]. Stress from actual or anticipated handling and immobilization leads to variability and inaccuracy in tonometry estimates of resting IOP that can only be overcome by contactless telemetry systems. The IOP stress response is important to consider in the interpretation of tonometry data.

Unlike acute stress there is less consensus about the effect of general anesthetics on IOP, and the consensus that does exist may be faulty or misleading. Most studies report that isoflurane decreases IOP [23, 24, 43-46], but some have seen IOP increase [47] or not change [48, 49]. Even more contradictory is ketamine, with numerous studies reporting an IOP decrease [23, 24, 47, 50-52], increase [53-57], or no change [58, 59]. An implicit and likely mistaken assumption of these tonometry studies is that IOP measured before anesthetic induction reflects resting IOP. Our and other telemetry [35] results show that animal handling induces a stress response that raises IOP long past the handling event. There was actually little-to-no effect of isoflurane or ketamine anesthesia on rat IOP, which agrees with a monkey telemetry study [26]. Hence, the IOP decrease reported by tonometry studies may instead reflect anesthetic inhibition of the stress response. In support of this interpretation, early tonometry studies notice no significant IOP change in children that were already sedated [48, 60]. Another potential complication is the effect of anesthetics on thermoregulation [61]. Some tonometry studies report IOP decreases of 5 mmHg or more in mice and rats under isoflurane and ketamine anesthesia [23, 24, 46]. Such large drops were recorded in this study only from implanted animals that were not provided heat support. None of the cited rodent studies monitored BT to confirm it was stable, one does not mention heat support, and one explicitly states a heat pad was not used. Reported IOP decreases may thereby be explained by a combination of stress-elevated baseline and BT loss and not necessarily a direct anesthesia effect. However, our results cannot reconcile reported IOP increases. IOP elevation is primarily seen for ketamine, which is known to increase heart rate, blood pressure, and vascular resistance [62]. Perhaps anesthetic effects on IOP depend on species, dosage amount, or delivery method (intravenous versus intramuscular).

There is comparatively less research on the effect of temperature on IOP. Two groups put individuals in a heated room and neither noticed changes in IOP [19, 20]. One detected a few mmHg increase after 3 h that was attributed to a rise in BT since it was not observed in acclimated subjects [20, 28]. No IOP change was noted here either when conscious rats were exposed to different surface temperatures, presumably because thermoregulatory processes held BT constant. IOP decreases were though reported in humans and rabbits immersed to the head in warm water [63, 64]. They might not have been seen in implanted rats because the thermal challenge to the body is much greater than a heat pad, causing elevated heart rate and reduced blood pressure in immersed humans and elevated episcleral venous pressure and reduced aqueous humor formation in immersed rabbits. Our results are not only consistent with tonometry studies that demonstrate IOP increases upon warming the eye via prolonged eyelid closure and IOP decreases upon cooling with a cold mask or air stream [65-67], but also reveal the fast dynamics of temperature driven IOP changes.

### 2.5.2 Limitations

Two limitations of the work should be noted. One is the external locus of the pressure sensor, which introduces non-physiological variability in IOP records due to hydrodynamic effects of head and body rotation [8]. The extraneous noise is heightened during hyperactivity, such as when animals are stressed or waking from anesthesia. Another is that physiological mechanisms underlying observed effects were not investigated. While IOP startle and stress response can be broadly attributed to the autonomic nervous system [68] since they were blocked by anesthetics, the precise mode of action is uncertain. Autonomic signals could alter IOP in rats by changing ocular blood flow or components of aqueous humor dynamics [69]. Also, IOP still fluctuated in anesthetized rats, so some autonomic signals are not inhibited by isoflurane or ketamine. The

autonomic nervous system could mediate temperature effects as well given that circadian BT and IOP rhythms are strongly coupled [70]. A biophysical explanation cannot though be discarded since aqueous outflow depends on temperature-sensitive factors like fluid viscosity and metabolic activity [71, 72], which is suggested by the sensitivity of rat IOP to ocular heating. To address these limitations, a telemetry system that mounts to the skull and records additional parameters like BT, heart rate, and motor activity is being developed to reduce extraneous noise and better understand the mechanisms of IOP variation.

## **2.6 Conclusion**

The principal findings of the study are that IOP is dynamically modulated in conscious rats by physical and physiological processes that are sensitive to temperature and animal stress but not anesthetics. The processes can act rapidly and produce IOP changes that last long after initiation. Continuous IOP telemetry is required to record these fast changes without disturbing the animal. Rebound tonometry gives accurate snapshots of IOP but animal handling elevated IOP in conscious rats. A better estimate of resting IOP may be obtained by anesthetizing animals while maintaining resting BT.



## **Chapter 3: Characterization of Intraocular Pressure Variability in Rats**

### **3.1 Introduction**

It is well established that a sustained elevation in mean intraocular pressure (IOP) is a risk factor for glaucoma in humans and glaucoma-like damage in animal models. However, little is known about IOP fluctuation moment-to-moment and the impact it has on the retina. Previous studies represent IOP as the mean and standard deviation of a distribution of variable tonometry readings, but it is unclear whether this variability is due to measurement error or if it reflects true IOP fluctuation. Tonometry has been used for decades as the gold standard for measuring IOP, however it only provides a snapshot estimate and data collection is laborious. Tonometry also requires investigator-subject interaction, which has been shown to elevate IOP above resting levels when compared to telemetered IOP data [73]. Other studies have also suggested that anticipation of investigator or physician presence contributes to IOP variability and may be explained by whitecoat hypertension, which, for some, can affect the accuracy of glaucoma diagnosis [37, 38].

Previous 24-h studies revealed that IOP of various species follows a diurnal pattern when entrained to a normal 12-h light:12-h dark cycle [34, 74-77]. However, many of these studies performed tonometry or another method of intermittent IOP data collection. Although tonometry provides a good estimate of mean IOP change over time, it does not accurately capture IOP fluctuation moment-to-moment. Unlike tonometry, telemetry offers a hands-off approach that allows for collection of resting IOP with minimal confounds and experimental bias. IOP telemetry has been used in various animal models [9-11, 78-80] as well as human studies [27, 81] to prove that IOP is not constant, but fluctuates continuously. Our previous telemetry study revealed

that IOP fluctuated in isolated, idle animals as well as in anesthetized animals, which suggests that IOP is modulated by internal physiological processes [73]. Others have used telemetered IOP data to correlate fast pressure fluctuations on the order of seconds with blinks and saccades in pigs and monkeys [9, 80]. However, little is known on the extent of IOP variability and how it changes over time. To further investigate the relative contribution of slower and faster IOP fluctuations to daily IOP change, we used a novel telemetry system to monitor IOP round-the-clock for weeks on end to characterize IOP variability in the rat.

### **3.2 Materials and Methods**

All experiments were conducted in accordance with the National Institutes of Health guide for the care and use of laboratory animals and compliance with a protocol approved by the Institutional Animal Care and Use Committee (IACUC) at the University of South Florida.

#### **3.2.1 Animal Preparation**

Male retired-breeder Brown-Norway rats (300-400 g) were housed in a temperature-controlled room (22 °C) under a 12-h light (6AM):12-h dark (6PM) cycle with food and water available ad libitum. The anterior chamber of the right eye was implanted with a silicone microcannula (OD: 200  $\mu\text{m}$ , ID: 100  $\mu\text{m}$ , AS One International, Santa Clara, CA, USA) connected to an IOP telemetry device worn as a backpack. Pressure sensors were calibrated against a mercury manometer and validated with rebound tonometry. Device functionality and eye cannulation surgery were explained previously in Section 2.3.1 as well as in previous publications [8, 73]. Rat IOP data was collected at 0.25 Hz for weeks to months.

#### **3.2.2 Data Analysis**

MATLAB software (The MathWorks, Natick, MA) was used to both median and lowpass filter data with a filtering window of 28s to remove spurious data. To determine IOP variability

over different timescales, filtered data were subjected to both a mean and variance analysis as well as a quantification of transient and sustained IOP fluctuations. Statistical analyses were conducted in SigmaPlot software (Systat, San Jose, CA), with significance assessed at  $\alpha$  of 0.05. Results are expressed as mean  $\pm$  standard deviation following a test of normality. Mean differences between groups were evaluated with paired t-tests unless otherwise noted.

### 3.2.3 Daily IOP Mean and Variance Analysis

To compare results of previous tonometry studies, mean changes in telemetered IOP data were analyzed. Daily IOP mean changes were found by normalizing 24-h data segments to the respective daily mean and averaging in consecutive 30-minute intervals. In addition to mean changes, telemetered data has shown that IOP varies continuously. To quantify the extent that IOP deviates from mean changes, data were also subjected to a daily IOP variance analysis. The extent of deviation was found by normalizing 24-h data segments to the running 30-minute average and calculating the variance in consecutive 30-minute periods. Average IOP mean and variance statistics of 7 days of data were compared across animals.

### 3.2.4 Transient and Sustained IOP Fluctuation Analysis

Transient and sustained IOP fluctuations were detected using a custom MATLAB algorithm. The algorithm employed the “findpeaks()” command to detect the peak of an event using two name-value arguments: minimum peak prominence and minimum peak separation. Minimum peak prominence, or the amount a peak stands out relative to the highest local minima, was determined from sensor resolution. Since the sensor accurately detects pressure changes  $> 0.3$  mmHg, a minimum peak prominence of  $\geq 1$  mmHg was used to ensure that signal noise went undetected. An illustration showing the application of this parameter is shown in Figure 3.1A. The peaks marked with asterisks would go undetected because they are  $< 1$  mmHg in amplitude with

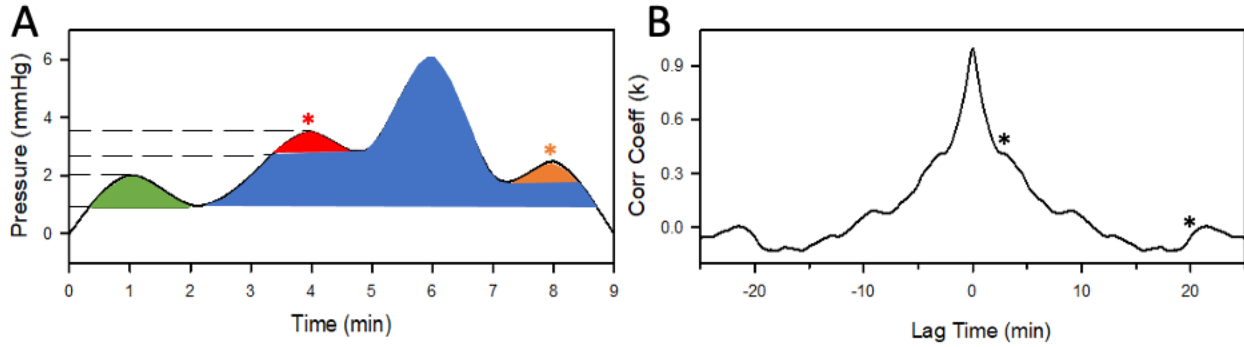


Figure 3.1: Determination of peak detection parameters. (A) A schematic showing the application of a 1 mmHg minimum peak prominence to a randomly generated data set. Peaks marked with \* would go undetected as they are  $< 1$  mmHg in amplitude with respect to the highest local minima. (B) Representative autocorrelation of a 4-hour IOP data segment. Minimum peak separations of 2 mins and 20 mins were used to detect transient and sustained events respectively based on changes in slope from the autocorrelation (marked by \*'s).

respect to the highest neighboring minima. Minimum peak separation was determined from an autocorrelation of IOP data. Figure 3.1B shows a representative autocorrelation of a 4-hour IOP data segment. Since an autocorrelation is a cross-correlation of a data set with itself, the maximum correlation was found at zero lag time. The asterisks mark the 2 min and 20 min lag times where transient and sustained IOP fluctuations were respectively most correlated across animals ( $n = 12$ ).

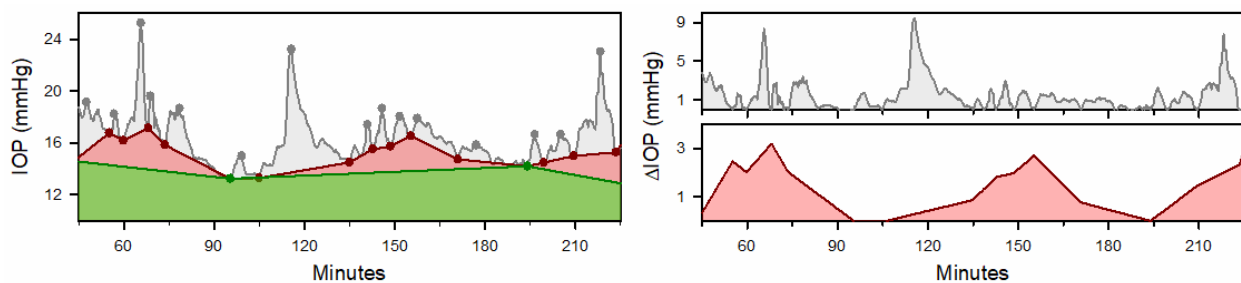


Figure 3.2: Detection of transient and sustained IOP fluctuations. Left, representative data set showing fast and slow IOP fluctuations over the course of 3 hours. Grey dots mark the peaks of transient events. Local minima between peaks (red dots) were linearly interpolated to generate the new sustained IOP waveform. The peaks of sustained events were detected and local minima between those peaks (green dots) were linearly interpolated to reveal baseline IOP. Right, examples of transient (grey) and sustained (red) IOP fluctuations that were peeled away from underlying baseline fluctuations (green).

Figure 3.2 illustrates the method used to detect transient and sustained IOP fluctuations. First, transient peaks were detected (grey dots) using a minimum peak prominence of 1 mmHg and minimum peak separation of 2 mins. Local minima were linearly interpolated and subtracted from the original data set to peel away the transient IOP signal (grey). The remaining IOP signal was subjected to the algorithm again to detect sustained peaks (red dots) using a minimum peak prominence of 1 mmHg and minimum peak separation of 20 mins. The minima between sustained peaks were linearly interpolated to generate an underlying baseline IOP signal (green) with the sustained IOP signal peeled off (red). The frequency, amplitude, and interval of transient and sustained IOP fluctuations were quantified across animals and represented as probability density functions (PDF). Serial correlations were performed on the amplitude and interval of transient and sustained events to determine if there was any relationship between a given event and past events. Serial correlations  $s_k$  between characteristics of one IOP event  $\tau_i$  in relation to another that occurs  $k$ -intervals later  $\tau_{i+k}$  (Equation 3.1) were calculated using the following relationship where length of the IOP record was given as  $N$ :

$$s_k = \frac{N \sum_{i=1}^N \tau_i \tau_{i+k} - \sum_{i=1}^N \tau_i \sum_{i=1}^N \tau_{i+k}}{\sqrt{[N \sum_{i=1}^N \tau_i^2 - (\sum_{i=1}^N \tau_i)^2][N \sum_{i=1}^N \tau_{i+k}^2 - (\sum_{i=1}^N \tau_{i+k})^2]}} - \frac{k-N}{N(N-1)} \quad [3.1]$$

Equation 3.1 is an interpretation of a relationship previous used to assess the temporal pattern of neuron output spiking [82]. A high serial correlation would indicate that IOP event amplitude and/or interval of a given event likely depends on those of previous events. Serial correlations were also performed on data sets in which IOP event amplitude and interval were shuffled in time to determine if any relationships were due to chance. To determine coherence in IOP fluctuations between simultaneously recording animals, cross-correlations were performed across transient, sustained, and baseline IOP waveforms. IOP events of one animal were shuffled and cross-correlated again with the other animal to determine any relationship due to chance.

### 3.2.5 IOP-Related Mechanical Energy Calculation

The individual contribution of transient, sustained, and baseline IOP fluctuations to the mechanical energy expenditure on a given intraocular tissue was calculated. The following relationship of energy dissipation over time in a direct current (DC) circuit was used to calculate IOP-related mechanical energy expenditure  $E$ , where IOP is represented as voltage  $V$ :

$$E = \int_0^T V(t)I(t)dt, I = \frac{V}{R}, G = \frac{1}{R} \rightarrow E = G \int_0^T IOP^2(t)dt \quad [3.2]$$

The integral portion of Equation 3.2 represents the area under the squared transient, sustained, and baseline IOP records, which yields units of mmHg<sup>2</sup>·sec. Since conductance  $G$  is equivalent to the reciprocal of resistance  $R$ , we multiplied the area under the IOP<sup>2</sup> versus time curve by the average conductance  $G$  of the rat trabecular meshwork,  $3.83 \times 10^{-4}$  μL/sec/mmHg [69] to determine energy expenditure  $E$  on the conventional outflow pathway specifically. This yields an energy term in units of mmHg·μL. To get the term in units of μJ, the conversion factor of 1 mmHg·μL is equal to  $133.32 \times 10^{-3}$  μJ was applied. The daily average IOP-related mechanical energy expenditure was compared across animals and expressed as average μJ/day.

### 3.3 Results

This study considers IOP statistics of 12 animals that collected data for at least 7 consecutive days in 12-h light:12-h dark conditions. All rats exhibited diurnal IOP changes with lower values in the light phase and higher values in the dark phase (Figure 3.3A). The average light-phase (10AM - 2PM) and dark-phase (10PM - 2AM) IOP's were  $14.6 \pm 6.0$  mmHg and  $19.3 \pm 8.4$  mmHg, respectively ( $n = 12$ ). Daily changes in IOP mean were variable across animals as well as across 7 days in a single animal. Analysis of IOP mean across animals revealed a maximum diurnal IOP swing of  $8.6 \pm 2.2$  mmHg ( $n = 12$ ) (Figure 3.3B, left). IOP deviation from the mean on the other hand fluctuated randomly throughout the day independent of mean changes (Figure

3.3B, right). There was, however, slightly higher IOP variation right before lights came on and right after lights turned off.

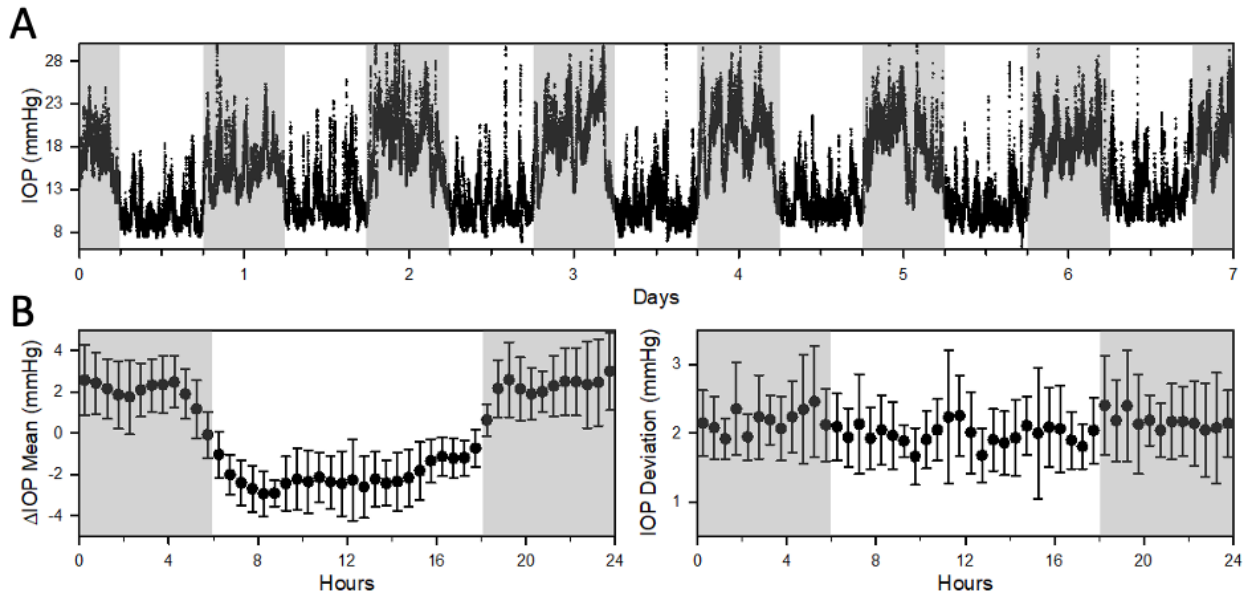


Figure 3.3: IOP mean and variance statistics. (A) IOP data from a given animal housed in 12-h light: 12-h dark conditions. There were noticeable differences in amplitude of the diurnal swing from day to day. (B) Graphs showing average change in IOP mean and the extent that IOP deviates from the mean over 24 hours. Dark-phase IOP was higher than light-phase IOP (left). Over 30-min intervals, IOP varied independently of mean changes (right).

IOP data was also subjected to a MATLAB algorithm that parsed the signal into three distinct waveforms: transient, sustained, and baseline IOP. There were on average  $231 \pm 79$  transient events and  $16 \pm 2$  sustained events daily ( $n = 12$ ). About 77% of daily transient IOP fluctuations were  $\leq 4$  mmHg in amplitude, but some animals had transient fluctuations up to 15 mmHg (Figure 3.4A). Transient IOP fluctuations were short in duration, lasting 2 to 6 minutes, however, this was rather variable across animals (Figure 3.4B). Sustained IOP fluctuations were less frequent than transient fluctuations and lasted much longer. About 80% of sustained events were  $\leq 5$  mmHg (Figure 3.5A) and typically lasted 20 to 90 minutes (Figure 3.5B). Serial correlations were performed on the amplitude and interval of transient and sustained events to

determine if there were any dependencies on previous event characteristics. It was found that there was a likelihood for the amplitude and interval of a given transient event to be serially correlated with the amplitude and interval of the three previous transient events. Sustained event amplitude and interval were not serially correlated. Serial correlation analysis of shuffled amplitude and interval data revealed no correlation due to chance.

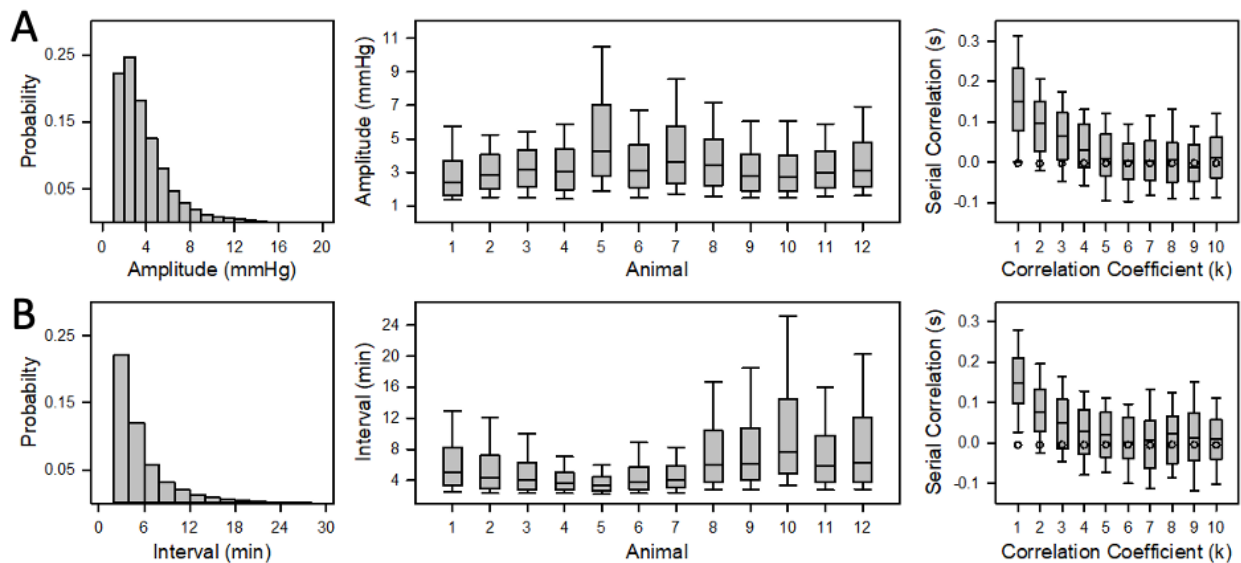


Figure 3.4: Transient IOP fluctuation statistics. (A) Statistics pertaining to the amplitude of transient IOP fluctuations. (B) Statistics pertaining to the interval of transient IOP fluctuations. PDFs for transient IOP amplitude and interval (left). Distribution of transient amplitude and interval for each animal showing inter-animal variability (middle). Serial correlations showing that amplitude and interval of a given transient event is serially correlated with the amplitude and interval of the 3 previous events (right).

Plots of average transient, sustained, and baseline IOP fluctuations for all animals are shown in Figure 3.6A. Both sustained and baseline IOP waveforms displayed long-lasting diurnal characteristics, however, transient IOP did not. Like IOP variance statistics, rats experienced slightly larger transient events just before lights turned on and just after lights turned off. Averaging across animal data highlighted the similarities between waveforms but could mask any



differences. The individual contributions of transient, sustained, and baseline fluctuations to the IOP-induced mechanical energy expenditure on the trabecular meshwork was calculated. On average, transient, sustained, and baseline IOP respectively amounted to  $26.0 \pm 10.9$ ,  $40.1 \pm 15.9$ , and  $964.5 \pm 770.6 \mu\text{J}/\text{day}$  ( $n = 12$ ). The amount of energy due to transient events was significantly smaller than the amount of energy due to sustained events ( $p = 0.02$ ). The sum of energy due to transient and sustained events is also significantly less than energy due to baseline fluctuations ( $p < 0.001$ ). Baseline IOP was separated further into diurnal IOP fluctuations and DC IOP offset. Average light-phase IOP (dashed line in Figure 3.6A, bottom) was used as the DC offset, which was subtracted out of the baseline IOP record to isolate diurnal changes.

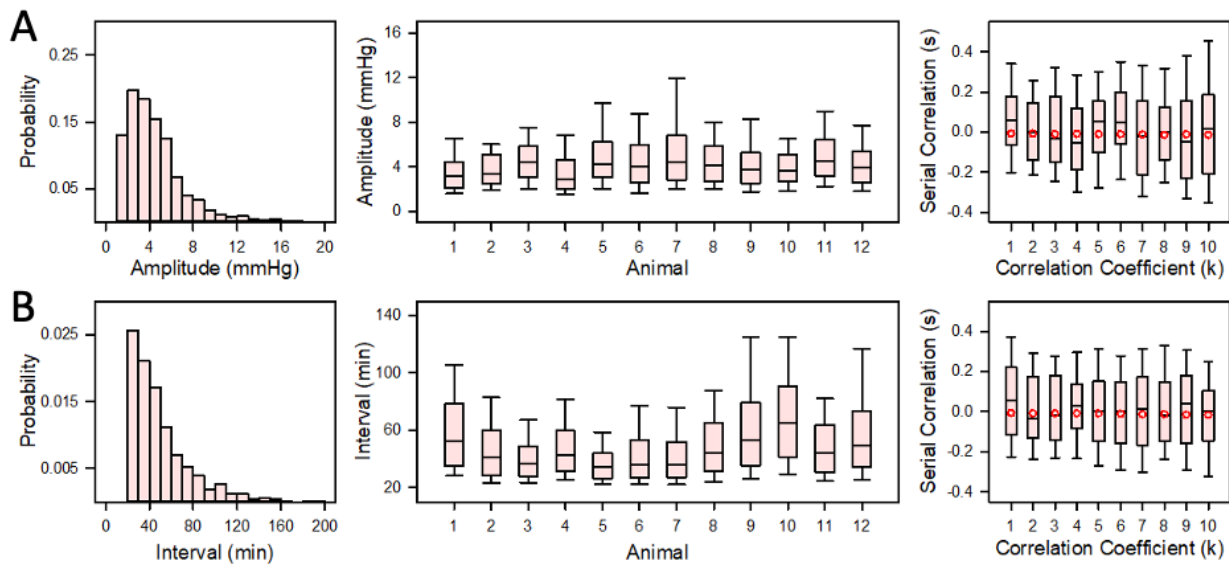


Figure 3.5: Sustained IOP fluctuation statistics. (A) Statistics pertaining to the amplitude of sustained IOP fluctuations. (B) Statistics pertaining to the interval of sustained IOP fluctuations. PDFs for sustained IOP amplitude and interval (left). Distribution of sustained amplitude and interval for each animals showing inter-animal variability (middle). Serial correlations showing that amplitude and interval of a given sustained event were not serially correlated with previous events (right).

It was found that diurnal IOP and DC IOP offset respectively contributed  $112.1 \pm 134.4$  and  $648.3 \pm 590.4 \mu\text{J}/\text{day}$  to the relative energy expenditure. The sum of energy due to transient,

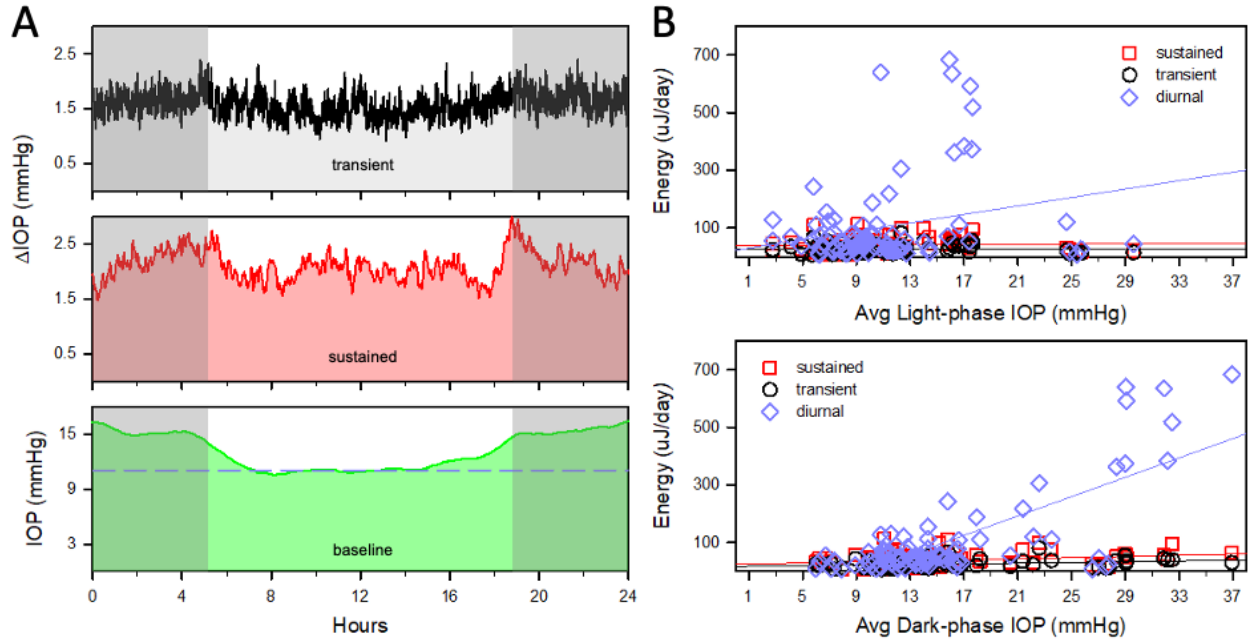


Figure 3.6: Daily IOP-related mechanical energy expenditure. (A) Average daily transient, sustained, and baseline IOP fluctuations across animals. No diurnal trend existed for transient fluctuations (top). There was a diurnal rhythm for both sustained (middle) and baseline (bottom) IOP fluctuations. The dashed line on the baseline IOP waveform marks average daytime IOP. (B) Comparison of average light-phase and dark-phase IOP to daily IOP-related mechanical energy expenditure. There was a stronger linear relationship between average light-phase IOP and energy due to diurnal fluctuations ( $m = 7.3$ ,  $R^2 = 0.061$ ) than transient and sustained fluctuations ( $m = 0.1$  &  $0.3$ ,  $R^2 = 0.001$  &  $0.004$ , respectively) (top). There was a stronger linear relationship between average dark-phase IOP and energy due to diurnal fluctuations ( $m = 16.8$ ,  $R^2 = 0.565$ ) than transient and sustained fluctuations ( $m = 0.6$  &  $0.9$ ,  $R^2 = 0.091$  &  $0.070$ , respectively) (bottom).

sustained, and diurnal IOP fluctuation alone is equivalent to a 6.4 mmHg elevation in DC IOP over 24 hours. Figure 3.6B is a linear regression analysis of average light-phase and dark-phase IOP with daily pressure-related energy expenditure. There was a strong positive linear relationship of light-phase and dark-phase IOP with energy due to diurnal IOP change ( $m = 7.3$  and  $16.8$ , respectively). This suggests that animals experiencing larger diurnal IOP changes were more likely to have a higher IOP mean, which is associated with a higher risk of glaucomatous damage. There was a weak positive linear relationship of light-phase and dark-phase IOP with energy due to

transient ( $m = 0.1$  and  $0.6$ , respectively) and sustained ( $m = 0.3$  and  $0.9$ , respectively) IOP fluctuations. This suggests that animals with a higher mean IOP do not necessarily experience higher amplitude transient and sustained IOP fluctuations.

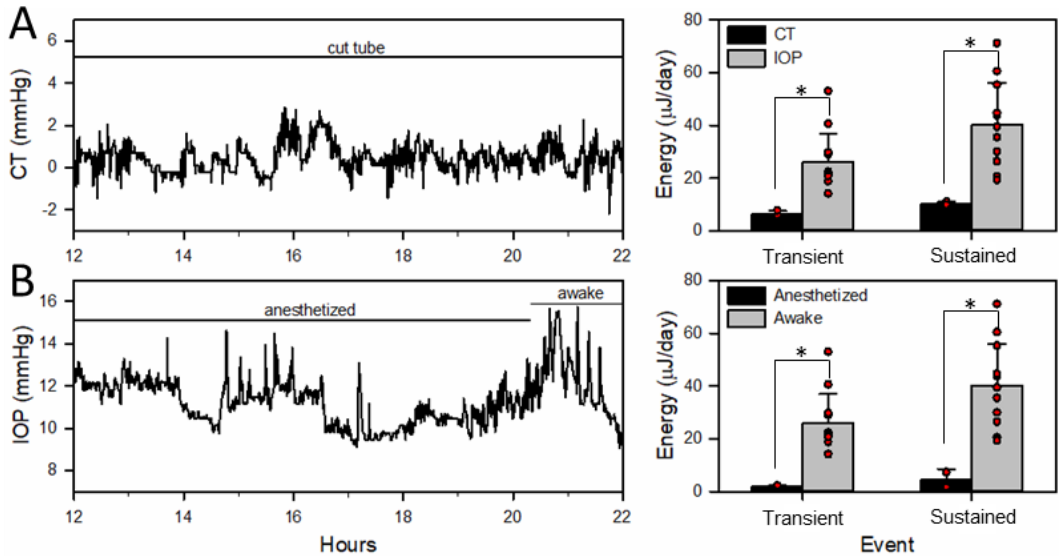


Figure 3.7: Analysis of cut tube data and effect of isoflurane on IOP variability. (A) Raw pressure data from a control experiment in which the cannula was removed from the eye, cut, and sutured under the conjunctiva (left). Analysis revealed that there was significantly less transient and sustained pressure-related energy from hydrodynamic effects of fluid in the tubing ( $n = 3$ ) compared to IOP recordings ( $n = 12$ ) (right). (B) Raw IOP data of an animal that was anesthetized under isoflurane (left). Analysis revealed that anesthetized rats ( $n = 2$ ) experience significantly less transient and sustained IOP-related mechanical energy than awake rats ( $n = 12$ ) (right). Red circle represent average daily energy expenditure from each animal.

Two additional experiments were conducted to corroborate results. In one set of experiments, the cannula was removed from the anterior chamber and sutured under the conjunctiva to detect pressure fluctuations due to head rotation. Figure 3.7A shows a raw plot of pressure fluctuations from a cut tube (CT) experiment. These fluctuations were random in occurrence and  $< 2$  mmHg in amplitude. 7 days of CT data from three different rats were subjected to the transient and sustained fluctuation analysis to determine the relative contribution of hydrodynamic effects of fluid in the tubing to the perceived IOP-induced mechanical energy

expenditure. It was found that transient and sustained CT fluctuations were significantly less than those of IOP ( $p = 0.01$  and  $0.007$ , respectively). Transient and sustained CT fluctuations amounted to  $6.3 \pm 1.3$  and  $10.2 \pm 0.8$   $\mu\text{J}/\text{day}$ , respectively ( $n = 3$ ). This suggests that CT fluctuations contribute at most 25% to the combined daily transient and sustained IOP-related energy expenditure and no more than 1% to total IOP-related energy expenditure. The second set of experiments involved monitoring IOP of an anesthetized animal over several hours. Figure 3.7B shows that IOP of isoflurane anesthetized rats fluctuates spontaneously. There were noticeably fewer IOP fluctuations in the anesthetized state compared to the awake state. This was expected since anesthesia inhibits the autonomic response. Transient and sustained fluctuation analysis was performed on IOP data of two isoflurane anesthetized rats to determine the extent of IOP variability. It was found that transient and sustained IOP-related energy expenditure in anesthetized rats was significantly less than that of awake rats ( $p = 0.036$  and  $0.01$ , respectively).

Figure 3.8A shows IOP data of two simultaneously recording rats in the same room on the same shelf. IOP fluctuation analysis was performed on a 3-day record from each animal to determine the coherence of IOP fluctuation patterns between animals. Figure 3.8B shows the resulting cross-correlations of transient, sustained, and baseline IOP waveforms between animals (solid lines). The cross-correlation analysis was repeated on IOP data that had been shuffled for one animal to detect similarities due to chance (dotted lines). The highest positive correlations due to chance (dashed lines) were used as reference for significance of original correlation analysis. It was found that sustained and baseline IOP fluctuations were significantly correlated between the two animals, but not transient fluctuations. This suggests that transient events may be the result of physiological phenomenon that are unique to a given animal such as blinking or activity level, which are short-lasting. Sustained events may be the result of environmental stimuli such as

presence of an investigator or loud noises in the animal facility, which have long-lasting, correlated effects. Baseline IOP includes the diurnal IOP fluctuations, therefore, correlation of this signal between animals was expected since animals were housed in the same lighting condition.

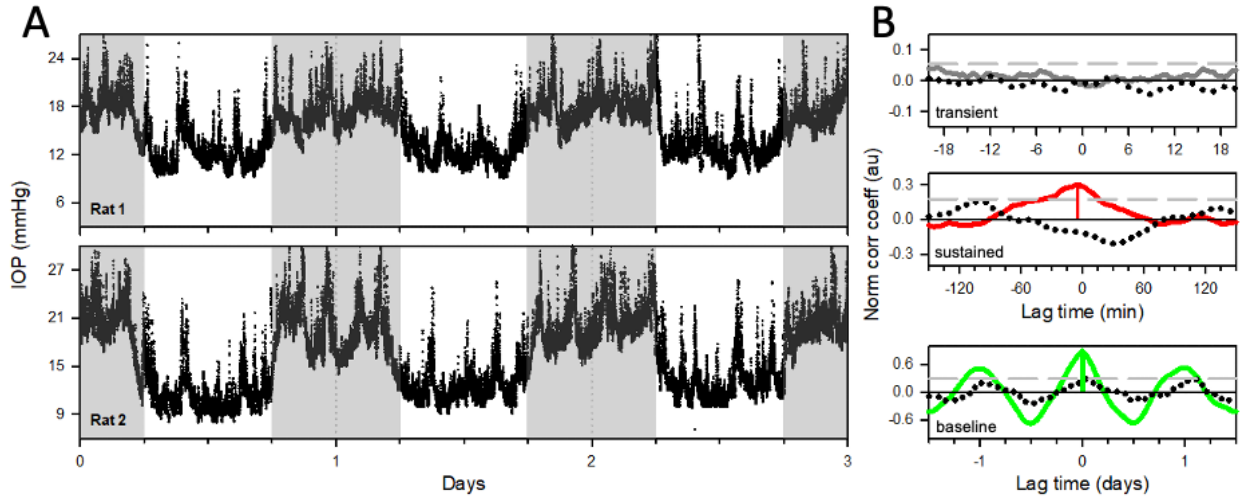


Figure 3.8: Cross-correlation of IOP fluctuations between simultaneously recording rats. (A) Raw IOP record of two rats simultaneously collecting on the same shelf in the housing room. Both had similar patterns of IOP fluctuation. (B) Cross-correlation statistics showing coherence of transient, sustained, and baseline IOP fluctuations between animals (solid line). IOP events of one animal were randomized and cross-correlated with the other to determine coherence due to chance (dotted line). The dashed line shows the highest correlation due to chance. It is possible that correlation of transient events may be due to chance (top). However, there was significant correlation between sustained (middle) and baseline events (bottom).

### 3.4 Discussion

In this study, our novel telemetry system was used to continuously monitor IOP in conscious rats for weeks on end. It was found that rats housed in normal 12-h light:12-h dark conditions experienced a diurnal IOP rhythm, with higher values in the dark phase. This finding supports and confirms results of prior tonometry studies that show diurnal IOP changes in rats [34, 77]. However, there is a lot of information pertaining to IOP fluctuation day-to-day and moment-to-moment that is lacking in previous tonometry studies. Telemetered data suggests that IOP is sensitive to environmental stimuli such as visual, auditory, and tactile cues. We suspect that these

stimuli contribute to daily IOP fluctuation in addition to time of day. Although mean IOP changes were diurnal, IOP deviation from the mean was random over 24 hours and thus varied independent of mean changes. To further characterize IOP variability, data was separated into transient, sustained, and baseline IOP fluctuations. Transient fluctuations occurred more often than sustained fluctuations daily. However, they had a smaller contribution to the daily IOP-related mechanical energy expenditure on ocular tissues than sustained fluctuations since they were short lasting. Sustained IOP fluctuations were synchronous across simultaneously collecting rats, which provided further evidence that IOP is impacted by environmental stimuli.

#### 3.4.1 Relation to Prior Work

The results of this study add a new understanding of how IOP fluctuates moment-to-moment in the rodent model, which builds to the existing characterization of monkey IOP fluctuation. A previous study conducted in monkeys used a dual-band finite impulse response (FIR) filter to extract low and high frequency transient IOP fluctuations from the underlying baseline signal [83, 84]. Investigators used this filter to identify sources of IOP fluctuation as well as quantify the magnitude and frequency of transient fluctuations on the scale of milliseconds. The area under the IOP versus time curve was calculated to give the relative IOP-related mechanical energy the eye must withstand over time due to IOP transients. They found that transients contributed to 12% of the total IOP energy during waking hours, which was attributed to blinks and saccades. This is an important finding since IOP plays a large role in ocular biomechanics and is representative of the relative mechanical strain on ocular tissues. The method we used to identify and characterize fluctuations found in the IOP waveform differs from the one used in the monkeys since our telemetry system has a lower sampling rate than the commercial system they used. Thus, transient fluctuation statistics in the rat are not a reproduction of what has been previously reported

but tells a different part of the same story of how IOP fluctuates continuously and is affected by various internal and external processes. We also reported on sustained IOP fluctuations, which has yet to be discussed in previous literature. In addition to transient fluctuations, it is important to consider the impact of long-lasting IOP fluctuations on ocular tissues since glaucoma is heavily associated with sustained IOP elevation.

Rabbit and mice IOP telemetry studies show a distinct 24-h mean IOP change [10, 11, 78], with higher values during the dark phase, which is consistent with our results. These telemetry studies provide a detailed description of how mean IOP fluctuates over time compared to tonometry studies, however, they lack variability statistics of IOP on smaller time scales. It is important to consider faster IOP fluctuations in addition to slower mean changes because there are studies suggesting that repeated transient IOP elevation has just as much damage to the retina as sustained IOP elevation [85, 86]. It is thought that progressive damage following transient IOP elevation occurs due to temporary occlusion of blood flow to the retina. Although the induced transient IOP fluctuations of that study are significantly higher than typical fluctuations we see moment-to-moment in the rat, it is still important to consider that natural fluctuations occur over a lifetime and contribute to the constant mechanical stress on ocular tissues.

### 3.4.2 Limitations

There are two limitations of this study that are worth noting. The first limitation is that an extraocular pressure transducer is used to detect changes in IOP through a fluid-filled pressure line that starts in the eye and runs to the back. Although it was statistically insignificant, the cut tube experimental results revealed that there was some contribution of head and body rotation to the pressure fluctuations recorded from the eye. This issue could be solved in future device designs where the pressure sensor is mounted on the head instead of the back. It would also be beneficial

to eliminate the external fluid line completely and implant a pressure transducer directly in the anterior segment. This approach has been proven successful in the monkey IOP telemetry model [87]. Another limitation of this study is that animals were housed in a housing room where investigators and technicians frequented during work hours. The effect of visual and auditory cues on IOP variability were not specifically studied but most likely contributed to the transient and sustained IOP fluctuation results. To study IOP variability in the absence of environmental stimuli, animals would need to be housed in isolation. Since the results of this study are intended for translational evidence of IOP variability in humans, it would be beneficial to know the added mechanical stress on ocular tissues due to environmental stimuli that mirror presumably stressful scenarios in rats. It would also be beneficial to include other parameters in the telemetry system such as continuous body temperature and locomotor activity to determine if there are any modulatory effects of these physiological parameters.

### **3.5 Conclusion**

The principal findings of the study are that IOP fluctuates continuously on different time scales. IOP fluctuations are seen in both awake and anesthetized rats. IOP telemetry is required to detect and characterize IOP variability moment-to-moment without additional experimental bias. In addition to a diurnal mean change, IOP varies randomly throughout the day. These variations in IOP have been categorized as either transient or sustained fluctuations, which have differing properties. Transient IOP fluctuations are short lasting and tend to be unique to a given animal whereas sustained IOP fluctuations are long-lasting and can be correlated across simultaneously recording animals. This suggests that IOP variability is modulated not only by physiological processes, but also environmental stimuli.



## **Chapter 4: Effects of Ambient Lighting on Intraocular Pressure Variability in Rats**

### **4.1 Introduction**

Circadian rhythms are physiological processes that are intrinsic to a given animal and follow a near 24-hour cycle. The endogenous timing of all circadian rhythms is controlled by the master clock, a group of neurons comprising the suprachiasmatic nucleus (SCN). The SCN is part of the hypothalamus and is responsible for regulation of hormones that are necessary for maintaining homeostasis. There are also biological clocks located in tissues other than the SCN that assist in regulation of local circadian rhythms. Local clocks have been identified in various ocular tissues including the cornea [88, 89], iris-ciliary body complex [90, 91], and retina [92, 93]. Various internal and external factors contribute to the coordination of local clocks within a given tissue. Overall, the job of the master clock is to synchronize local clocks and disruption of this can lead to cognitive and behavioral issues [94].

Intraocular pressure (IOP) rhythmicity has been studied for decades in humans and various animal models. An endogenous IOP rhythm has been detected in a variety of small mammals including mice [95], rats [34, 77], rabbits [96, 97], and cats [76], as well as larger mammals including goats [98], pigs [99], and horses [100]. In these studies, animals were housed in constant darkness (DD) following initial entrainment to a normal 12-h light:12-h dark (LD) cycle. Results showed that the IOP rhythm previously detected in LD persisted in DD, concluding that IOP is controlled and regulated by a circadian clock. To completely understand the impact ambient lighting has on IOP rhythm, it is important to test the effects of various light cycles. There are at least 3 groups that have studied the effects of constant light (LL) on IOP rhythm, but results

conflict. Two groups reported a complete loss of IOP rhythm after a week of LL [11, 101], whereas the third group reported a dampened free-running IOP rhythm that persisted for a significantly longer time [77]. The re-entrainment of IOP rhythm to a shifted or reversed LD cycle has also been reported [11, 34, 101]. However, no studies have considered the effect of ambient lighting on IOP variability moment-to-moment and day-to-day since most employ tonometry to measure IOP.

Tonometry is the gold-standard for estimating IOP both clinically and experimentally. Unfortunately, this method provides only snap-shot measurements that are limited in information pertaining to IOP fluctuation. Tonometry is frequently performed in both awake and anesthetized subjects. However, the act of tonometry in awake subjects requires close contact and handling, which has been shown to evoke a stress response that leads to IOP elevation [37, 73]. To avoid this response, some perform tonometry under anesthesia, but many fail to maintain physiological body temperature. Without thermoregulation, there is a decrease in IOP [73]. To avoid confounding variables, we developed a novel telemetry system to record IOP round-the-clock in free-moving, conscious rats. In this study, we attempt to clarify existing results pertaining to effects of ambient light on IOP rhythmicity using this telemetry system. With extensive IOP information we also seek to determine if there are any effects of ambient lighting on IOP variability moment-to-moment.

## **4.2 Materials and Methods**

All experiments were conducted in accordance with the National Institutes of Health guide for the care and use of laboratory animals and compliance with a protocol approved by the Institutional Animal Care and Use Committee (IACUC) at the University of South Florida.

#### 4.2.1 Animal Preparation

In this study, a silicone microcannula (OD: 200um, ID: 100um, AS One International, Santa Clara, CA, USA) was implanted in the right anterior chamber of male retired-breeder Brown-Norway rats. This cannula was guided to a custom Delrin head-mount coupler connected to a pressure transducer worn as a backpack. The cannulation surgery and device specifications are explained in Section 2.3.1 and in previous publications [8, 73]. Data was sampled at 0.25 Hz and transmitted to a laptop where it was stored in real time. Animals were housed in a temperature-controlled room (22 °C) with food and water available ad libitum.

#### 4.2.2 Manipulation of Ambient Lighting

Light cycle experiments were conducted in an environmental control unit (ECU) (Tecniplast BIO-C36) to isolate the effects of ambient conditions and minimize other external stimuli that contribute to IOP variability. Animals were entrained to a normal LD cycle for a week before ambient light manipulation. IOP variability and rhythmicity were studied under the following conditions: reversed LD, DD, and LL (150 lux). LL was the last condition tested in each animal because extended periods of illumination are known to induce long-lasting physiological abnormalities [102, 103]. Additional experiments were conducted in anti-phasic 18-h light:6-h dark (18L:6D) and 6-h light:18-h dark (6L:18D) cycles to determine if the interval of ambient light alters IOP rhythmicity. Animals remained in the altered ambient condition for up to 2 weeks and were re-entrained to a normal LD cycle for at least a week before testing another condition.

#### 4.2.3 Data Analysis

Raw IOP records were processed using MATLAB software (The MathWorks, Natick, MA) with a combination of a running median and lowpass filter with a filtering window of 28s to remove spurious data. Statistical analyses were conducted in SigmaPlot software (Systat, San Jose,

CA), with significance assessed at  $\alpha$  of 0.05. Data collected in DD and LL were fit to a sinusoidal curve to assess changes in IOP rhythm amplitude, period, and phase with respect to LD entrainment. Data were also analyzed using a custom MATLAB algorithm to detect transient and sustained IOP fluctuations (Section 3.2.4). Analysis of transient and sustained IOP fluctuations previously characterized in LD conditions (Figure 3.4 & 3.5) were compared to those found in DD and LL. Results are expressed as mean  $\pm$  standard deviation and mean differences between groups were evaluated with paired t-tests unless otherwise noted.

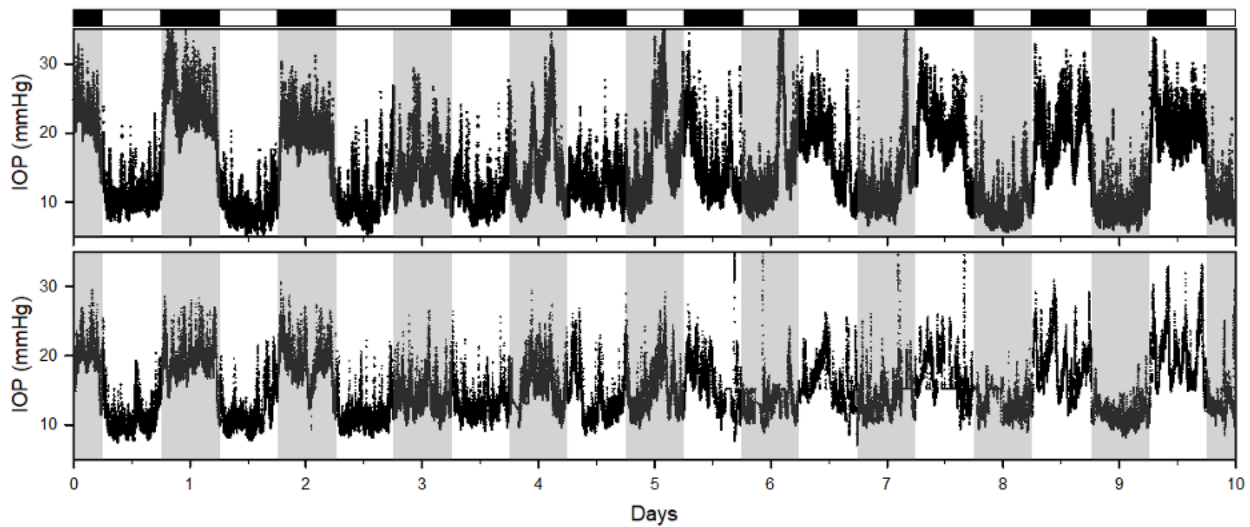


Figure 4.1: Effect of reversed light cycle on IOP rhythm. Plotted are two rats that were housed on the same shelf and recorded IOP simultaneously. There was a noticeable disruption in the IOP rhythm when lights were reversed. It took several days for the IOP rhythm to re-entrain to the shifted cycle.

### 4.3 Results

Rats entrained to a LD cycle experienced a diurnal IOP rhythm with higher values in the dark phase. LD data was fit to a sinusoid with a forced period of 24 hours which revealed an average diurnal amplitude change of  $8.6 \pm 3.5$  mmHg and phase of  $0.1 \pm 0.6$  hours ( $n = 15$ ). For all figures within this document, the bar across the top of the plot represents the ambient condition

within the ECU and the shaded regions within the graph represent the ambient condition outside of the ECU. Figure 4.1 provides data of two simultaneously recording rats that were both initially entrained to a LD cycle. LD reversal occurred between days 2 and 3 when lights were left on into the anticipated dark phase. Both animals experienced a noticeable disruption in the period, amplitude, and phase of the IOP rhythm. It wasn't until day 7 that diurnal IOP rhythm came back in phase with the new light cycle. On average, it took 3 to 5 days for IOP to resynchronize to the shifted cycle (n = 9).

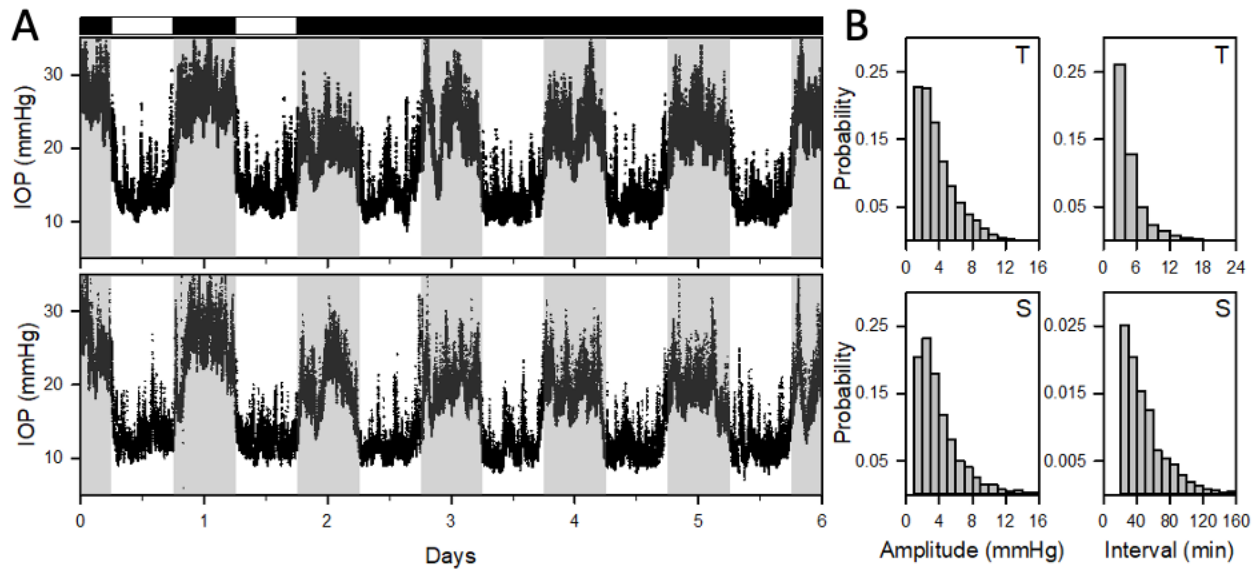


Figure 4.2: Effect of constant darkness on IOP rhythm. (A) IOP data of two simultaneously recording rats that were initially entrained to a LD cycle. After day 2, the IOP rhythm persisted when animals were subjected to DD. (B) Cumulative statistics for transient (T) and sustained (S) IOP fluctuations of rats housed in DD. Left, PDFs of T and S fluctuation amplitude in DD. Right, PDFs of T and S interval in DD.

Rat IOP rhythm was also assessed in DD. Figure 4.2A shows IOP data of two simultaneously collecting rats, both of which exhibited a diurnal IOP rhythm that persisted in DD. This suggests that in the absence of a regulated light cycle, IOP rhythm is reinforced by a circadian clock. Sinusoid fitting of DD IOP data produced an average free-running period of  $24.1 \pm 0.2$

hours, amplitude of  $12.2 \pm 3.8$  mmHg, and phase of  $1.2 \pm 4.2$  hours ( $n = 10$ ). The free-running DD period was not significantly different from the 24-h period enforced by the LD cycle ( $p = 0.443$ ). The peak-to-trough amplitude change of IOP rhythm from LD to DD increased by  $3.6 \pm 1.5$  mmHg in 7 animals and decreased by  $3.1 \pm 1.3$  mmHg in 3 animals. IOP fluctuation statistics of DD data

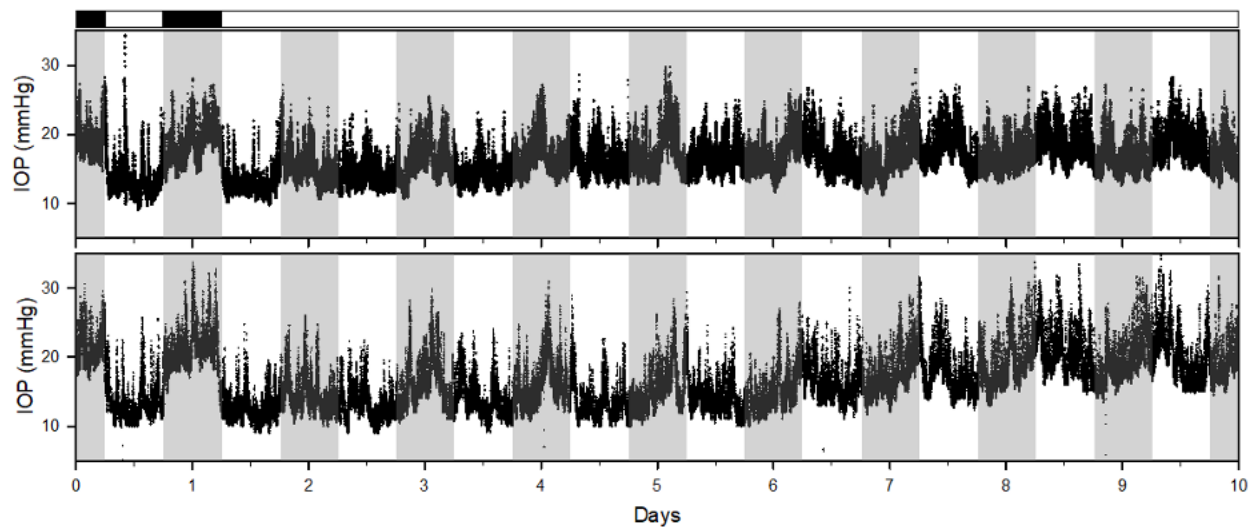


Figure 4.3: Effect of constant light on IOP rhythm. Plotted are two simultaneously recording rats that were initially entrained to a LD cycle. There was an immediate change in IOP rhythm after day 1 when rats were subjected to LL. There was a noticeable decrease in amplitude change from subjective light phase to subjective dark phase as well as a change in periodicity. After about a week in LL, there was an upwards drift in mean IOP.

were also compared to those of LD data (Section 3.3). There were on average  $289 \pm 46$  DD transient events daily which was not significantly different from the number of daily LD transient events ( $p = 0.055$ ). Sustained events were, however, significantly more prevalent in DD than LD with  $28 \pm 2$  sustained events occurring daily ( $p < 0.001$ ). The amplitude and interval of DD transient and sustained IOP fluctuations were expressed as probability density functions (PDFs) (Figure 4.2B). About 75% of daily DD transient IOP fluctuations were  $\leq 4$  mmHg and occurred 2 - 4 min apart (Figure 4.2B, top). Transient events in DD were significantly larger in amplitude and occurred significantly closer together than in LD ( $p = 0.001$  and  $p < 0.001$ , respectively). About

75% of daily DD sustained IOP fluctuations were  $\leq 4$  mmHg and occurred 20 - 50 min apart (Figure 4.2B, bottom). Sustained events in DD were significantly smaller in amplitude but occurred on similar intervals in LD ( $p < 0.001$  &  $p = 0.187$ , respectively).

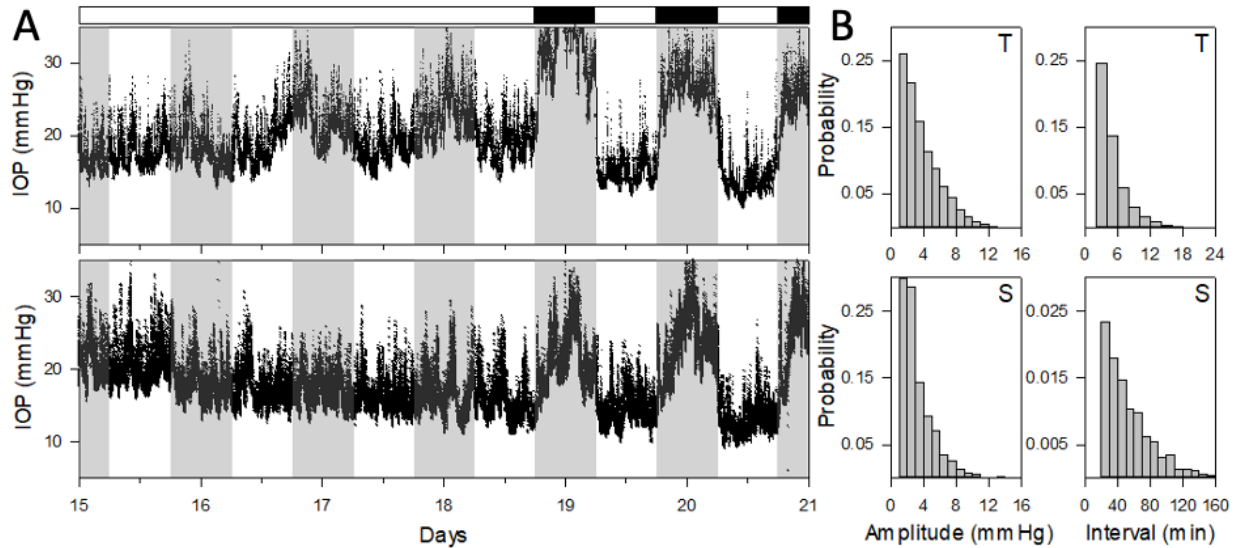


Figure 4.4: Inter-animal variability of constant light effects on IOP rhythm. (A) Plotted is data of a later time from the same two rats shown previously in Figure 4.3. Notice that IOP rhythm of one rat persisted for the full two weeks in LL (top), while the rhythm of the other rat was abolished (bottom). Also, the peak-to-trough amplitude of the IOP rhythm was drastically larger following re-entrainment to a LD cycle. (B) Cumulative statistics for transient (T) and sustained (S) IOP fluctuations of rats housed in LL. Left, PDFs for amplitude of T (top) and S (bottom) events. Right, PDFs for interval of T (top) and S (bottom) events.

The effect of LL conditions on IOP were also assessed. Figure 4.3 shows data of two simultaneously recording rats that were initially entrained to a LD cycle. After day 1, the lights were left on in the ECU for an extended period. The IOP rhythm initially persisted, but there was an immediate decrease in peak-to-trough amplitude when the light remained on during the anticipated dark phase. On average, animals experienced a  $3.9 \pm 2.6$  mmHg decrease in peak-to-trough amplitude with the onset of LL ( $n = 8$ ). It was also noted that the attenuated LL IOP rhythm was shifting out of phase with the light cycle of the outside environment. Sinusoid fitting the first week of LL data produced an average free-running LL period of  $25.0 \pm 0.5$  hours, amplitude of

$4.6 \pm 1.4$  mmHg, and phase of  $2.6 \pm 3.5$  hours ( $n = 8$ ). The free-running LL period was significantly longer than 24 hours, which led to the time shift seen from day to day. On average, mean IOP rose  $4.3 \pm 1.9$  mmHg linearly after the first week of LL ( $n = 8$ ).

Unlike in DD, the circadian IOP rhythm was lost in 5 out of 8 animals within 2 weeks of LL. It is unknown whether the 3 other animals would have lost their IOP rhythm if they were left in LL for longer. Figure 4.4A shows data of a later time from the same two rats shown in Figure 4.3. The animal in the top plot retained its IOP rhythm for the full experiment, whereas the animal in the bottom plot lost its IOP rhythm completely. Upon re-entrainment to a normal LD cycle, the IOP rhythm came back instantaneously with a peak-to-trough amplitude greater than or comparable to that of LD data prior to LL onset. On average, the LD amplitude increased by  $6.2 \pm 3.2$  mmHg in 6 animals coming out of LL but was the same as the previous LD amplitude in 2 animals.

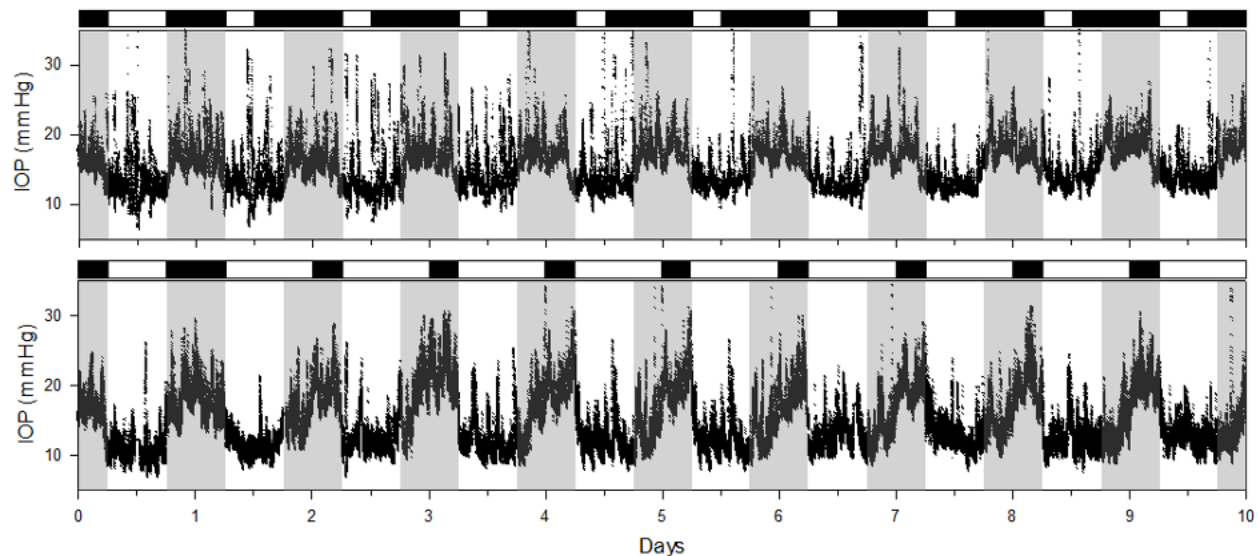


Figure 4.5: Effect of anti-phasic lighting conditions on IOP rhythm. Plotted are two separate experiments conducted in different rats. There were no obvious changes in IOP rhythm of the rat subjected to a 6L:18D cycle (top). However, IOP rhythm of the rat subjected to a 18L:6D cycle was modulated to match the periodicity of the light cycle (bottom).



IOP fluctuation statistics of LL data were also compared to those of LD data (Section 3.3). There were on average  $293 \pm 27$  LL transient events daily which was not significantly different from the number of LD transient events daily ( $p = 0.114$ ). Sustained events were, however, significantly more prevalent in LL than LD with  $27 \pm 3$  sustained events occurring daily ( $p < 0.001$ ). There was no significant difference in the number of transient and sustained events occurring in DD versus LL ( $p = 0.828$  and  $0.199$ , respectively). The amplitude and interval of LL transient and sustained IOP fluctuations were expressed as PDFs (Figure 4.4B). About 75% of daily LL transient IOP fluctuations were  $\leq 4$  mmHg and occurred 2 - 4 min apart (Figure 4.4B, top). Transient events in LL were significantly smaller in amplitude and interval than in LD ( $p = 0.05$  and  $p < 0.001$ , respectively). About 75% of daily LL sustained IOP fluctuations were  $\leq 3$  mmHg and occurred 20 - 50 min apart (Figure 4.4B, bottom). Sustained events in LL were

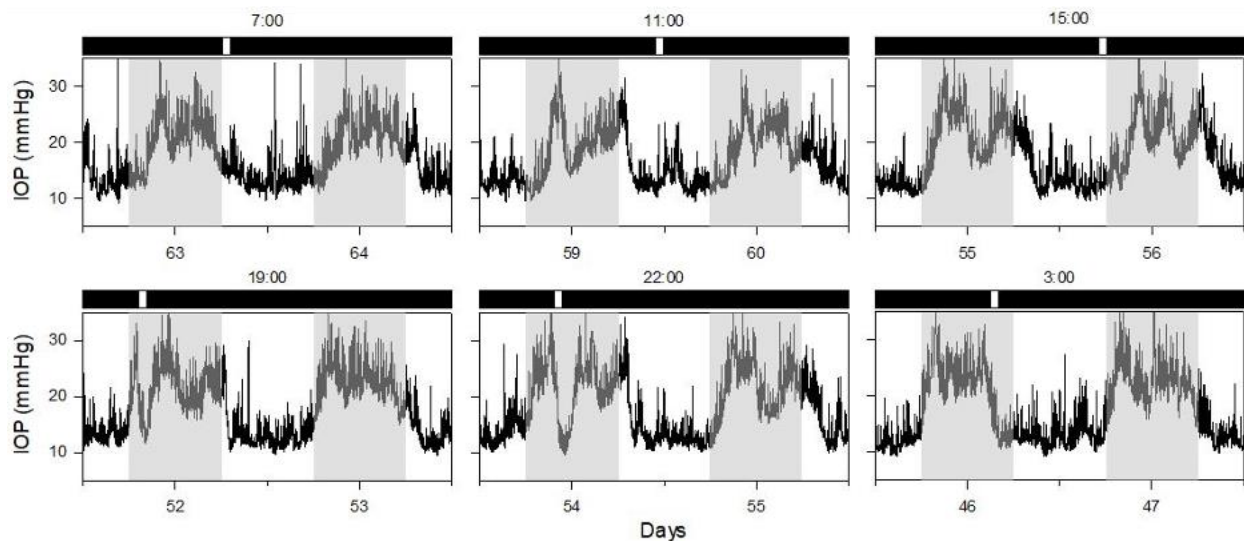


Figure 4.6: IOP phase response to a single light pulse. Light pulses administered during the subjective light phase of the free-running DD IOP rhythm produced no obvious phase change in the IOP rhythm (top). There were, however, noticeable phase shifts in the IOP rhythm following light pulses administered during the subjective dark phase (bottom). When lights were turned on during the subjective dark phase, IOP fell to light-phase levels.

significantly smaller in amplitude and significantly larger in interval than those found in LD ( $p < 0.001$  and  $p < 0.001$ , respectively). Comparison of DD and LL IOP fluctuation statistics revealed that the amplitudes of transient and sustained events were significantly greater in DD than in LL ( $p < 0.001$  and  $p < 0.001$ , respectively). Conversely, the intervals of transient and sustained fluctuations were significantly longer in LL than in DD ( $p < 0.001$  and  $p = 0.009$ , respectively).

Results of LL exposure were indicative that the duration of light has a significant effect on IOP fluctuation. Two additional experiments were conducted to determine the effects of anti-phasic light cycles on IOP rhythm. Figure 4.5 shows IOP data of two different animals from two separate experiments. These experiments tested the effects of both a shortened (6L:18D, top) and extended (18L:6D, bottom) light phase. There were no changes in IOP rhythmicity when the light phase was shortened ( $n = 2$ ). However, IOP rhythm was greatly affected when the light phase was extended ( $n = 4$ ). After 5 - 6 days of 18L:6D, there was a noticeable shortening of the dark-phase elevated IOP interval. In a separate set of experiments, animals were entrained to DD conditions for several days before 1-hour light pulses were administered at different times during an animals' circadian rhythm (Figure 4.6). Light pulses given during an animals' subjective light phase had no effect on IOP rhythm ( $n = 2$ ). Light pulses given during an animals' subjective dark phase produced an instantaneous decrease in IOP to light-phase values ( $n = 2$ ). In experiments where light pulses were administered at 19:00 and 3:00, there were noticeable phase advancements in the IOP rhythm of the following day. Conversely, phase delays were seen in experiments where light pulses were given at 22:00. Results suggest that the IOP rhythm can shift forward or backward by varying amounts depending on the onset time of the 1-hour light pulse with respect to an animal's subjective dark phase.

## 4.4 Discussion

Results of this study suggest that IOP was greatly affected by changes in ambient lighting. As shown previously, rats housed in a normal LD cycle experienced a diurnal IOP rhythm with higher values in the dark phase when rats are presumably more active. IOP rhythm was temporarily abolished during light cycle reversal and completely abolished in about 60% of rats housed in LL. The free-running period, amplitude, and phase of the IOP rhythm differed in rats housed in DD versus LL as well as those housed in LD. We also saw that transient and sustained IOP fluctuation statistics differed in rats housed in DD and LL when compared to those found in LD. Although, it is possible that differences may partially stem from inter-animal variability, lighting conditions are important to consider when conducting studies in which IOP measurement is pertinent. It was found that rat IOP rhythm was more sensitive to extended periods of light rather than extended periods of dark. This observation may be attributed to the rat being a nocturnal animal. Further experimentation should be performed to see whether this result holds true for diurnal animals.

### 4.4.1 Relation to Prior Work

Upon reversal of the LD cycle, the IOP rhythm was desynchronized, but returned after 3 to 5 days. A similar result was seen in a rabbit IOP telemetry study where the LD cycle was advanced by 6 hours and it took upwards of 10 to 14 days for the IOP rhythm to resynchronize with the shifted light cycle [11]. This effect on IOP rhythm is analogous to jet lag, where an individuals' internal clock is out of sync with external time. Jet lag usually occurs following extensive travel to different time zones when the internal clock differs from the external clock. This phenomenon may be explained by disruption of melatonin production, which is pertinent for the sleep/wake cycle. A related study showed that when the LD cycle was shifted by 12 hours, it took 5 to 7 days for melatonin levels in rats to re-entrain to the new cycle [104].

Transient and sustained IOP fluctuations in animals housed in constant lighting conditions were compared to statistics of animals housed in LD (Section 3.3). Significantly more sustained IOP events were found in animals isolated in DD and LL conditions than those that were kept in the housing room under LD conditions. This was a rather interesting outcome, since we previously found that sustained events were significantly correlated in simultaneously recording rats and were most likely due to environmental stimuli (Section 3.3, Figure 3.8). Results here suggest that although animals were isolated from other environmental stimuli, psychological stress evoked by constant lighting may contribute to IOP variability. Animals housed in DD also experienced much larger circadian fluctuations than those in LL. Although inter-animal variability may contribute to differences between test groups, long-lasting IOP events seem to be activated by involuntary physiological processes. It is therefore possible that these processes are affected by constant lighting conditions as well as physical isolation. Further investigation of IOP variability in isolated animals housed under LD conditions is necessary. A study in rats found that adrenomedullin (ADM), a hormone responsible for regulation and protection of the hypothalamo-pituitary-adrenal (HPA) axis, was upregulated in both DD and LL conditions [105]. The HPA axis is a major component of the autonomic nervous system, which is responsible for regulation of involuntary physiological processes such as respiration, blood pressure, and heart rate [106]. It is unknown if regulation of ADM is related to IOP fluctuation, however, it is possible that spontaneous IOP fluctuations [73] are directly or indirectly affected by the autonomic nervous system, which is light cycle dependent. It is also known that ocular blood flow is controlled directly by the autonomic system [68] and increased blood pressure is correlated with increased IOP [107]. This phenomenon may also explain the steady rise in mean IOP of rats housed in LL conditions, which is presumably more stressful than DD for nocturnal animals.

The effect of constant lighting conditions on the neural and behavioral systems have been studied for decades. The circadian behavior of animals housed in DD and LL can be explained by Aschoff's Rules of photoperiod sensitivity, which were developed to characterize free-running periods of physiological processes in both diurnal and nocturnal animals [108]. In this study, we found that the free-running period of rat IOP rhythm was longer in LL than DD. This is supported by Aschoff's first rule which states that the endogenous circadian period is extended in LL for nocturnal animals and extended in DD for diurnal animals [108]. Aschoff's second rule states that light intensity plays a crucial role on the severity of the effect constant conditions have on endogenous rhythms. We found that transient IOP fluctuations that occur both spontaneously as well as in response to environmental stimuli were significantly smaller in LL, but larger in DD when compared to those detected in LD conditions [73]. Similarly, Aschoff found that daily activity decreases with increasing light intensity in nocturnal animals [108]. Rats in LL also experienced a dampened circadian IOP rhythm and most animals in DD experienced an amplified rhythm. A similar study found that rats housed in continuous dim light (40-90 lux) experienced dampened IOP and body temperature rhythms that persisted for up to 7 weeks [77]. In our study, the circadian IOP rhythm was abolished in about 60% of animals housed in significantly higher light intensity (150 lux) for up to 2 weeks. A different study that collected rat IOP twice a day via tonometry at set external times and averaged across animal data reported a complete loss of the endogenous IOP rhythm in both DD and LL [101]. However, each animal has a unique endogenous rhythm that shifts with time and averaging across animals that are most likely out-of-phase with one another could mask the underlying circadian rhythm. Also, an IOP record consisting of 2 data points per day does not provide sufficient information about circadian IOP rhythm. IOP telemetry provides extensive information on IOP variability moment-to-moment and day-to-day and results

indicate that IOP rhythm of rats housed in DD persists with a period close to 24 hours. Aschoff's third rule states that nocturnal animals experience a free-running DD period that is less than 24 hours [108], which conflicts with our results. However, circadian rhythm studies of locomotor activity in mice and hamsters, suggest that it could take weeks or months for the free-running rhythm to be attained [109]. It remains unknown whether circadian IOP fluctuations are controlled by the master clock located within the SCN or by local clocks in the eye. To determine this, it is necessary to conduct experiments in which tetrodotoxin (TTX), a neurotoxin that inhibits sodium ion-gated channels, is applied on the optic nerve to block communication of local clocks with the master clock in the SCN. Rhythm persisting after TTX application would indicate that a local clock exists in the eye that controls IOP circadian fluctuations.

Additionally, we tested the effect of modulating the photoperiod length (light phase) a rat receives daily. We found that a short photoperiod (6L:18D) had no significant effect on the IOP rhythm, however a longer photoperiod (18L:6D) did. Similar experiments were conducted on circadian rhythm of locomotor activity in mice and sparrows [109-111]. It was found that both species experienced a shorter circadian after entrainment to a light cycle with a longer photoperiod. This supports and confirms results in the rat where dark phase IOP is significantly shortened when animals are entrained to a longer photoperiod compared to a shorter photoperiod. We also studied the phase response of the IOP rhythm to a single 1-hour light pulse administered at different times during an animals intrinsic free-running DD clock. We found that a 1-hour light pulse given during the animals' subjective dark phase induced a phase shift in the circadian IOP rhythm. The amount by which the rhythm shifted depended on how far into the subjective dark phase the rat was when the pulse was administered. A similar result was seen in the hamster and finch when the circadian rhythm of locomotor activity was reset following a brief light flash [112]. In the rat, we also found

that a single light pulse given during the animals' respective dark phase temporarily lowered IOP to light-phase values. This result is significant since there is increasing evidence that glaucoma may be linked to a dark-phase elevation in IOP [113].

#### 4.4.2 Limitations

There are two limitations worth mentioning for this study. The first limitation is that constant white noise was not provided for animals housed in constant ambient conditions. Constant white noise would have prevented any unanticipated entrainment of animals to external auditory cues, which could impact circadian IOP rhythms. However, it was noted during experimentation that the ECUs that animals were housed in made a low humming noise that may act as white noise. We are not certain whether louder noises within the vivarium were masked by this constant hum. Another limitation of this study pertains to the sinusoid fitting of IOP data. The sinusoid-fitting algorithm spits out an average amplitude, phase, and period of each waveform, therefore, any spontaneous or random changes in the IOP rhythm could be masked by this analysis. However, performing the sinusoid fitting on too small of a data segment could result in a weak fit and including more data can increase the accuracy of the model.

#### 4.5 Conclusion

The principal findings of the study are that IOP rhythm and variability are affected by ambient lighting conditions. The periodicity of IOP rhythm was dramatically impacted by extended durations of high intensity light. The period of rats in LL was significantly longer than those in DD. IOP rhythm also shifted in response to light exposure while in DD conditions. IOP variability also differed under constant ambient conditions compared to normal LD. The results of this study suggest that IOP fluctuation patterns are partially dependent on the intensity and duration of ambient light. Therefore, it is important for clinicians to consider work schedule and

geographical location of patients with abnormal IOP and circadian patterns. It is also beneficial for researchers to consider light conditions when monitoring IOP in longitudinal experiments such as testing therapeutic medications or studying behavioral responses.



## **Chapter 5: A Wearable Device for Continuous Monitoring of Intraocular Pressure, Body Temperature, and Locomotor Activity in Conscious Rats**

### **5.1 Introduction**

Intraocular pressure (IOP) is the only treatable risk factor for glaucoma and has been studied extensively using tonometry. Tonometry is a technique that is used both clinically and experimentally to non-invasively measure IOP. There have been various forms of tonometry over the years including applanation, rebound, and non-contact air puff tonometry. Although studies have shown that tonometry provides an adequate estimation of long-term mean changes [114] [115], it is not fully capable of capturing IOP fluctuations on shorter timescales. With advancement in medical technology, telemetry is now commonly used to continuously record biological signals from patients or subjects with minimal intervention. There are few investigators that have used telemetry as a tool for experimentally recording IOP in mice [78], rats [8], rabbits [11], and monkeys [9]. Clinically, telemetry has been used to indirectly monitor IOP in humans for extended durations using changes in corneal curvature [13, 81]. In all scenarios, IOP telemetry has allowed for detection of IOP fluctuation moment-to-moment and has thus become a key tool for characterizing IOP variability. It has been used to identify and quantify both transient and sustained IOP fluctuations that exist daily (Section 3.3) and study the impact various internal and external factors have on IOP variability and rhythmicity (Sections 2.4 & 4.3) [73, 83].

In previous studies, we used a novel telemetry system for continuous recording of IOP in conscious, freely moving rats. However, it has been shown that rat IOP is affected by various factors including but not limited to stress, anesthesia, and temperature [73]. To further characterize

the extent that IOP is modulated by internal and external processes, we have modified our existing wearable telemetry system to continuously monitor other physiological parameters in addition to IOP. It now includes the ability to simultaneously monitoring body temperature (BT) and locomotor activity (LMA). This improved rat telemetry system will provide more information on the mechanisms leading to IOP variation as well as the impacts they have on the retina and overall health of the eye.

## 5.2 Material and Methods

All experiments were conducted in accordance with the National Institutes of Health guide for the care and use of laboratory animals and compliance with a protocol approved by the Institutional Animal Care and Use Committee (IACUC) at the University of South Florida.

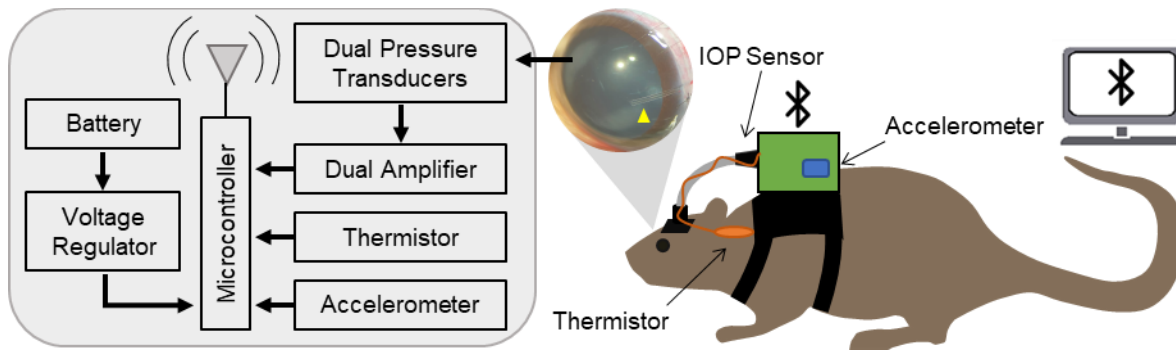


Figure 5.1: Telemetry system design and experimental setup. The device diagram on the left shows a breakdown of components included in the new telemetry system and how they send and receive data. On the right is a cartoon showing how the system is used on the rat and where the components are implanted.

### 5.2.1 System Design and Data Acquisition

The new and improved IOP telemetry system (Figure 5.1) required fabrication of a custom printed circuit board (PCB). The board was designed using EAGLE software (Autodesk, San Rafael, CA) and printed using OSH Park PCB (Portland, OR) services. The microcontroller was updated to the Simblee, which is equipped with a 32-bit ARM Cortex-M0 processor and

communicates Simblee-to-Simblee via Bluetooth (RFD77101, RF Digital Corporation, ams AG). Arduino Integrated Development Environment (IDE) Software along with the Simblee BSP (board support package) and Simblee Library were used to interface with the microcontroller. The device is powered by a rechargeable 3.7 V, 500 mAh lithium-ion polymer battery (ASR00035, TinyCircuits™, Akron, OH). The Simblee requires an operational 3.3 V power supply, which is set by an ultra-low noise, low drop out (LDO) voltage regulator (NCP167, ON Semiconductor®, Phoenix, AZ).

Two analog output piezoresistive pressure transducers with silicone-gel coated membranes (TBP Series, Honeywell, Morristown, NJ) were included for dual pressure monitoring. These sensors are temperature compensated and produce a measure of pressure resulting from a change in membrane resistance due to mechanical stretch [116]. A dual operational amplifier (op-amp) (AD8606, Analog Devices Inc., Norwood, MA) was used to convert the two analog pressure outputs to information usable by the Simblee. An implantable, epoxy coated negative temperature coefficient (NTC) thermistor (KC Series, Littelfuse®, Chicago, IL) was included to monitor BT. NTC thermistors are temperature dependent variable semiconductors that increase in resistance when temperature decreases. This happens because as the semiconductor material heats up, more thermal energy is available for electrons to absorb [117]. Sufficient energy allows electrons to easily cross the energy bandgap between the valence band and the conduction band, which increases flow or conduction of electrons in the material. The implantable thermistor was connected to the PCB with flexible, silicone-coated braided wires. Silicone coated wires were used instead of PVC coated wires, because they have a much higher resistance to thermal change, superior flexibility, and are more biocompatible [118].

The new telemetry system also includes a 3-axis MEMS (micro-electromechanical system) accelerometer (ICM-42605, TDK InvenSense, San Jose, CA) to monitor LMA. Acceleration along a particular axis is detected by displacement of a known mass connected to a spring located within the component. The accelerometer has on-chip Analog-to-Digital Converters (ADCs) that convert the voltage output to digital information used by the Simblee. The Simblee interfaces with the accelerometer using I<sup>2</sup>C communication, which is typical for communication between a master and slave devices. All electronic components, excluding the implantable thermistor, were housed in a sealed 3D-printed plastic box with dimensions of 1.5 x 1.0 x 0.5 inches in length, width, and height respectively.

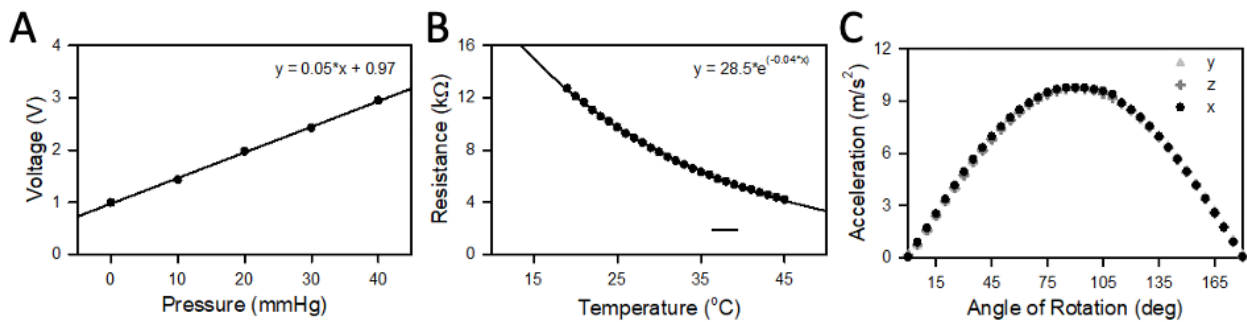


Figure 5.2: Calibration of telemetry system. (A) Linear regression of pressure transducer output voltage with varying gauge pressure to determine operational parameters. (B) Calibration curve for change in thermistor resistance due to varying temperature of a water bath. The curve was fit with an exponential decay to determine operational parameters. (C) Confirmation of accelerometer manufacturing calibration by rotating the device about each of the 3 axes.

### 5.2.2 Benchtop Testing of System

The pressure transducers were calibrated against a mercury manometer in a stepwise fashion from 0 to 40 mmHg above atmospheric pressure. The calibration curve for a given pressure transducer is shown in Figure 5.2A. Transducers had a positive linear response to the stepwise elevation in gauge pressure. Operational gain and offset parameters were found from a linear

regression of pressure calibration data. Thermistors were calibrated against a mercury thermometer placed in a water bath that was varied from 23 to 45 °C. Figure 5.2B shows an example calibration curve for a given thermistor. The calibration temperature range included rat physiological core temperature which varies from 37 to 39 °C in mammals [119]. These thermistors have a negative non-linear response to a stepwise increase in temperature, so data was fit with a decaying exponential to determine the operational parameters. The 3-axis MEMS accelerometer sensor was surface mounted on the PCB and was pre-calibrated by the manufacturer so when placed on a flat surface, the x- and y-axes read 0 g and the z-axis read +1 g or 9.81 m/s<sup>2</sup>. Accelerometer calibration was confirmed by incrementally rotating the system about each axis (Figure 5.2C). At a sampling rate of 0.25 Hz, the battery life of the telemetry system was approximately 10 days on a single rechargeable 3.7 V, 500 mAh lithium-ion battery.

### 5.2.3 Animal Preparation

Male retired-breeder Brown-Norway rats (300-400 g) were housed in a temperature-controlled room (22 °C) under a 12-h light:12-h dark (LD) cycle with food and water available ad libitum. The anterior chamber of the right eye was implanted with a silicone microcannula (OD: 200µm, ID: 100µm, AS One International, Santa Clara, CA, USA) connected to one of the two pressure transducers located in the backpack via a 16G silicon tube covered with a spring to prevent kinking (Figure 5.1). Surgical procedures for anterior segment cannulation were detailed in previous publications as well as in Section 2.3.1 [8, 73]. In short, the cannula was inserted in the anterior segment through a trans-limbal hole made by a 33G needle. The cannula was secured to the sclera with sutures and guided subcutaneously from the eye to a head-mounted coupler secured to the skull with 4 bone screws. The pressure line was filled with a balanced salt solution, 3 mM moxifloxacin hydrochloride (Vigamox®, Alcon, Fort Worth, TX), 1.3 mM enoxaparin sodium

(Lovenox®, Henry Schein, Melville, NY) and 2.2 mM triamcinolone acetonide (Triessence®, Alcon, Fort Worth, TX) to prevent microbial and fibrin buildup that can clog the cannula over time. A new surgical protocol was developed to implant the thermistor for continuous BT monitoring. The thermistor was inserted into a subcutaneous pocket on the mid-posterior neck created by blunt dissection. The thermistor was sutured to the surrounding tissue to reduce flexion of wires inside the body (Figure 5.1). Changes in acceleration along each of the 3 axes were detected by the board-mounted MEMS device located within the rat backpack (Figure 5.1). LMA was defined as the combined magnitude calculation of the acceleration along all the axes. Data was sampled at 0.25 Hz or every 4 secs in conscious, freely moving rats for weeks to months. Each sampled data point was an average of 20 consecutive measurements over a 4 sec duration.

#### 5.2.4 Data Analysis

Raw IOP, BT, and LMA data were processed in MATLAB software (The MathWorks, Natick, MA) using a median and lowpass filter with a filtering window of 28s to remove spurious data points and smooth each record. Cross-correlation analysis was performed in an hourly fashion to assess the coherence between IOP, BT, and LMA fluctuations. Temporal relationships were also evaluated using transient and sustained IOP event times to trigger a running average of BT and LMA records with a window of  $\pm 1$  hour about the event peak. The MATLAB algorithm used to detect transient and sustained IOP events was explained previously in Section 3.2.4. Statistical analyses were conducted in SigmaPlot software (Systat, San Jose, CA), with significance assessed at  $\alpha$  of 0.05 and results are expressed as mean  $\pm$  standard deviation. Mean differences between groups were evaluated with paired t-tests unless otherwise noted.

### 5.3 Results

The results of this study consider data from 14 rats. The upgraded telemetry system was used to simultaneously collect IOP and BT in all rats. A diurnal IOP rhythm was detected in all 14 rats, while only 8 exhibited diurnal BT rhythm. LMA was also simultaneously collected in 3 of the 14 rats, none of which exhibited diurnal LMA rhythm. Figure 5.3A shows IOP and BT data that were simultaneously recorded from a rat housed in LD conditions. This animal exhibited both diurnal IOP and BT fluctuations with higher values in the dark phase. Figure 5.3B shows IOP, BT, and LMA data that were simultaneously collected from a different rat housed in LD conditions. This rat exhibited a diurnal IOP rhythm, but diurnal BT and LMA rhythms were not detected. This result suggests that some animals experience changes in mean BT and LMA that are independent from diurnal mean IOP changes, which have shown to be driven by ambient lighting. However, there are fast and slow IOP fluctuations that seem to be correlated with changes in BT and LMA that last minutes to hours.

Cross-correlation analysis was performed on 7 days of data for each animal to determine the coherence between IOP, BT, and LMA fluctuations. A running window of  $\pm 1$  hour was used to insure inclusion of both short- and long-lasting fluctuations. The left panel of Figure 5.4A shows a 2-day snippet of data collected from a given animal housed in LD conditions and the boxed 2-hour region of this plot is shown zoomed in on the right panel. The zoomed in section shows a noticeable correlation between IOP, BT, and LMA with slight lag between event onsets, marked by the vertical line. Cross-correlation statistics across animals revealed that BT lagged IOP by 38 sec ( $n = 14$ ) and LMA by 2 min ( $n = 3$ ), while IOP lagged LMA by 4 sec ( $n = 3$ ). Figure 5.4B provides exemplary correlation waveforms for 2 different rats. Both rats have similar IOP vs BT and BT vs LMA cross-correlation waveforms. This suggests that BT changes were more likely to

occur when both IOP and LMA changed. The IOP vs LMA waveforms on the other hand, were quite different. The animal on the left, j118, had a stronger, more pronounced correlation between IOP and LMA than the animal on the right, j117. The difference in the cross-correlation waveforms for IOP vs LMA across animals suggests that IOP and BT changes can also occur during periods of inactivity and activity level is variable between rats.

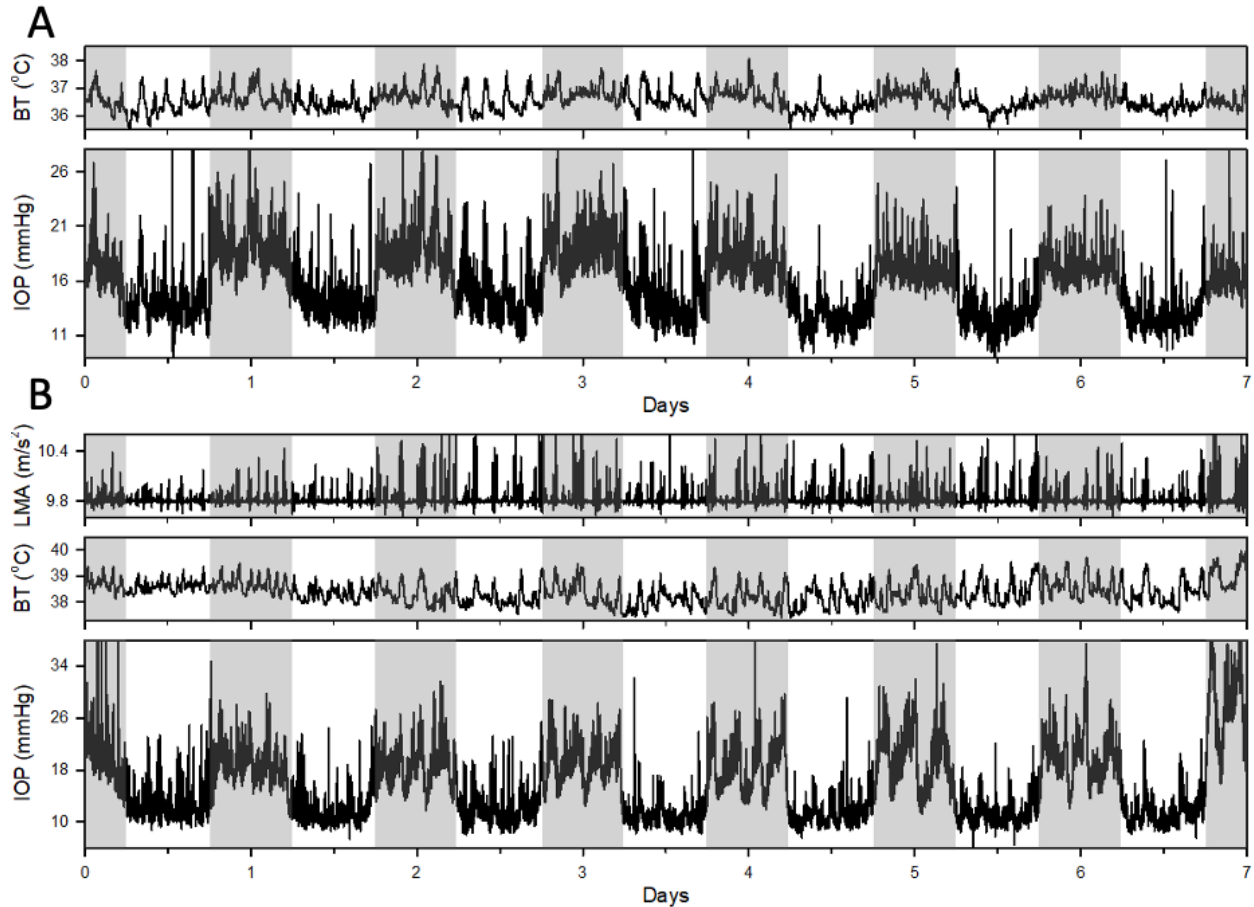


Figure 5.3: Continuous recording of IOP, BT, and LMA. Plotted are data from two rats that were not simultaneously recording. (A) Shown is data of a rat that experienced diurnal fluctuations in both IOP and BT. Mean IOP and BT were higher during the dark phase than in the light phase. (B) Shown is data of a rat that experienced diurnal IOP fluctuations but no diurnal changes in BT or LMA. Changes in mean BT and LMA were independent of changes in mean IOP and ambient light. However, there were fast and slow IOP fluctuations that seemed to be correlated with BT fluctuations and bursts in LMA.



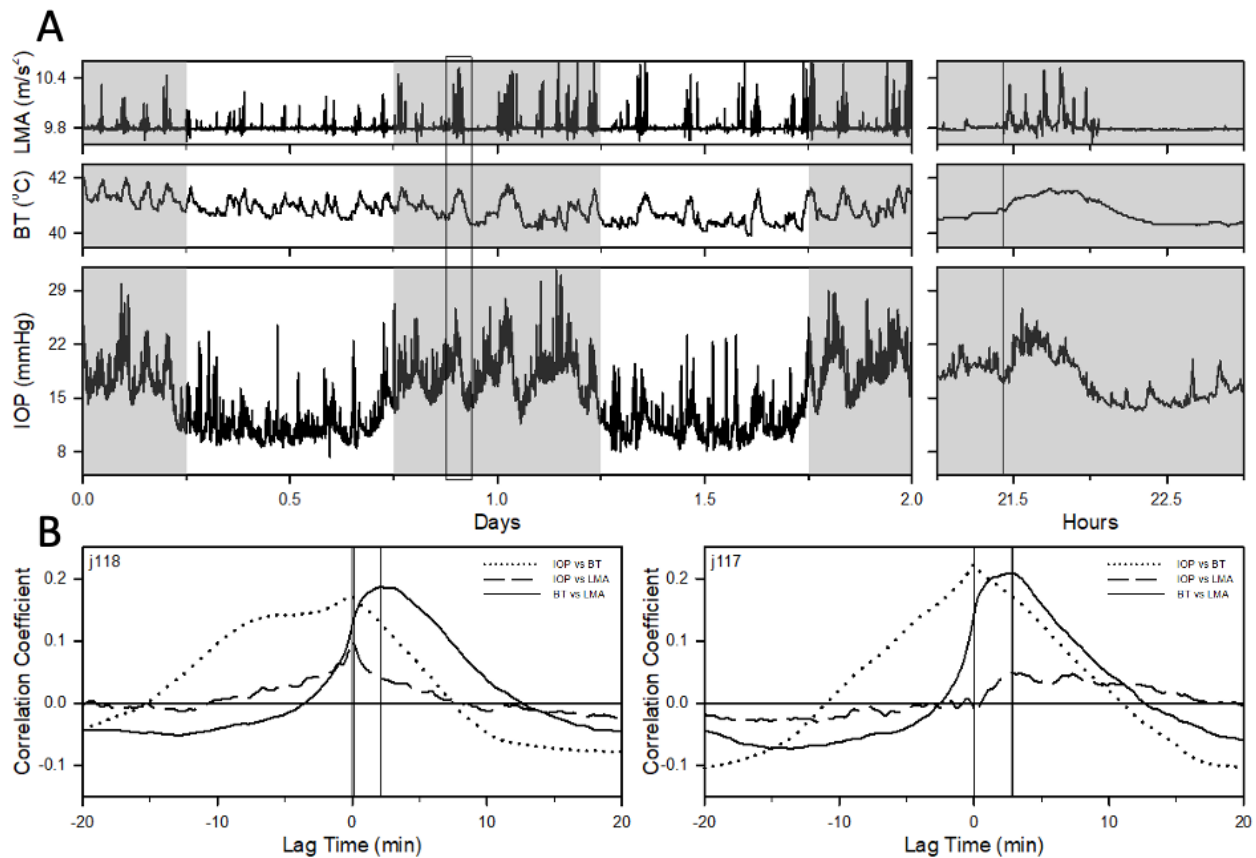


Figure 5.4: Cross-correlations of IOP, BT, and LMA data. (A) Left, plot showing a 2-day record of raw IOP, BT, and LMA data with a box marking the zoomed in 2-hour record plotted on the right. There was noticeable coherence between IOP, BT, and LMA data. (B) Representative correlograms from two different rats, both showing strong correlation of IOP vs BT and BT vs LMA. However, the correlation of IOP vs LMA differs between animals.

To determine the temporal relationship between IOP, BT, and LMA fluctuations, the peak times of transient and sustained IOP events were used to trigger averaging of BT and LMA records. The bottom plot of Figure 5.5A shows an example of how transient (grey) and sustained (red) IOP events were detected and peeled away from underlying mean changes (green). Also plotted are simultaneous records of BT (middle) and LMA (top). The boxed areas mark changes in BT and LMA that occur with transient and sustained IOP fluctuation. An example of transient and sustained IOP event triggered averaging for a given animal is shown in Figure 5.5B (left and right,

respectively). This example suggests that BT rises after transient and sustained IOP fluctuations peak. It also suggests that bursts in LMA led to near instantaneous transient IOP fluctuations. There was, however, a slight delay in LMA following peak sustained IOP fluctuations. When

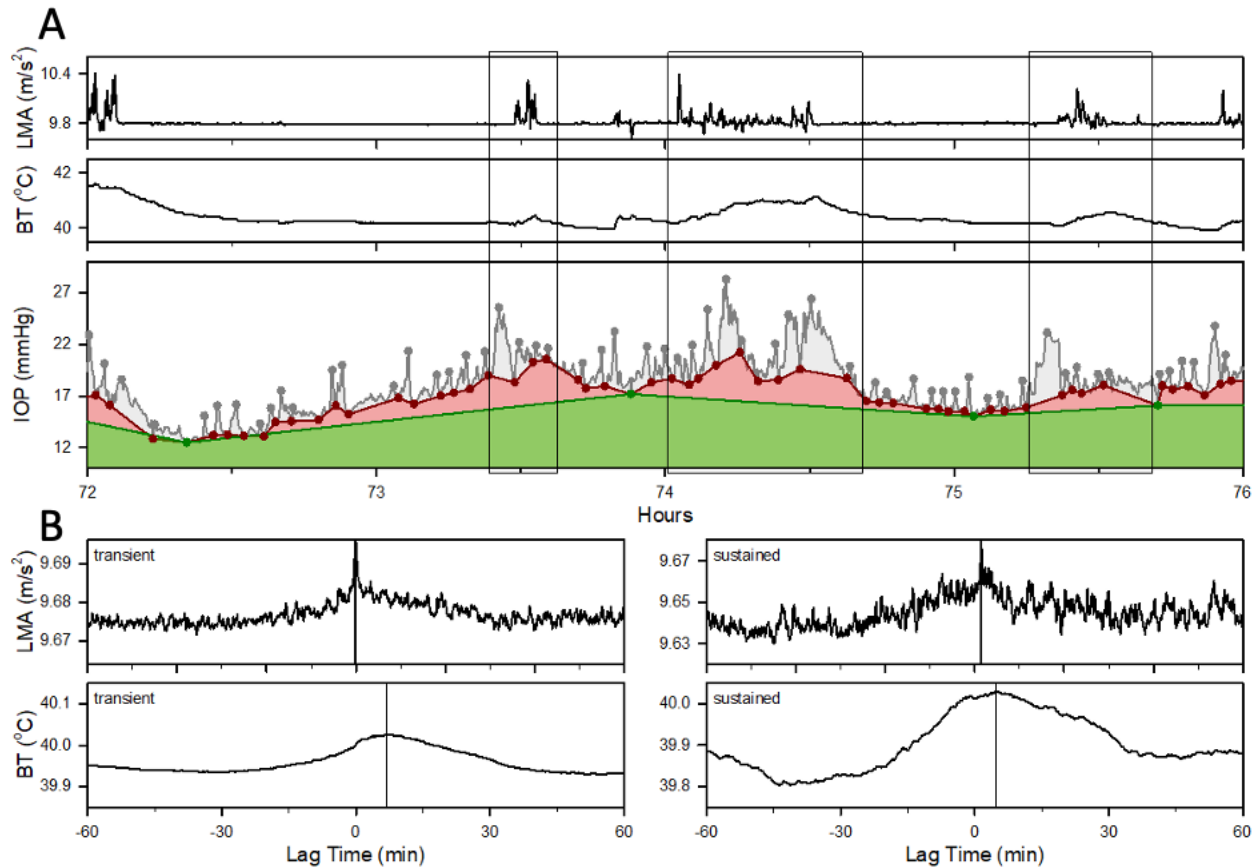


Figure 5.5: Transient and sustained IOP event triggered average of BT and LMA. (A) Raw IOP, BT, and LMA data of a given animal. Transient (grey) and sustained (red) IOP fluctuations were detected and peeled away from baseline IOP (green). The peaks of transient and sustained events were used to trigger averaging of BT and LMA. The boxed regions highlight times when changes in BT and LMA occurred congruently with transient and sustained IOP fluctuations. (B) An example of transient (left) and sustained (right) IOP event triggered averages of both BT and LMA for a given animal. Results show a noticeable delay in BT change and a near instantaneous change in LMA.

analyzed across animals, BT elevation lagged peak transient and sustained IOP fluctuation by 5 min and 3 min, respectively ( $n = 14$ ). In the 3 animals that recorded LMA, there was zero lag time between peak transient IOP fluctuation and onset of LMA. The onset of LMA lagged peak

sustained IOP fluctuation by 4 min in 2 rats and were uncorrelated in the third rat. The delay seen in the 2 animals, however, could be a coincidence of the animal moving during a sustained IOP event that either occurred spontaneously or was initiated by a previous burst of activity.

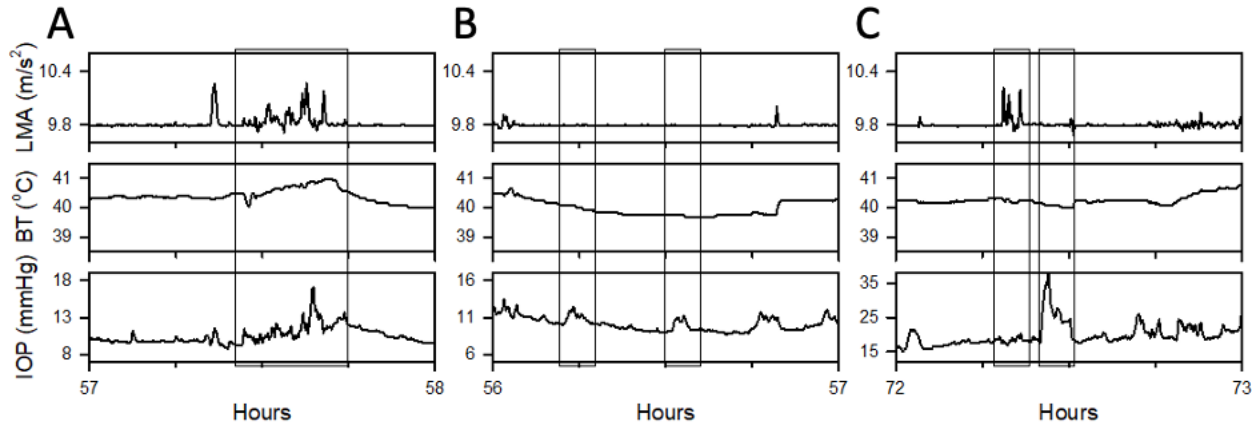


Figure 5.6: Telemetry system functionality. (A) IOP fluctuation occurring instantaneously with LMA as well as a delayed rise in BT. (B) Boxed regions showing spontaneous IOP fluctuations without LMA or change in BT. (C) The first boxed region marks LMA without changes in BT or IOP showing that thermistor output is not due to flexion of wires. The second boxed region marks a large, long-lasting pressure fluctuation in the absence of LMA and BT change.

Proper functionality of the telemetry system can be confirmed by the three snippets of simultaneously collected IOP, BT, and LMA data presented in Figure 5.6. The left most plot shows that IOP fluctuations can occur congruently with bursts in LMA, both of which are followed by a BT elevation. This result suggests that IOP and BT variability are highly influenced by LMA. In the middle plot, the boxed regions are incidents where the animal was idle and experienced no BT change, yet there were IOP fluctuations that lasted several minutes. This result suggests that IOP fluctuates spontaneously in response to internal physiological process. It also confirms that the pressure fluctuations seen in the IOP record are not purely due to hydrodynamic changes of fluid in the external tubing connecting to the sensor. Control experiments shown previously in Figure 3.7A also showed that head and body rotations had an insignificant contribution to the

hydrodynamic effects of fluid in the external tubing. The right plot shows that changes in IOP, BT, and LMA can also occur independent of one another. The first boxed region shows that there was a burst in LMA with minimal change in IOP and BT. This result confirms that the thermistor output is truly a measure of temperature and not a change in resistance due to wire flexion that could occur during LMA. The second boxed region shows a huge IOP spike without change in BT or LMA. This reinforces what is shown in the middle plot and confirms that IOP fluctuations can occur spontaneously without changes in BT or activity level.

## **5.4 Discussion**

In this study, a new and improved animal monitoring telemetry system was developed and tested in a rat model. Like previous experiments, IOP was recorded from an external pressure transducer located within the backpack. New components of the device included an implantable thermistor to monitor BT, an on-board accelerometer to track LMA, and an additional pressure transducer to record from a second physiological pressure source. This upgraded system successfully collected IOP, BT, and LMA round-the-clock in conscious, freely moving animals. Statistical analyses revealed significant correlation between the three physiological parameters on different timescales. In future experiments, the dual pressure sensors may be used together to determine the coherence between bilateral IOP measurements, the effect of intracranial pressure on IOP, as well as the direct impact of blood pressure on IOP, all of which will improve our understanding of IOP variability and its contribution to glaucoma.

### **5.4.1 Relation to Prior Work**

Following implantation of the new telemetry system, diurnal IOP rhythm was detected in all rats, which confirms results of previous tonometry studies in rats [34], mice [120], and rabbits [121]. Statistics pertaining to IOP rhythm and variability of rats housed in LD conditions were

discussed in detail previously in Section 3.3. Continuous measurement of BT revealed that 60% of rats experienced a diurnal BT rhythm. In a past study, researchers found that rat BT followed a diurnal rhythm that coincided with a diurnal IOP rhythm in all animals [77]. This group recorded BT continuously from an intraperitoneal temperature sensor. Differing results between studies may be explained by temperature sensor placement. Deeper regions such as muscle tissue and the peritoneal cavity are more comparable to core temperature than subcutaneous space, which is 1 - 2 °C lower than core temperature [122]. However, it has been reported in humans that subcutaneous temperature in the trunk or torso region is also comparable to that of core temperature [123, 124]. It is possible that the subcutaneous thermistor shifted away from the trunk or torso region in the 40% of rats that diurnal BT rhythm went undetected. It is also possible that diurnal BT changes were masked due to accumulation of heat brought on by inflammation of the implant site. Although the diurnal component of BT fluctuation was absent in some animals, the thermistor was still able to detect BT changes on shorter timescales.

In this study, diurnal LMA was not detected in any rats, which is contrary to what is presented in previous literature. Diurnal LMA rhythm has been seen in various animal models including but not limited to mice [125], rats [126], hamsters, rabbits, sheep, goats, cows, and horses [127]. In these studies, nocturnal animals were more active during the dark phase, while diurnal animals were more active in the light phase [127]. We suspect that one of the main reasons diurnal changes in LMA were not detected is because rats were not provided a running wheel. Most studies that found a diurnal rhythm in LMA of rodents housed animals in a cage equipped with a running wheel. When provided a running wheel, most rodents will voluntarily use it as a means of habitual exercise [128]. Another potential reason that diurnal LMA was not detected is that animals were housed in a room where investigators and vivarium staff frequently entered during working hours

(7 AM - 3 PM). It was previously shown in Figure 2.2 that rats experience an IOP spike in response to the housing room door opening [73]. We also saw previously using cage mounted cameras that these IOP spikes were sometimes coupled with bursts in LMA. It is therefore possible that LMA seen during the photopic phase is not habitual, but rather a response to environmental stimuli. It is also possible that the rats lacked diurnal LMA patterns because they were retired-breeders and activity level tends to fade with age [129, 130].

Results from this study also suggest that IOP and BT fluctuations on smaller time scales are highly influenced by bursts in LMA. A previous study looked at the acute effects of LMA on BT and CO<sub>2</sub> elimination in rats housed at room temperature (23 °C) and found that during times of activity or grooming, there was a near instantaneous elevation in CO<sub>2</sub> elimination followed by a delayed BT rise [131]. Both CO<sub>2</sub> and BT levels recovered to baseline after LMA ceased due to homeostatic regulation. The delay in BT change following LMA has also been seen in mice [125]. They attributed this delay to the thermal capacity of the body and its ability to distribute heat generated by muscle tissue during movement to prevent immediate change of core temperature. This is an important thermoregulatory task of the body to maintain temperatures within physiological range. In a separate study, researchers found that manipulating mean arterial pressure (MAP) has an effect on ocular hemodynamics and IOP in rabbits [132]. Doppler flowmetry revealed a linear correlation between changes in orbital venous pressure (OVP), episcleral venous pressure (EVP), and IOP resulting from MAP changes. This suggests that regulation of ocular hemodynamics plays a crucial role in IOP variability. These studies also support the idea that heart rate and blood pressure changes associated with LMA cause near instantaneous changes in IOP by altering ocular hemodynamics.

Another interesting result from this study was that IOP fluctuated spontaneously in the absence of LMA and BT change. These IOP fluctuations were discovered previously with older versions of our telemetry system [73] as well as in rabbit and monkey telemetry models [11, 37]. However, previous studies failed to report the physiological mechanism that led to these IOP fluctuations, which is why they were categorized as spontaneous. Since we saw IOP fluctuations without changes in LMA and BT, we suspect that there are other involuntary physiological processes that heavily influence IOP variability. These processes may include but are not limited to hormone production, metabolism, respiration, and blood pressure. In future studies, periodic blood samples can be taken to determine if IOP variability is associated with changes in hormone concentration and glucose levels. The telemetry system can be upgraded further to include a CO<sub>2</sub> concentration sensor to get an estimate of respiration rate. As mentioned previously, the dual pressure transducers can be used to simultaneously monitor IOP and blood pressure to better understand effects of hemodynamics on IOP variation. Finally, we must also consider the effect of visual and auditory cues as sources of IOP variability, which were not monitored in this study.

#### 5.4.2 Limitations

One limitation of this study is that IOP is still being collected from an external pressure transducer located in the backpack. It was previously mentioned that head and body rotations had a slight contribution to hydrodynamic effects of fluid in the tubing (Figure 3.7A). Accelerometer data also suggests that not all activity leads to pressure fluctuations. To eliminate any skepticisms that pressure fluctuations are due to kinking of the tubing, future designs of the device should include a head-mounted extraocular pressure transducer or a fully implanted intraocular pressure transducer. Another limitation of this study was that the wire of the thermistor would break a few weeks after implantation. Flexion and extension of wires due to chronic body movements over

time led to metal fatigue and eventual failure near the head mount. To enhance durability and flexibility, the thermistor wires should be helically wound and encased in medical grade silicone. This method has proven successful for the group that uses this type of wire for their fully implantable IOP telemetry system in monkeys [9].

## **5.5 Conclusion**

In this study, we employed a new and improved telemetry device capable of recording various physiological parameters. We used it to record IOP, BT, and LMA simultaneously. Our results suggest that individual IOP fluctuations often correlate with bursts in LMA, both of which are followed by a delayed rise in BT. We speculate that heart rate and blood pressure changes associated with LMA cause near instantaneous changes in IOP by altering blood hemodynamics and prolonged LMA leads to changes in BT. Although we used this device to further our understanding of mechanisms leading to IOP fluctuations, the applications of this device are endless.



## **Chapter 6: Conclusions and Future Works**

### **6.1 Summary of Major Findings**

In summary, we successfully developed and implemented novel telemetry systems to study factors affecting intraocular pressure (IOP) variability in free-moving conscious rats. IOP was measured by an extraocular pressure transducer connected to a fluid-filled cannula implanted in the anterior segment of the eye. This technology offered a hands-off approach to monitoring IOP variability with minimal confounding variables. In chapter 2, we reported that acute stress triggers an elevation in IOP. Results revealed that IOP elevated when animals were temporarily placed in a confined space and remained elevated long after removal. A similar IOP stress-response was seen when tonometry was performed in awake rats. Although cortisol, the hormone released during psychological stress, was not monitored during experimentation, we found that this IOP response was absent in anesthetized rats. This may be explained by the inhibition of the autonomic response to external stimuli during anesthesia. When used properly, anesthesia itself had little to no effect on IOP. There was, however, a significant IOP decrease in anesthetized animals that were not provided heat support. This is presumably due to the inhibition of thermoregulation following anesthesia induction. It is important for clinicians and researchers to consider the impact environmental and core temperature have on IOP during surgical procedure and experiments in which anesthesia is used. Improper thermoregulation can be injurious to patients suffering from IOP-related diseases.

Telemetry also revealed that IOP varies constantly. Although IOP fluctuations were commonly seen in animals subjected to environmental stimuli, they were also detected in idle and

isolated rats as well as anesthetized rats. In anesthetized experiments, rats exhibited considerably less IOP variation than awake rats. This result was introduced in chapter 2 but clarified in chapter 3 when a custom MATLAB algorithm was used to characterize the various components that comprise the IOP waveform. The algorithm used peak detection to peel away faster and slower IOP fluctuations from underlying mean changes. The faster fluctuations on the order of minutes were classified as transient fluctuations and the slower components ranging from tens of minutes to over an hour were classified as sustained fluctuations. The remaining mean changes were termed baseline IOP fluctuations. In awake rats, there were far more transient fluctuations than sustained fluctuations daily and amplitudes of both were typically between 1 and 6 mmHg. The area under the IOP<sup>2</sup> versus time waveform was used to calculate and quantify the IOP-related biomechanical stress on ocular tissues due to daily IOP fluctuation. Although transient and sustained fluctuations were similar in amplitude, sustained fluctuations contributed more mechanical stress than transients since they were longer in duration. Overall, baseline fluctuations contributed the most to daily IOP-related stress on the eye, which suggests that changes in mean IOP are significant for glaucoma diagnosis. Results also suggest that acute IOP fluctuations over a lifetime may contribute to age-related glaucomatous damage, but most of the damage comes from extended durations of IOP elevation.

The effects of different ambient lighting conditions on IOP variability were also tested. In constant dark (DD) conditions, the IOP rhythm persisted, which confirmed the circadian characteristics seen in previous studies [34]. Reversed light cycle as well as constant light (LL) experiments revealed that period, amplitude, and phase of the IOP circadian rhythm was disrupted by extended durations of high intensity light. These phenomena may be explained by Aschoff's rules of photoperiod sensitivity [108]. LL conditions also evoked a gradual rise in mean IOP, which

we know is a major risk factor for hypertensive glaucoma. The frequency of IOP transients on smaller time scales was not impacted by constant lighting conditions, however sustained events were significantly more prevalent. It is possible that this difference may stem from inter-animal variability, but it may also be tied to psychological stress. It has been seen in many other species that when animals are subjected to constant lighting conditions, they present behavioral abnormalities including depression and heightened anxiety [133, 134]. Therefore, lack of light cycle regulation disrupts the sleep/wake cycle leading to alteration of the IOP fluctuation patterns, which may have implications for glaucoma and other IOP-related diseases.

## **6.2 Technological Advancement**

To better understand the physiological processes associated with IOP fluctuation, modifications were made to the existing telemetry system for collection of additional information. The new version of the device was equipped with a thermistor for body temperature (BT) monitoring and an accelerometer to track locomotor activity (LMA). The device printed circuit board (PCB) was miniaturized by upgrading the microprocessor to a Simblee module, which is two-fold smaller than the previous RFDuino microcontroller. Although it has yet to be tested in an animal, the system also includes an additional pressure transducer to simultaneously monitor two different physiological pressure sources as well as circuitry to record heart rate. The single channel op-amp of the original device was upgraded to a dual op-amp to properly amplify the additional pressure transducer. To monitor heart rate, a circuit developed by a previous graduate student to acquire electroretinograms (ERGs) and compound actions potentials (CAPs) was incorporated into the design [135]. It consists of implantable bipolar electrodes amplified by a multistage differential amplifier with an incorporated bandpass filter. This component can be used to collect a one-lead electrocardiogram (EKG) by recording a difference in voltage potential using the bipolar

electrodes on opposite sides of the heart. When connected to an interrupt pin of the Simblee, each QRS complex generates a potential large enough to trigger the microcontroller and record a heartbeat. Additional device capabilities required upgrading of the power supply. To extend the battery life and reduce electronic waste, the previously used 3 V coin cell battery was replaced with a rechargeable 3.7 V lithium-ion polymer battery with a much higher capacitance. To ensure a stable power supply to the device, a low-dropout (LDO) voltage regulator was also added to the circuit design. The LDO regulator minimizes noise in the output voltage and reduces power dissipation as heat to the device.

This modified telemetry system was used to simultaneously monitor IOP, BT, and LMA in conscious, free-moving rats. The simultaneous recording helped determine the coherence between changes in each physiological process. It was found that there was a strong correlation between bursts in LMA that led to near instantaneous IOP fluctuations followed by a delayed, gradual rise in BT. There were some instances where IOP fluctuated in the absence of LMA and BT changes, which re-enforced results collected using the original technology with cage-mounted cameras that revealed IOP fluctuations in idle, isolated rats. This suggests that IOP fluctuates spontaneously due to internal processes that are triggered by external stimuli including visual and auditory cues or by involuntary intrinsic mechanisms including hormone production, metabolism, respiration, and hemodynamic changes. We therefore speculate that IOP variability is modulated either directly or indirectly by the autonomic nervous system (ANS). Future use of our device would also involve dual monitoring of physiological pressure sources, which may include IOP with either systemic blood pressure or episcleral venous pressure (EVP) to identify and quantify direct effects of cardiovascular changes on IOP. It is also important to mention that applications for the pressure transducers to monitor different physiological pressures are endless.

### **6.3 IOP and the Autonomic Nervous System**

There is increasing evidence that the ANS interacts with the central nervous system (CNS) via the modulation of circadian rhythms and other physiological processes [136]. The CNS is comprised of two parts: the brain and spinal cord. The brain is responsible for major bodily functions including the 5 senses: visual, auditory, tactile, gustatory, and olfactory perception as well as cognition, motor activity, speech, and intellection. The brainstem is an extension of the brain that is used to communicate with the peripheral nervous system (PNS), which is divided into the somatic nervous system (SoNS) and the ANS. The SoNS controls the contraction and relaxation of muscles that allow for motor activity and collects information for the brain from the 5 major senses. The ANS controls and regulates involuntary physiological processes including but not limited to respiration, digestion, blood pressure, and heart rate. In addition to maintaining homeostasis, the ANS is involved in the sympathetic (fight or flight) and parasympathetic (rest and digest) subsystems.

Like the sleep/wake cycle, our results suggest that IOP is regulated through similar circadian processes. Previous literature indicates that EVP is a key determinant of IOP and therefore changes in vasculature can impact IOP value [132]. There is evidence that systemic blood pressure also has a significant impact on IOP variation [30, 137]. Acute changes in blood pressure are due to the regulation of cardiovascular output by the ANS to maintain homeostasis and long-term variations in blood pressure have circadian tendencies, which are controlled by the brain. Researchers have proposed the Central Autonomic Network (CAN) model to determine the interaction between the ANS and CNS to describe the two-way interaction between the brain and the heart [136]. The vagus nerves, which run on either side of the neck, have been identified as part of the ANS that interact with the heart and play a crucial role in circadian rhythm. Since our

results suggest that IOP is driven by an intrinsic mechanism it would be possible to use the device to further investigate the intrinsic mechanisms driving IOP fluctuation. Along with simultaneous recording of IOP and other physiological signals such as blood pressure, temperature, and heart rate, electrical or chemical stimulation could be used to inhibit or excite neural pathways between the eye and the brain to further study this. There are studies that have performed similar experiments to determine the neural connection between IOP and intracranial pressure (ICP) [138] as well as IOP and EVP [139]. Also, tetrodotoxin (TTX), a potent neurotoxin, can be applied to the optic nerve to inhibit sodium ion-gated channels and block the communication between the eye and the brain. If free-running circadian IOP persists following application of TTX, it would suggest that there are local clock genes within the eye that drive circadian IOP. To completely map the neural pathway, one could also individually knock out local circadian clocks that are known to exist in the eye.

#### **6.4 Future Works**

It was reported in 2014 that there were 80 million individuals suffering from glaucoma and it is estimated to increase 40% by the year 2040 [140]. This statistic indicates an overwhelming need for answers pertaining to the cause and progression of IOP-related diseases, specifically glaucoma. The next and most appropriate direction for application of IOP telemetry would be to characterize IOP variability in an experimental model of glaucoma. Common models of experimental glaucoma target IOP value by manipulating aqueous humor excretion from the eye. The injection of varying diameter microbeads has been used to elevate IOP by occluding the porous like structure of the trabecular meshwork, which is the major component of the conventional outflow pathway [141]. Translimbal laser photocoagulation has also been used to successfully elevate IOP by scarring the trabecular meshwork [142]. Since episcleral vasculature

plays a key role in regulating the rate of aqueous outflow, cauterization of episcleral veins can induce a pressure blockage that elevates IOP [143]. Other methods that successfully elevate IOP in an animal model for extended durations include application of pharmacological corticosteroids that block calcium channels [144, 145], circumlimbal suturing to compress the eye [146], and injection of hypertonic saline leading to sclerosis of the aqueous outflow pathway [147]. IOP telemetry can be used to determine differences in IOP variability before and after induction of any of the previously stated models, which is crucial in understanding IOP as a risk factor for the development and progression of glaucoma.

There are relatively few studies that have attempted to characterize IOP variability in clinical and experimental forms of glaucoma. In humans, an external contact lens equipped with a strain gauge uses corneal curvature as an indirect estimate of IOP [81, 148-150]. Although this technique provides a unique, non-invasive approach for monitoring IOP round-the-clock, there are concerns with measurement accuracy. One major limitation is that these contact lenses are not custom fit for patient specific corneal thickness and globe shape. It was reported that lenses were uncomfortable to wear and, extensive use led to corneal erosion. There are, however, other commercial telemetry systems available that are fully implantable. There is a group that performs IOP telemetry in monkeys that use a total implant system made by Konigsberg Instruments [9]. This group has had tremendous success over the last decade identifying and characterizing sources of IOP variability that coincide with risk factors for glaucoma. There was also a recent groundbreaking clinical case study in which a patient was implanted with the EYEMATE-IO, an implantable sensor, to measure IOP before and after glaucoma surgery [151]. Being the first of its kind, this clinical trial was a huge success as it led doctors to timely surgical intervention and the ability to monitor postoperative response to treatment.

Another rather important future direction would be to study the effects of various pharmacological agents on IOP. One could study the impacts of various drugs that are known to increase the risk of glaucoma development as well as drugs that are commonly used as therapeutic treatments for IOP-related diseases. Typically, the effectiveness of these medications is tested in animal models before clinical approval for use in humans. Our telemetry system can be used to better understand both the acute and chronic effects of various pharmacological agents on IOP variability. Telemetry would also reveal any unanticipated changes in behavior during and after treatment that may negatively impact patients, which would go undetected with tonometry alone.

There is also increasing evidence that glaucoma may be related to dark-phase IOP elevation. A previous tonometry study found that rats with experimental glaucoma experienced significantly higher dark phase IOP than healthy animals, with no change in light phase IOP level [113]. We saw a similar result in a few rats implanted with our telemetry system. Since glaucoma is an age-related disease, it is possible that the retired-breeder rats used in our study can spontaneously develop glaucoma. It is unclear whether abnormally elevated dark phase IOP is a result of changes in aqueous humor dynamics that are somehow impacted by the pupillary response in the dark phase. Further investigation is necessary to understand the mechanism by which IOP rhythm and variability is affected by glaucoma. Fortunately, IOP telemetry allows for detection of these changes. To understand the impact of pupil modulation on IOP, the effects of various drugs such as mydriatics and miotics, which are used to dilate and constrict the pupil during routine diagnostic procedures, should be tested.



## References

1. Quigley HA, Broman AT: The number of people with glaucoma worldwide in 2010 and 2020. *British Journal of Ophthalmology* 2006, 90(3):262-267.
2. Goel M, Picciani RG, Lee RK, Bhattacharya SK: Aqueous humor dynamics: A review. *The Open Ophthalmology Journal* 2010, 4:52.
3. Fine HF, Biscette O, Chang S, Schiff W: Ocular hypotony: A review. *Comprehensive Ophthalmology Update* 2007, 8(1):29-37.
4. Downs JC, Roberts MD, Sigal IA: Glaucomatous cupping of the lamina cribrosa: A review of the evidence for active progressive remodeling as a mechanism. *Experimental Eye Research* 2011, 93(2):133-140.
5. Steinmetz JD, Bourne RR, Briant PS, Flaxman SR, Taylor HR, Jonas JB, Abdoli AA, Abrha WA, Abualhasan A, Abu-Gharbieh EG: Causes of blindness and vision impairment in 2020 and trends over 30 years, and prevalence of avoidable blindness in relation to VISION 2020: The Right to Sight: An analysis for the Global Burden of Disease Study. *The Lancet Global Health* 2021, 9(2):e144-e160.
6. Weinreb RN, Aung T, Medeiros FA: The pathophysiology and treatment of glaucoma: A review. *Journal of the American Medical Association* 2014, 311(18):1901-1911.
7. Wang K, Read AT, Sulchek T, Ethier CR: Trabecular meshwork stiffness in glaucoma. *Experimental Eye Research* 2017, 158:3-12.
8. Bello SA, Passaglia C: A wireless pressure sensor for continuous monitoring of intraocular pressure in conscious animals. *Annals of Biomedical Engineering* 2017, 45(11):2592–2604.
9. Downs JC, Burgoyne CF, Seigfreid WP, Reynaud JF, Strouthidis NG, Sallee V: 24-Hour IOP telemetry in the nonhuman primate: Implant system performance and initial characterization of IOP at multiple timescales. *Investigative Ophthalmology & Visual Science* 2011, 52(10):7365-7375.
10. C RS, C. Debon, and C. L. Percicotf: Measurement of intraocular pressure by telemetry in conscious, unrestrained rabbits. *Investigative Ophthalmology & Visual Science* 1996, 37(6):958-965.
11. McLaren JW, Brubaker RF, FitzSimon S: Continuous measurement of intraocular pressure in rabbits by telemetry. *Investigative Ophthalmology & Visual Science* 1996, 37(6):966-975.

12. Agnifili L, Mastropasqua R, Frezzotti P, Fasanella V, Motolese I, Pedrotti E, Iorio AD, Mattei PA, Motolese E, Mastropasqua L: Circadian intraocular pressure patterns in healthy subjects, primary open angle and normal tension glaucoma patients with a contact lens sensor. *Acta Ophthalmologica* 2015, 93(1):e14-e21.
13. Gillmann K, Bravetti GE, Niegowski LJ, Mansouri K: Using sensors to estimate intraocular pressure: A review of intraocular pressure telemetry in clinical practice. *Expert Review of Ophthalmology* 2019, 14(6):263-276.
14. Morrison JC, Guo WOCY, Johnson EC: Pathophysiology of human glaucomatous optic nerve damage: Insights from rodent models of glaucoma. *Experimental Eye Research* 2011, 93(2):156-164.
15. Malihi M, Sit AJ: Effect of head and body position on intraocular pressure. *Ophthalmology* 2012, 119(5):987-991.
16. Nelson ES, Myers Jr JG, Lewandowski BE, Ethier CR, Samuels BC: Acute effects of posture on intraocular pressure. *Plos One* 2020, 15(2):e0226915.
17. Turner DC, Samuels BC, Huisingh C, Girkin CA, Downs JC: The magnitude and time course of IOP change in response to body position change in nonhuman primates measured using continuous IOP telemetry. *Investigative Ophthalmology & Visual Science* 2017, 58(14):6232.
18. Bruttini C, Verticchio Vercellin A, Klersy C, De Silvestri A, Tinelli C, Riva I, Oddone F, Katsanos A, Quaranta L: The Mont Blanc Study: The effect of altitude on intra ocular pressure and central corneal thickness. *Plos One* 2020, 15(8):1-10.
19. Van de Veire S, Germonpre P, Renier C, Stalmans I, Zeyen T: Influences of atmospheric pressure and temperature on intraocular pressure. *Investigative Ophthalmology & Visual Science* 2008, 49(12):5392-5396.
20. Shapiro A, Shoenfeld Y, Shapiro Y: The effect of exposure to heat on intraocular pressure. *Albrecht von Graefes Archiv für klinische und experimentelle Ophthalmologie* 1979, 210(3):183-185.
21. Chandrasekaran S, Rochtchina E, Mitchell P: Effects of caffeine on intraocular pressure: The Blue Mountains Eye Study. *Journal of Glaucoma* 2005, 14(6):504-507.
22. Wang MT, Danesh-Meyer HV: Cannabinoids and the eye. *Survey of Ophthalmology* 2021, 66(2):327-345.
23. Jia L, Cepurna WO, Johnson EC, Morrison JC: Effect of general anesthetics on IOP in rats with experimental aqueous outflow obstruction. *Investigative Ophthalmology & Visual Science* 2000, 41(11):3415-3419.
24. Ding C, Wang P, Tian N: Effect of general anesthetics on IOP in elevated IOP mouse model. *Experimental Eye Research* 2011, 92(6):512-520.

25. Mikhail M, Sabri K, Levin AV: Effect of anesthesia on intraocular pressure measurement in children. *Survey of Ophthalmology* 2017, 62(5):648-658.
26. Jasien JV, Girkin CA, Downs JC: Effect of anesthesia on intraocular pressure measured with continuous wireless telemetry in nonhuman primates. *Investigative Ophthalmology & Visual Science* 2019, 60(12):3830.
27. Cooper R, Beale D, Constable I, Grose G: Continual monitoring of intraocular pressure: Effect of central venous pressure, respiration, and eye movements on continual recordings of intraocular pressure in the rabbit, dog, and man. *British Journal of Ophthalmology* 1979, 63(12):799-804.
28. Shapiro A, Shoenfeld Y, Konikoff F, Udassin R, Shapiro Y: The relationship between body temperature and intraocular pressure. *Ann Ophthalmol* 1981, 13(2):159-161.
29. Gökhan N, Gökçe S: Influence of hypercapnia on intraocular pressure in rabbits. *Experimental Eye Research* 1975, 21(1):71-78.
30. Klein BEK, Klein R, Knudtson MD: Intraocular pressure and systemic blood pressure: Longitudinal perspective: The Beaver Dam Eye Study. *British Journal of Ophthalmology* 2005, 89(3):284-287.
31. Berdahl JP, Fautsch MP, Stinnett SS, Allingham RR: Intracranial pressure in primary open angle glaucoma, normal tension glaucoma, and ocular hypertension: a case-control study. *Investigative Ophthalmology & Visual Science* 2008, 49(12):5412-5418.
32. Ficarrota KR, Passaglia CL: Intracranial pressure modulates aqueous humour dynamics of the eye. *The Journal of Physiology* 2020, 598(2):403-414.
33. Ren R, Zhang X, Wang N, Li B, Tian G, Jonas JB: Cerebrospinal fluid pressure in ocular hypertension. *Acta Ophthalmologica* 2011, 89(2):e142-e148.
34. Moore CG, Johnson EC, Morrison JC: Circadian rhythm of intraocular pressure in the rat. *Current Eye Research* 1996, 15(2):185-191.
35. Sven Dinslage JM, and Richard Brubaker: Intraocular pressure in rabbits by telemetry II: Effects of animal handling and drugs. *Investigative Ophthalmology & Visual Science* 1998, 39(12):2485-2489.
36. Miyazaki Y, Matsuo T, Kurabayashi Y: Immobilization stress induces elevation of intraocular pressure in rabbits. *Ophthalmic Research* 2000, 32(6):270-277.
37. Turner DC, Miranda M, Morris JS, Girkin CA, Downs JC: Acute stress increases intraocular pressure in nonhuman primates. *Ophthalmology Glaucoma* 2019, 2(4):210-214.

38. Méndez-Ulrich JL, Sanz A, Feliu-Soler A, Álvarez M, Borràs X: Could white coat ocular hypertension affect to the accuracy of the diagnosis of Glaucoma? Relationships between anxiety and intraocular pressure in a simulated clinical setting. *Applied Psychophysiology and Biofeedback* 2018, 43(1):49-56.
39. Bello SA, Malavade S, Passaglia CL: Development of a smart pump for monitoring and controlling intraocular pressure. *Annals of Biomedical Engineering* 2017, 45(4):990–1002.
40. Reina-Torres E, Bertrand JA, O'Callaghan J, Sherwood JM, Humphries P, Overby DR: Reduced humidity experienced by mice in vivo coincides with reduced outflow facility measured ex vivo. *Experimental Eye Research* 2019, 186:107745.
41. B.G. S: Psychophysiological stress, elevated intraocular pressure, and acute closed-angle glaucoma. *Optometry and Vision Science* 1987, 64(11):866-870.
42. Dada T, Mittal D, Mohanty K, Faiq MA, Bhat MA, Yadav RK, Sihota R, Sidhu T, Velpandian T, Kalaivani M: Mindfulness meditation reduces intraocular pressure, lowers stress biomarkers and modulates gene expression in glaucoma: a randomized controlled trial. *Journal of Glaucoma* 2018, 27(12):1061-1067.
43. Craig J, Cook J: A comparison of isoflurane and halothane in anaesthesia for intra-ocular surgery. *Anaesthesia* 1988, 43(6):454-458.
44. Mirakhur RK, Elliot P, Shepherd WFI, Mcgalliard JN: Comparison of the effects of isoflurane and halothane on intraocular pressure. *Acta Anaesthesiologica Scandinavica* 1990, 34:282-285.
45. Buehner E, Pietsch U-C, Bringmann A, Foja C, Wiedemann P, Uhlmann S: Effects of propofol and isoflurane anesthesia on the intraocular pressure and hemodynamics of pigs. *Ophthalmic Research* 2011, 45(1):42-46.
46. Tsuchiya S, Higashide T, Hatake S, Sugiyama K: Effect of inhalation anesthesia with isoflurane on circadian rhythm of murine intraocular pressure. *Experimental Eye Research* 2021, 203:108420.
47. Chae JJ, Prausnitz MR, Ethier CR: Effects of general anesthesia on intraocular pressure in rabbits. *Journal of the American Association for Laboratory Animal Science* 2021, 60(1):91-95.
48. Ausinsch B GS, Munson ES, Levy NS: Intraocular pressures in children during isoflurane and halothane anesthesia. *Anesthesiology* 1975, 42(2):167-172.
49. Dear GdL, Hammerton M, Hatch D, Taylor D: Anaesthesia and intra-ocular pressure in young children: A study of three different techniques of anaesthesia. *Anaesthesia* 1987, 42(3):259-265.
50. Trim C, Colbern G, Martin C: Effect of xylazine and ketamine on intraocular pressure in horses. *The Veterinary Record* 1985, 117(17):442-443.

51. Holve DL, Gum GG, Pritt SL: Effect of sedation with xylazine and ketamine on intraocular pressure in New Zealand white rabbits. *Journal of the American Association for Laboratory Animal Science* 2013, 52(4):488-490.
52. Rajaei SM, Mood MA, Paryani MR, Williams DL: Effects of diurnal variation and anesthetic agents on intraocular pressure in Syrian hamsters (*Mesocricetus auratus*). *American Journal of Veterinary Research* 2017, 78(1):85-89.
53. Schutten W, Van Horn D: The effects of ketamine sedation and ketamine-pentobarbital anesthesia upon the intraocular pressure of the rabbit. *Investigative Ophthalmology & Visual Science* 1977, 16(6):531-534.
54. Antal M, Mucsi G, Faludi A: Ketamine anesthesia and intraocular pressure. *Annals of Ophthalmology* 1978, 10(9):1281-1284, 1289.
55. Hofmeister EH, Mosunic CB, Torres BT, Ralph AG, Moore PA, Read MR: Effects of ketamine, diazepam, and their combination on intraocular pressures in clinically normal dogs. *American Journal of Veterinary Research* 2006, 67(7):1136-1139.
56. Ghaffari MS, Moghaddassi AP: Effects of ketamine-diazepam and ketamine-acepromazine combinations on intraocular pressure in rabbits. *Veterinary Anaesthesia and Analgesia* 2010, 37:269-272.
57. Qiu Y, Yang H, Lei B: Effects of three commonly used anesthetics on intraocular pressure in mouse. *Current Eye Research* 2014, 39(4):365-369.
58. Blumberg D, Congdon N, Jampel H, Gilbert D, Elliott R, Rivers R, Munoz B, Quigley H: The effects of sevoflurane and ketamine on intraocular pressure in children during examination under anesthesia. *American Journal of Ophthalmology* 2007, 143(3):494-499.
59. Drayna PC, Estrada C, Wang W, Saville BR, Arnold DH: Ketamine sedation is not associated with clinically meaningful elevation of intraocular pressure. *The American Journal of Emergency Medicine* 2012, 30(7):1215-1218.
60. Ausinsch B, Rayburn RL, Munson ES, Levy NS: Ketamine and intraocular pressure in children. *Anesthesia and Analgesia* 1976, 55(6):773-775.
61. Lenhardt R: The effect of anesthesia on body temperature control. *Frontiers in Bioscience* 2010, S2(1):1145.
62. Reich DL, Silvay G: Ketamine: An update on the first twenty-five years of clinical experience. *Canadian Journal of Anesthesia* 1989, 36(2):186-197.
63. Nichols PF, Krupin T, Beatty JF, Fritz CA, Becker B: The effects of body immersion on aqueous humor dynamics in rabbits. *Experimental eye research* 1984, 38(1):81-86.

64. Findikoglu G, Cetin EN, Sarsan A, Senol H, Yildirim C, Ardic F: Arterial and intraocular pressure changes after a single-session hot-water immersion. *UnderseaHyperb Med* 2015, 42(1):65-73.
65. Ortiz GJ, Cook DJ, Yablonski ME, Masonson H, Harmon G: Effect of cold air on aqueous humor dynamics in humans. *Investigative Ophthalmology & Visual Science* 1988, 29(1):138-140.
66. Orgül S, Flammer J, Stümpfig D, Hendrickson P: Intraocular pressure decrease after local ocular cooling is underestimated by applanation tonometry. *International Ophthalmology* 1995, 19(2):95-99.
67. Fabiani C, Li Voti R, Rusciano D, Mutolo MG, Pescosolido N: Relationship between corneal temperature and intraocular pressure in healthy individuals: a clinical thermographic analysis. *Journal of Ophthalmology* 2016, 2016:1-7.
68. McDougal DH, Gamlin PD: Autonomic control of the eye. *Comprehensive Physiology* 2015, 5(1):439.
69. Ficarrota KR, Bello SA, Mohamed YH, Passaglia CL: Aqueous humor dynamics of the Brown-Norway rat. *Investigative Ophthalmology & Visual Science* 2018, 59(6):2529.
70. Ostrin LA, Jnawali A, Carkeet A, Patel NB: Twenty-four hour ocular and systemic diurnal rhythms in children. *Ophthalmic Physiol Opt* 2019, 39(5):358-369.
71. Boussommier-Calleja A, Li G, Wilson A, Ziskind T, Scinteie OE, Ashpole NE, Sherwood JM, Farsiu S, Challa P, Gonzalez P: Physical factors affecting outflow facility measurements in mice. *Investigative Ophthalmology & Visual Science* 2015, 56(13):8331-8339.
72. Reina-Torres E, Boussommier-Calleja A, Sherwood JM, Overby DR: Aqueous humor outflow requires active cellular metabolism in mice. *Investigative Ophthalmology & Visual Science* 2020, 61(10):45-45.
73. Nicou CM, Pillai A, Passaglia CL: Effects of acute stress, general anesthetics, tonometry, and temperature on intraocular pressure in rats. *Experimental Eye Research* 2021, 210:108727.
74. Aihara M, Lindsey JD, Weinreb RN: Twenty-four-hour pattern of mouse intraocular pressure. *Experimental Eye Research* 2003, 77(6):681-686.
75. Sugimoto E-i, Aihara M, Ota T, Araie M: Effect of light cycle on 24-hour pattern of mouse intraocular pressure. *Journal of Glaucoma* 2006, 15(6):505-511.
76. Del Sole MJ, Sande PH, Bernades JM, Aba MA, Rosenstein RE: Circadian rhythm of intraocular pressure in cats. *Veterinary Ophthalmology* 2007, 10(3):155-161.

77. Lozano DC, Hartwick ATE, Twa MD: Circadian rhythm of intraocular pressure in the adult rat. *Chronobiology International* 2015, 32(4):513-523.
78. Ruixia Li JHKL: Telemetric monitoring of 24 h intraocular pressure in conscious and freely moving C57BL/6J and CBA/CAJ mice. *Molecular Vision* 2008, 14:745-749.
79. Todani A, Behlau I, Fava MA, Cade F, Cherfan DG, Zakka FR, Jakobiec FA, Gao Y, Dohlman CH, Melki SA: Intraocular pressure measurement by radio wave telemetry. *Investigative Ophthalmology & Visual Science* 2011, 52(13):9573.
80. Sánchez I, Laukhin V, Moya A, Martin R, Ussa F, Laukhina E, Guimera A, Villa R, Rovira C, Aguiló J: Prototype of a nanostructured sensing contact lens for noninvasive intraocular pressure monitoring. *Investigative Ophthalmology & Visual Science* 2011, 52(11):8310-8315.
81. Mansouri K, Shaarawy T: Continuous intraocular pressure monitoring with a wireless ocular telemetry sensor: initial clinical experience in patients with open angle glaucoma. *British Journal of Ophthalmology* 2011, 95(5):627-629.
82. Liu JS, Passaglia CL: Spike firing pattern of output neurons of the *Limulus* circadian clock. *Journal of Biological Rhythms* 2011, 26(4):335-344.
83. Markert JE, Jasien JV, Turner DC, Huisinigh C, Girkin CA, Downs JC: IOP, IOP transient impulse, ocular perfusion pressure, and mean arterial pressure relationships in nonhuman primates instrumented with telemetry. *Investigative Ophthalmology & Visual Science* 2018, 59(11):4496-4505.
84. Turner DC, Edmiston AM, Zohner YE, Byrne KJ, Seigfreid WP, Girkin CA, Morris JS, Downs JC: Transient intraocular pressure fluctuations: Source, magnitude, frequency, and associated mechanical energy. *Investigative Ophthalmology & Visual Science* 2019, 60(7):2572-2582.
85. Selles-Navarro I, Villegas-Perez MP, Salvador-Silva M, Ruiz-Gomez JM, Vidal-Sanz M: Retinal ganglion cell death after different transient periods of pressure-induced ischemia and survival intervals. A quantitative in vivo study. *Investigative Ophthalmology & Visual Science* 1996, 37(10):2002-2014.
86. Yang X, Yu X, Zhao Z, He Y, Zhang J, Su X, Sun N, Fan Z: Endoplasmic reticulum stress is involved in retinal injury induced by repeated transient spikes of intraocular pressure. *Journal of Zhejiang University-SCIENCE B* 2021, 22(9):746-756.
87. Jasien JV, Zohner YE, Asif SK, Rhodes LA, Samuels BC, Girkin CA, Morris JS, Downs JC: Comparison of extraocular and intraocular pressure transducers for measurement of transient intraocular pressure fluctuations using continuous wireless telemetry. *Scientific Reports* 2020, 10(1):1-10.

88. Buhr ED, Yue WW, Ren X, Jiang Z, Liao H-WR, Mei X, Vemmaraju S, Nguyen M-T, Reed RR, Lang RA: Neuropeptide Y (NPY)-mediated photoentrainment of local circadian oscillators in mammalian retina and cornea. *Proceedings of the National Academy of Sciences* 2015, 112(42):13093-13098.
89. Huynh AV, Buhr ED: Melatonin adjusts the phase of mouse circadian clocks in the cornea both ex vivo and in vivo. *Journal of Biological Rhythms* 2021, 36(5):470-482.
90. Otori Y, Cagampang FRA, Yamazaki S, Inouye S-IT, Mano T, Tano Y: Circadian rhythm of neuropeptide Y-like immunoreactivity in the iris-ciliary body of the rat. *Current Eye Research* 1993, 12(9):803-807.
91. Tsuchiya S, Buhr ED, Higashide T, Sugiyama K, Van Gelder RN: Light entrainment of the murine intraocular pressure circadian rhythm utilizes non-local mechanisms. *PLoS One* 2017, 12(9):e0184790.
92. Ribelayga C, Cao Y, Mangel SC: The circadian clock in the retina controls rod-cone coupling. *Neuron* 2008, 59(5):790-801.
93. Tosini G, Pozdeyev N, Sakamoto K, Iuvone PM: The circadian clock system in the mammalian retina. *Bioessays* 2008, 30(7):624-633.
94. Walker WH, Walton JC, DeVries AC, Nelson RJ: Circadian rhythm disruption and mental health. *Translational Psychiatry* 2020, 10(1):1-13.
95. Maeda A, Tsujiya S, Higashide T, Toida K, Todo T, Ueyama T, Okamura H, Sugiyama K: Circadian intraocular pressure rhythm is generated by clock genes. *Investigative Ophthalmology & Visual Science* 2006, 47(9):4050-4052.
96. Katz R, Henkind P, Weitzman E: The circadian rhythm of the intraocular pressure in the New Zealand White rabbit. *Investigative Ophthalmology & Visual Science* 1975, 14(10):775-780.
97. Smith SD, Gregory DS: A circadian rhythm of aqueous flow underlies the circadian rhythm of IOP in NZW rabbits. *Investigative Ophthalmology & visual science* 1989, 30(4):775-778.
98. Ziółkowska N, Ziółkowski H, Magda J, Bućko M, Kaczorek-Łukowska E, Lewczuk B: Diurnal and circadian variations in intraocular pressure in goats exposed to different lighting conditions. *Chronobiology International* 2019, 36(12):1638-1645.
99. Christie AH: Circadian rhythm of intraocular pressure in minipigs: First time mapping of rhythmicity and response to environmental and pharmaceutical factors. Tarleton State University; 2018.
100. Bertolucci C, Giudice E, Fazio F, Piccione G: Circadian intraocular pressure rhythms in athletic horses under different lighting regime. *Chronobiology International* 2009, 26(2):348-358.



101. Morrison JC, Johnson EC, Cepurna W, Jia L: Understanding mechanisms of pressure-induced optic nerve damage. *Progress in Retinal and Eye Research* 2005, 24(2):217-240.
102. Jing J-N, Wu Z-T, Li M-L, Wang Y-K, Tan X, Wang W-Z: Constant light exerted detrimental cardiovascular effects through sympathetic hyperactivity in normal and heart failure rats. *Frontiers in Neuroscience* 2020, 14(248):1-11.
103. Coomans CP, van den Berg SA, Houben T, van Klinken JB, van den Berg R, Pronk AC, Havekes LM, Romijn JA, van Dijk KW, Biermasz NR: Detrimental effects of constant light exposure and high-fat diet on circadian energy metabolism and insulin sensitivity. *The FASEB Journal* 2013, 27(4):1721-1732.
104. Adler J, Lynch HJ, Wurtman RJ: Effect of cyclic changes in environmental lighting and ambient temperature on the daily rhythm in melatonin excretion by rats. *Brain Research* 1979, 163(1):111-120.
105. Yuksel S: Altered adrenomedullin levels of the rats exposed to constant darkness and light stress. *Journal of Photochemistry and Photobiology B: Biology* 2008, 91(1):20-23.
106. Waxenbaum JA, Reddy V, Varacallo M: Anatomy, autonomic nervous system. 2019.
107. Tsai ASH, Aung T, Yip W, Wong TY, Cheung CY-L: Relationship of intraocular pressure with central aortic systolic pressure. *Current Eye Research* 2016, 41(3):377-382.
108. Aschoff J: Circadian rhythms: Influences of internal and external factors on the period measured in constant conditions. *Zeitschrift für Tierpsychologie* 1979, 49(3):225-249.
109. Pittendrigh CS, Daan S: A functional analysis of circadian pacemakers in nocturnal rodents. *Journal of Comparative Physiology* 1976, 106(3):223-252.
110. Eskin A: The Sparrow Clock: Behavior of the free running rhythm and entrainment analysis. *PhD Thesis, University of Texas at Austin* 1969.
111. Eskin A: Some properties of the system controlling the circadian activity rhythm of sparrows: National Academy of Sciences Washington, DC; 1971.
112. Pittendrigh CS: Circadian rhythms and the circadian organization of living systems. In: *Cold Spring Harbor symposia on quantitative biology: 1960*: Cold Spring Harbor Laboratory Press; 1960: 159-184.
113. Kwong JM, Vo N, Quan A, Nam M, Kyung H, Yu F, Piri N, Caprioli J: The dark phase intraocular pressure elevation and retinal ganglion cell degeneration in a rat model of experimental glaucoma. *Experimental Eye Research* 2013, 112:21-28.
114. Morrison JC, Jia L, Cepurna W, Guo Y, Johnson E: Reliability and sensitivity of the TonoLab rebound tonometer in awake Brown Norway rats. *Investigative Ophthalmology & Visual Science* 2009, 50(6):2802-2808.

115. Millar JC, Pang I-H: Non-continuous measurement of intraocular pressure in laboratory animals. *Experimental Eye Research* 2015, 141:74-90.
116. Fiorillo A, Critello C, Pullano S: Theory, technology and applications of piezoresistive sensors: A review. *Sensors and Actuators A: Physical* 2018, 281:156-175.
117. Scarr R, Settingington R: Thermistors, their theory, manufacture and application. *Proceedings of the IEE-Part B: Electronic and Communication Engineering* 1960, 107(35):395-405.
118. Dexter J, Servais P: Silicone rubber as cable insulation. In.: Dow Corning Corporation Midland, Michigan; 1953.
119. Refinetti R, Menaker M: The circadian rhythm of body temperature. *Physiology & Behavior* 1992, 51(3):613-637.
120. Dalvin LA, Fautsch MP: Analysis of circadian rhythm gene expression with reference to diurnal pattern of intraocular pressure in mice. *Investigative Ophthalmology & Visual Science* 2015, 56(4):2657-2663.
121. Rowland J, Potter D, Reiter R: Circadian rhythm in intraocular pressure: A rabbit model. *Current Eye Research* 1981, 1(3):169-173.
122. Webb P: Temperatures of skin, subcutaneous tissue, muscle and core in resting men in cold, comfortable and hot conditions. *European Journal of Applied Physiology and Occupational Physiology* 1992, 64:471-476.
123. Aschoff J: Thermal conductance in man: Its dependence on time of day and on ambient temperature. *Advances in Climatic Physiology* 1972:334-348.
124. Hilderbrandt G: Circadian variations of thermoregulatory response in man. *Chronobiology* 1974:234-240.
125. Weinert D, Waterhouse J: Diurnally changing effects of locomotor activity on body temperature in laboratory mice. *Physiology & behavior* 1998, 63(5):837-843.
126. Iuvone PM, Van Hartesveldt C: Diurnal locomotor activity in rats: Effects of hippocampal ablation and adrenalectomy. *Behavioral Biology* 1977, 19(2):228-237.
127. Caola G, Casella S, Giannetto C, Piccione G: Daily locomotor activity in five domestic animals. *Animal Biology* 2010, 60(1):15-24.
128. Sherwin C: Voluntary wheel running: A review and novel interpretation. *Animal Behaviour* 1998, 56(1):11-27.
129. Jakubczak LF: Frequency, duration, and speed of wheel running of rats as a function of age and starvation. *Animal Learning & Behavior* 1973, 1(1):13-16.

130. Morin LP: Age, but not pineal status, modulates circadian periodicity of golden hamsters. *Journal of Biological Rhythms* 1993, 8(3):189-197.
131. Poole S, Stephenson J: Body temperature regulation and thermoneutrality in rats. *Quarterly Journal of Experimental Physiology and Cognate Medical Sciences: Translation and Integration* 1977, 62(2):143-149.
132. Reitsamer HA, Kiel JW: A rabbit model to study orbital venous pressure, intraocular pressure, and ocular hemodynamics simultaneously. *Investigative Ophthalmology & Visual Science* 2002, 43(12):3728-3734.
133. Zhou Y, Zhang H-k, Liu F, Lei G, Liu P, Jiao T, Dang Y-h: Altered light conditions contribute to abnormalities in emotion and cognition through HINT1 dysfunction in C57BL/6 mice. *Frontiers in Behavioral Neuroscience* 2018, 12:110.
134. Fonken LK, Finy MS, Walton JC, Weil ZM, Workman JL, Ross J, Nelson RJ: Influence of light at night on murine anxiety-and depressive-like responses. *Behavioural Brain Research* 2009, 205(2):349-354.
135. Mohamed Y: Aqueous humor dynamics and compound action potentials in the anesthetized and conscious freely moving rat. University of South Florida; 2022.
136. Riganello F, Prada V, Soddu A, Di Perri C, Sannita WG: Circadian rhythms and measures of CNS/autonomic interaction. *International Journal of Environmental Research and Public Health* 2019, 16(13):2336.
137. Castejon H, Chiquet C, Savy O, Baguet J-P, Khayi H, Tamisier R, Bourdon L, Romanet J-P: Effect of acute increase in blood pressure on intraocular pressure in pigs and humans. *Investigative Ophthalmology & Visual Science* 2010, 51(3):1599-1605.
138. Siaudvytyte L: Interactions between IOP, ICP, OPP. *Biophysical Properties in Glaucoma: Diagnostic Technologies* 2019:31-34.
139. Strohmaier CA, Reitsamer HA, Kiel JW: Episcleral venous pressure and IOP responses to central electrical stimulation in the rat. *Investigative Ophthalmology & Visual Science* 2013, 54(10):6860-6866.
140. Tham Y-C, Li X, Wong TY, Quigley HA, Aung T, Cheng C-Y: Global prevalence of glaucoma and projections of glaucoma burden through 2040: a systematic review and meta-analysis. *Ophthalmology* 2014, 121(11):2081-2090.
141. Sappington RM, Carlson BJ, Crish SD, Calkins DJ: The microbead occlusion model: A paradigm for induced ocular hypertension in rats and mice. *Investigative Ophthalmology & Visual Science* 2010, 51(1):207-216.
142. Bellezza AJ, Rintalan CJ, Thompson HW, Downs JC, Hart RT, Burgoyne CF: Deformation of the lamina cribrosa and anterior scleral canal wall in early experimental glaucoma. *Investigative Ophthalmology & Visual Science* 2003, 44(2):623-637.

143. Ruiz-Ederra J, Verkman AS: Mouse model of sustained elevation in intraocular pressure produced by episcleral vein occlusion. *Experimental Eye Research* 2006, 82(5):879-884.
144. Beatty JF, Krupin T, Nichols PF, Becker B: Elevation of intraocular pressure by calcium channel blockers. *Archives of Ophthalmology* 1984, 102(7):1072-1076.
145. Overby DR, Clark AF: Animal models of glucocorticoid-induced glaucoma. *Experimental Eye Research* 2015, 141:15-22.
146. Liu H-H, Bui BV, Nguyen CTO, Kezic JM, Vingrys AJ, He Z: Chronic ocular hypertension induced by circumlimbal suture in rats. *Investigative Ophthalmology & Visual Science* 2015, 56:2811-2820.
147. Morrison JC, Cepurna WO, Johnson EC: Modeling glaucoma in rats by sclerosing aqueous outflow pathways to elevate intraocular pressure. 2015, 141:23-32.
148. Faschinger C, Mossböck G: Intraocular pressure contact lenses – suitable for everyday use yet? *European Ophthalmic Review* 2011, 5(2):136–138.
149. De Smedt S, Mermoud A, Schnyder C: 24-hour intraocular pressure fluctuation monitoring using an ocular telemetry sensor: tolerability and functionality in healthy subjects. *Journal of Glaucoma* 2012, 21(8):539-544.
150. Zhang J, Kim K, Kim HJ, Meyer D, Park W, Lee SA, Dai Y, Kim B, Moon H, Shah JV: Smart soft contact lenses for continuous 24-hour monitoring of intraocular pressure in glaucoma care. *Nature Communications* 2022, 13(1):5518.
151. Saxby E, Mansouri K, Tatham AJ: Intraocular pressure monitoring using an intraocular sensor before and after glaucoma surgery. *Journal of Glaucoma* 2021, 30(10):941-946.
152. Ito YA, Belforte N, Vargas JLC, Di Polo A: A magnetic microbead occlusion model to induce ocular hypertension-dependent glaucoma in mice. *Journal of Visualized Experiments* 2016(109):e53731.
153. Gordon DM, Ehrenberg MH: Cyclopentolate hydrochloride: A new mydriatic and cycloplegic agent: A pharmacologic and clinical evaluation. *American Journal of Ophthalmology* 1954, 38(6):831-838.
154. Esteve-Taboada JJ, Águila-Carrasco D, Antonio J, Bernal-Molina P, Ferrer-Blasco T, López-Gil N, Montés-Micó R: Effect of phenylephrine on the accommodative system. *Journal of Ophthalmology* 2016, 2016:1-13.
155. Stadtbäumer K, Frommlet F, Nell B: Effects of mydriatics on intraocular pressure and pupil size in the normal feline eye. *Veterinary Ophthalmology* 2006, 9(6):233-237.
156. Ansari Mood M, Rajaei SM, Faghihi H, Ghiadi A: Effect of topical 1% cyclopentolate hydrochloride on tear production, intraocular pressure, and pupil size in healthy turkman horses. *Journal of Equine Veterinary Science* 2019, 75:25-29.

157. Ribeiro AP, Crivelaro RM, Teixeira PPM, Trujillo DY, Guimaraes P1J, Vicente WRR, Martins BdC, Laus† JL: Effects of different mydriatics on intraocular pressure, pupil diameter, and ruminal and intestinal motility in healthy sheep. *Veterinary Ophthalmology* 2014, 17(6):397-402.
158. Kovalcuka L, Ilgazs A, Bandere D, Williams DL: Changes in intraocular pressure and horizontal pupil diameter during use of topical mydriatics in the canine eye. *Open Veterinary Journal* 2017, 7(1):16-22.
159. Atalay E, Tamcelik N, Cicik ME: The impact of pupillary dilation on intraocular pressure and anterior segment morphology in subjects with and without pseudoexfoliation. *Current Eye Research* 2015, 40(6):646-652.
160. Laojaroenwanit S, Layanun V, Praneeprachachon P, Pukrushpan P: Time of maximum cycloplegia after instillation of cyclopentolate 1% in children with brown irises. *Clinical Ophthalmology* 2016:897-902.
161. Hancox J, Murdoch I, Parmar D: Changes in intraocular pressure following diagnostic mydriasis with cyclopentolate 1%. *Eye* 2002, 16(5):562-566.
162. Kinney LM, Johnson AD, Reddix M, McCann MB: Temporal effects of 2% pilocarpine ophthalmic solution on human pupil size and accommodation. *Military Medicine* 2020, 185:435-442.
163. Skaat A, Rosman MS, Chien JL, Mogil RS, Ren R, Liebmann JM, Ritch R, Park SC: Effect of pilocarpine hydrochloride on the Schlemm canal in healthy eyes and eyes with open-angle glaucoma. *JAMA Ophthalmology* 2016, 134(9):976-981.
164. Linnér E: The effect of pilocarpine and acetazolamide on the outflow resistance in normal and glaucomatous human eyes. *Documenta Ophthalmologica* 1966, 20(1):170-174.
165. Grierson I, Lee WR, Abraham S: The effects of topical pilocarpine on the morphology of the outflow apparatus of the baboon (*Papio cynocephalus*). *Investigative Ophthalmology & Visual Science* 1979, 18(4):346-355.
166. Overby DR, Bertrand J, Schicht M, Paulsen F, Stamer WD, Lütjen-Drecoll E: The structure of the trabecular meshwork, its connections to the ciliary muscle, and the effect of pilocarpine on outflow facility in mice. *Investigative Ophthalmology & Visual Science* 2014, 55(6):3727-3736.
167. Naveh-Floman N, Stahl V, Korczyn A: Effect of pilocarpine on intraocular pressure in ocular hypertensive subjects. *Ophthalmic Research* 1986, 18(1):34-37.
168. Akaishi T, Odani-Kawabata N, Ishida N, Nakamura M: Ocular hypotensive effects of anti-glaucoma agents in mice. *Journal of Ocular Pharmacology and Therapeutics* 2009, 25(5):401-408.

169. Lamble J, Lamble A: The effect of miotics on the intraocular pressure of conscious owl monkeys. *Investigative Ophthalmology & Visual Science* 1976, 15(10):848-851.
170. Gwin RM, Gelatt KN, Gum GG, Peiffer RL, Williams L: The effect of topical pilocarpine on intraocular pressure and pupil size in the normotensive and glaucomatous beagle. *Investigative Ophthalmology & Visual Science* 1977, 16(12):1143-1148.
171. Roy Chowdhury U, Holman BH, Fautsch MP: A novel rat model to study the role of intracranial pressure modulation on optic neuropathies. *PLoS One* 2013, 8(12):e82151.
172. Lin JS, Liu JHK: Circadian variations in intracranial pressure and translaminar pressure difference in Sprague-Dawley rats. *Investigative Ophthalmology & Visual Science* 2010, 51(11):5739.
173. Jasien JV, Samuels BC, Johnston JM, Downs JC: Diurnal cycle of translaminar pressure in nonhuman primates quantified with continuous wireless telemetry. *Investigative Ophthalmology & Visual Science* 2020, 61(2):37-37.
174. Jasien JV, Samuels BC, Johnston JM, Downs JC: Effect of body position on intraocular pressure (IOP), intracranial pressure (ICP), and translaminar pressure (TLP) via continuous wireless telemetry in nonhuman primates (NHPs). *Investigative Ophthalmology & Visual Science* 2020, 61(12):18-18.

## **Appendix A: Microbead Occlusion Model**

Preliminary experiments were conducted in 4 female Brown-Norway rats to test the established microbead occlusion model. This model has been used to chronically elevate IOP and induce glaucoma-like damage in mice and rats by occluding the conventional outflow pathway [141]. Although polystyrene microbeads are commonly used, recent studies have shown that magnetic microbeads are more efficient because you can use a ring-magnet to draw them closer to the iridocorneal angle and into the outflow pathway. We wanted to compare the effects of both materials in a rat model [152]. On the first day of experimentation, rats were anesthetized with an intraperitoneal bolus of ketamine hydrochloride (75 mg/kg) and xylazine (7.5 mg/kg) and the head was secured in a stereotaxic apparatus. Pupils were dilated with 1% cyclopentolate hydrochloride. A 33G needle attached to a Hamilton syringe was advanced through the translimbal region into the anterior chamber using a micromanipulator. A 20  $\mu$ L solution of the same concentration of either 8  $\mu$ m diameter magnetic microbeads or 15.7  $\mu$ m diameter polystyrene beads in saline was injected into the eye. In preliminary experiments, rebound tonometry was used to measure IOP before injection and over the days following injection.

Figure A1 presents raw tonometry data from two different microbead injection experiments. The top plot shows IOP data of an animal that received an OD (right eye) injection of 8  $\mu$ m diameter magnetic beads, while OS (left eye) served as a control. Immediately after injection, a ring-shaped magnet was placed around the eye to pull the magnetic beads into the iridocorneal angle. This animal experienced elevated IOP 2 days post-injection that came back down to pre-injection levels after 4 days. The bottom plot shows IOP data of an animal that

received an OD injection of 15.7  $\mu\text{m}$  diameter polystyrene beads, while OS served as a control. IOP continued to creep upwards after 4 days post-injection. This animal, however, developed a fibrotic clot in the posterior chamber, just behind the iris. Overall, results suggest that the larger diameter polystyrene beads caused more damage to the eye than the smaller magnetic beads. It is also thought that polystyrene has toxicity effects that damage ocular tissues independent of trabecular meshwork occlusion. However, more experiments need to be conducted along with tissue toxicity tests to make any concluding arguments. Varying results may also reflect differences in trabecular meshwork structure between animals.

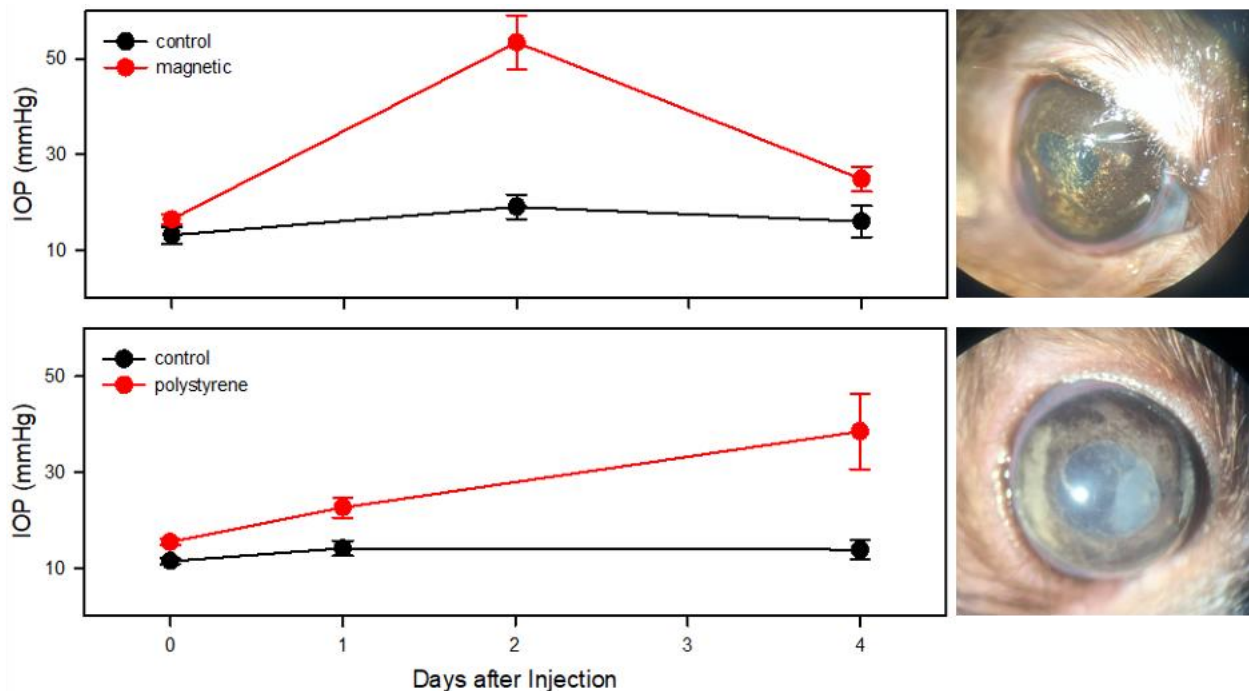


Figure A1: Effect of microbeads on IOP. Top, raw tonometry data of a rat that received an OD injection of 8  $\mu\text{m}$  diameter magnetic beads. Bottom, raw tonometry data of a rat that received an OD injection of 15.7  $\mu\text{m}$  diameter polystyrene beads. OS served as a control in both animals. Photos in the right panel were taken 4 days after microbead injection. Notice that the animal injected with polystyrene beads developed a fibrotic clot located in the posterior chamber just behind the iris.



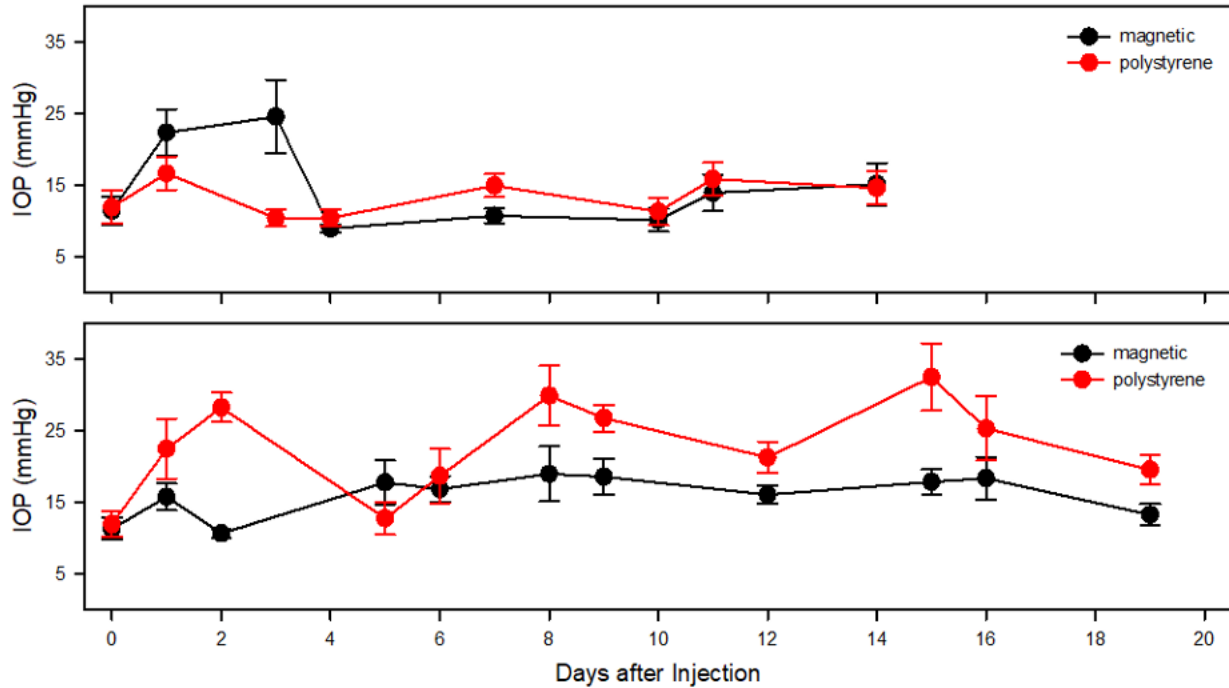


Figure A2: Effect of microbead material and diameter on IOP. Plotted are data from two different rats the underwent an OD injection of 8  $\mu\text{m}$  diameter magnetic microbeads and an OS injection of 15.7  $\mu\text{m}$  diameter polystyrene beads. There were varying results on the effect of bead diameter and material between the two animals.

Figure A2 shows the IOP data from two different rats that were injected with magnetic beads in one eye and polystyrene beads in the other. This set of experiments directly compared the effects of material type while minimizing inter-animal variability. However, following binocular injection, results were contradictory. One animal had a greater IOP response to the magnetic beads and the other animal had a greater IOP response to the polystyrene beads. Since the beads were injected by hand using a micromanipulator, it is possible that the 20  $\mu\text{L}$  volume was given at different rates, which may lead to transient biomechanical stress on ocular tissues. Therefore, tissue damage may result from not only trabecular meshwork occlusion, but also from the injection rate of the bead solution. It is also possible that some beads may escape the eye after the syringe is removed, resulting in fewer microbeads that remain in the anterior chamber. In future

experiments, it is necessary to standardize the injection procedure and use an automatic syringe pump to ensure a steady injection of beads into the eye as to not cause sudden pressure spikes.

One of the major limitations of this set of experiments is that IOP was measured using tonometry. Tonometry measurements were rather variable when taken at any given moment in time. Experiments were repeated in animals that were implanted with our wireless telemetry system, however, there were many failures. The fibrotic clot that formed soon after injection led to clogging of the implanted cannula, which inhibited proper conduction of pressure in the tubing. It is possible that clot formation is due to puncturing the cornea, which initiates the inflammation cascade. To solve this problem, investigators could try injecting beads into the eye through the cannula as to not cause corneal damage. Another solution would be to use a different model of glaucoma that doesn't involve intracameral injections.

## **Appendix B: Effect of Pharmacological Agents on IOP**

Mydriatics or cycloplegics are ophthalmic solutions that are typically used to dilate the pupil for diagnostic procedures. There are two ocular muscles that are responsible for pupil modulation, the iris sphincter, which is controlled by the parasympathetic nervous system (PNS) and the iris dilator, which is controlled by the sympathetic nervous system (SNS). Different types of mydriatics have varying mechanisms of action that target these muscles. For instance, cyclopentolate is an anticholinergic mydriatic that inhibits the PNS to relax the sphincter muscle and dilate the pupil [153]. Conversely, phenylephrine is a mydriatic that stimulates sympathetic adrenergic receptors to contract the dilator muscle and widen the pupil [154]. Previous studies have reported contradictory results pertaining to the effect of 1% cyclopentolate [155-157] and 10% phenylephrine [155, 158, 159] on IOP. These studies used tonometry in awake subjects to monitor IOP after drug application. However, we know that performing tonometry on awake rats induces a stress-response that leads to an IOP elevation [73]. Also, considering the time dependency of pupil modulation, infrequent tonometric measurements are unable to capture IOP changes on smaller time scales. Since mydriatics agents are commonly used for diagnostic and therapeutic purposes, it is important to understand the complete effects they have on IOP. We have used our novel telemetry system to collect preliminary data concerning the effects of cyclopentolate on IOP variability, while monitoring pupil diameter.

One experimental day, animals were transferred to a testing room where they were undisturbed for 30 minutes to allow recovery of IOP to near resting levels. Animals were anesthetized using 3% isoflurane with oxygen at 2 L/min. Heat support was provided and body

temperature was monitored with a rectal thermometer. A single drop of 1% cyclopentolate was instilled on the implanted eye. Drugs were administered at room temperature to eliminate corneal temperature changes. IOP was monitored before, during, and after drug application. Baseline was defined as the 1 min IOP average before animals were placed in the isoflurane chamber. Before was defined as the 1 min IOP average right before the drop was administered. After was defined as the 1 min IOP average 30 mins after drug application since that is when clinicians report maximum pupillary response [160]. Images of the pupil were taken every 10 mins to show roughly the time of maximum pupil dilation.

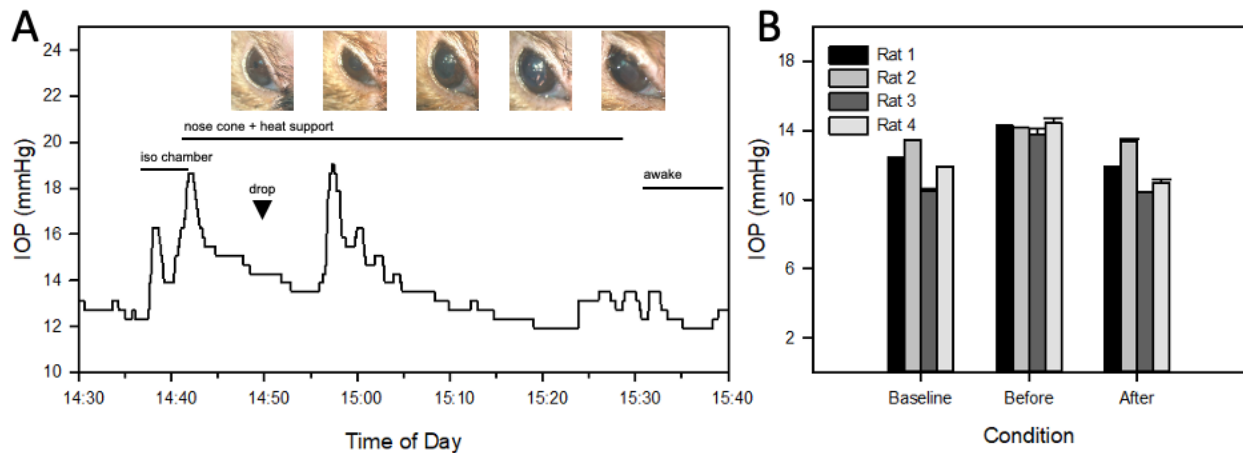


Figure B1: Effect of cyclopentolate on IOP. (A) Raw IOP data before and after application of a single drop of 1% cyclopentolate. Maximum pupil dilation was reached about 30 min following application. (B) Cumulative statistics from 4 rats showing no significant effect of the mydriatic on mean IOP around the time of maximum pupil dilation when compared to baseline levels. Elevated IOP just before drug application reflects the elicited stress response upon placement in the confined isoflurane chamber.

Figure B1 shows raw IOP data before and after application of cyclopentolate in a rat. IOP increased slightly during anesthetic induction but returned to near baseline levels soon after. A drop of cyclopentolate was administered after IOP stabilized. There was an IOP spike 5 mins following drug application. This IOP perturbation was not seen in the other 3 rats tested. Although

the spike was likely spontaneous, it provides evidence that IOP telemetry is superior in capturing short-term IOP perturbations compared to tonometry. Around the time of maximum pupil dilation, IOP had recovered to near baseline levels. Across all animals, IOP before drug application was slightly higher than baseline levels presumably due to the stress response associated with animal handling and placement in the confined isoflurane chamber. Across all animals, there were no significant differences between baseline IOP and IOP 30 mins after drug application. This suggests that mean IOP was unaffected by maximum pupil dilation. Our results contradict results of previous studies that report an IOP elevation following application of cyclopentolate [155, 156, 161] However, in these studies tonometry was performed over several hours in awake subjects and IOP elevation is likely a reflection of whitecoat hypertension.

IOP telemetry should be used in future studies to clarify and confirm effects of other ophthalmic medications on IOP. It would be beneficial to test other common mydriatics including atropine, phenylephrine, and epinephrine as well as miotics, which have been used to treat glaucoma. Miotics are ophthalmic solutions that stimulate the PNS to contract the iris sphincter and constrict the pupil. Pilocarpine is a miotic that acts directly on muscarinic acetylcholine receptors to widen Schlemm's canal [162]. It has been shown to increase aqueous humor outflow in humans [163, 164], baboons [165], and enucleated mouse eyes [166]. Previous tonometric studies suggest IOP reduction following pharmacological miosis in humans and other species besides rats [163, 165-170]. However, it is necessary to confirm these results using IOP telemetry as tonometry is suspected to confound results. If the proposed mechanism of pilocarpine holds true, it is expected that rats will also experience an IOP reduction as their iridocorneal angle resembles that of humans. Unlike tonometry, IOP telemetry allows continuous measurement

without intervention. Therefore, effects of mydriatics and miotics should also be tested in awake subjects, however, initial effects of applying the drug to the eye must be considered.

In future anesthesia experiments, pupil diameter should be monitored continuously in addition to IOP. Modifications were made to an existing image processing MATLAB algorithm that relates image pixel density to a measurement of length. Initial testing of the algorithm was done on a continuous video recording of the anterior segment that was converted to a stacked TIFF file. The algorithm converted TIFF files to binary images so that the pupil contrasted from the rest of the image. The 'boundingbox()' function was utilized to track the outer most edge of the pupil. Pupil diameter was converted from pixel density to units of millimeters using a ruler of known length provided within the frame. Continuous monitoring of pupil diameter in addition to IOP would allow us to determine if there is a relationship between pupil modulation and IOP variability.

### Appendix C: Continuous Intracranial Pressure Monitoring

Previous work done in our lab revealed that intracranial pressure (ICP) modulates aqueous humor dynamics of the eye [32]. It was found that elevated ICP resulted in decreased outflow of aqueous humor through the conventional pathway, which inevitably led to IOP elevation. When tetrodotoxin (TTX), a neurotoxin, was applied to the eye, elevations in ICP no longer effected IOP level. It was concluded that aqueous humor dynamics are modulated by an ICP-driven neural feedback mechanism from the brain. This means that the translaminal pressure gradient that is felt by the optic nerve head may be regulated by this neural protective feedback mechanism, which may have implications for future glaucoma treatment. To completely understand the relationship between IOP and ICP, it would be beneficial to be able to study both simultaneously in an animal model of glaucoma. Modifications to our existing IOP telemetry system now allow for dual pressure monitoring. To implement this system, Youssef Mohamed, a former lab member, and I worked together to develop a novel protocol for ICP cannula implantation in the rat.

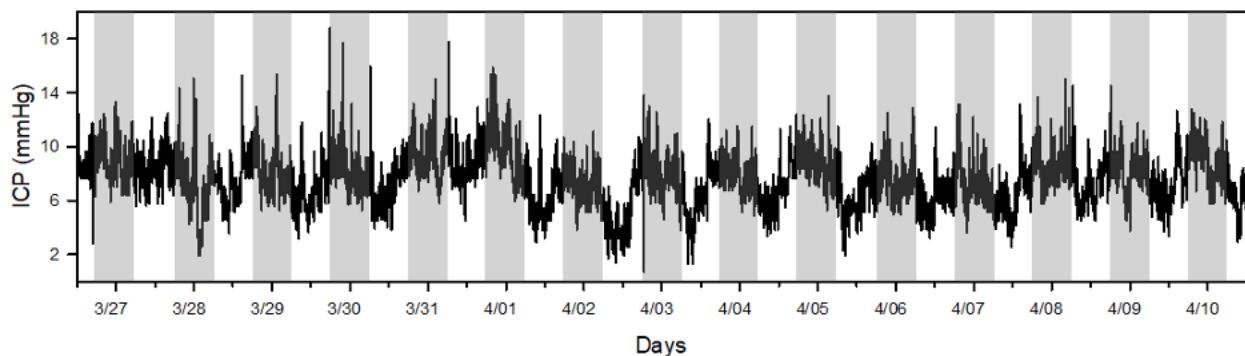


Figure C1: Continuous ICP recording using wireless telemetry. Raw ICP data of a rat housed in normal 12-h light: 12-h dark conditions. Like IOP, ICP was higher in the dark phase than in the light phase. It also fluctuated continuously on short and long timescales.

Like the existing protocol for anterior segment cannulation, an external pressure transducer was connected to a head-mount coupler secured to the skull with 4 bone screws in each of the skull plates. The holes for the bone screws were drilled to only half the skull thickness to ensure that the dura mater remained intact. A fifth hole was made in one of the frontal skull plates to expose the dura mater. The dura mater was punctured with a 33G needle thus releasing cerebral spinal fluid (CSF). A fluid filled silicone microcannula (OD: 200um, ID: 100um, AS One International, Santa Clara, CA, USA), also connected to the head-mount coupler, was inserted approximately 5 mm into this opening. The opening on the skull was plugged with gel-foam and covered with superglue. The entire apparatus was covered with bone cement and skin flaps were sutured. Animals were allowed to recover and ICP was recorded at 0.25 Hz for weeks.

Two different rats were implanted with the telemetry system to record ICP round-the-clock. ICP data was collected in 2 different rats. Figure C1 shows a raw ICP data collected from one of the two rats that were housed in normal 12-h light: 12-h dark conditions. Like IOP, ICP varied continuously. ICP of rats also followed a diurnal rhythm with higher values in the dark phase, which confirms results of another study that performed ICP telemetry in Brown-Norway rats in which the ventricle was cannulated [171]. Slight difference in mean pressure may be seen between the ventricle and the subdural space since the ventricle is the site of CSF production. Our results contradict results of another study in which there were no circadian variations found in the ICP of Sprague-Dawley rats [172]. This suggests that there may be an inter-species variability for diurnal ICP. A different group has also monitored diurnal ICP from the parenchyma in monkeys using a commercially available telemetry system [173, 174].



## Appendix D: Copyright Permissions

The following permission is for the inclusion of a previously published work in Chapter 1 of this dissertation. This article was published in *Experimental Eye Research*, Volume 210, Christina M Nicou, Aditi Pillai, and Christopher L Passaglia, Effects of acute stress, general anesthetics, tonometry, and temperature on intraocular pressure in rats, Pages 1-8, Copyright Elsevier (2021).

2/9/23, 11:07 AM

Mail - Christina Nicou - Outlook

Re: Copyright permissions [220920-029439]

Permissions Helpdesk <permissionshelpdesk@elsevier.com>

Thu 9/22/2022 12:43 PM

To: Christina Nicou

Dear Christina Nicou

We hereby grant you permission to reprint the material below at no charge in your thesis subject to the following conditions:

**RE: Effects of acute stress, general anesthetics, tonometry, and temperature on intraocular pressure in rats, *Experimental Eye Research*, Volume 210, 2021, Nicou et al**

1. If any part of the material to be used (for example, figures) has appeared in our publication with credit or acknowledgement to another source, permission must also be sought from that source. If such permission is not obtained then that material may not be included in your publication/copies.

2. Suitable acknowledgment to the source must be made, either as a footnote or in a reference list at the end of your publication, as follows:

"This article was published in Publication title, Vol number, Author(s), Title of article, Page Nos, Copyright Elsevier (or appropriate Society name) (Year)."

3. Your thesis may be submitted to your institution in either print or electronic form.

4. Reproduction of this material is confined to the purpose for which permission is hereby given.

5. This permission is granted for non-exclusive world English rights only. For other languages please reapply separately for each one required. Permission excludes use in an electronic form other than submission. Should you have a specific electronic project in mind please reapply for permission.

6. As long as the article is embedded in your thesis, you can post/share your thesis in the University repository.

7. Should your thesis be published commercially, please reapply for permission.

8. Posting of the full article/ chapter online is not permitted. You may post an abstract with a link to the Elsevier website [<http://www.elsevier.com%2C/www.elsevier.com>], or to the article on ScienceDirect if it is available on that platform.

Kind regards,

**Roopa Lingayath**

Senior Copyrights Coordinator

**ELSEVIER** | HCM - Health Content Management

Visit [Elsevier Permissions](#)

The following permission is for the “Three Internal chambers of the Eye” image used in Chapter 1: Background, Section 1.1: Importance of Intraocular Pressure. The image illustrates the anatomy of the eye and the fluids that contribute to pressure in the eye. The author of the image is Holly Fischer, and the file is licensed under the Creative Commons Attribution 3.0 Unported license.

2/9/23, 11:22 AM

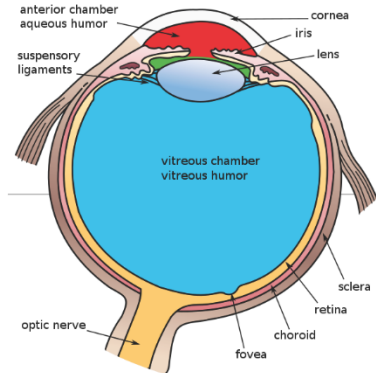
File:Three Internal chambers of the Eye.svg - Wikimedia Commons

WIKIMEDIA COMMONS

**File:Three Internal chambers of the Eye.svg**

From Wikimedia Commons, the free media repository

- Download all sizes
- Use this file on the web
- Use this file on a wiki
- Email a link to this file
- Information about reusing



Size of this PNG preview of this SVG file: 586 × 599 pixels.

Original file (SVG file, nominally 704 × 720 pixels, file size: 62 KB)

Open in Media Viewer

File information

Structured data



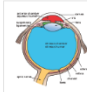
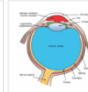
Captions

English

Add a one-line explanation of what this file represents

Edit

**Summary**

<b>Description</b>	<b>English:</b> This image focuses on the three internal layers of the eye.
<b>Date</b>	1 February 2021
<b>Source</b>	Own work based on <a href="#">Three Internal chambers of the Eye.png</a> by Holly Fischer
<b>Author</b>	<b>Original:</b> Holly Fischer. Vector: <a href="#">PixelSquid</a>
<b>Other versions</b>	<div style="display: flex; justify-content: space-around;"> <div style="text-align: center;">  <p>العربية (SVG)</p> </div> <div style="text-align: center;">  <p>English (PNG)</p> </div> <div style="text-align: center;">  <p>English (SVG)</p> </div> <div style="text-align: center;">  <p>español (PNG)</p> </div> </div>
<b>SVG development</b>	<p><b>W3C</b> The source code of this SVG is <b>invalid</b> (<a href="https://validator.w3.org/check?uri=https%3A%2F%2Fcommons.wikimedia.org%2Fwikimedia.org%2Fspecial%3AFilepath%2FThree_Internal_chambers_of_the_Eye.svg">https://validator.w3.org/check?uri=https%3A%2F%2Fcommons.wikimedia.org%2Fwikimedia.org%2Fspecial%3AFilepath%2FThree_Internal_chambers_of_the_Eye.svg</a>)</p> <p>This W3C-invalid diagram was created with <a href="#">Inkscape</a>. This diagram uses embedded text that can be easily translated using a text editor.</p>

**Licensing**

I, the copyright holder of this work, hereby publish it under the following license:

This file is licensed under the Creative Commons Attribution 3.0 Unported (<https://creativecommons.org/licenses/by/3.0/deed.en>) license.



- You are free:
- to share – to copy, distribute and transmit the work
  - to remix – to adapt the work
- Under the following conditions:
- attribution – You must give appropriate credit, provide a link to the license, and indicate if changes were made. You may do so in any reasonable manner, but not in any way that suggests the licensor endorses you or your use.

(<https://commons.wikimedia.org/wiki/File:Three Internal chambers of the Eye.svg#filelinks>)

The following permission is for the “Aqueous humor pathway” image used in Chapter 1: Background, Section 1.1: Importance of Intraocular Pressure. The image illustrates the secretion to excretion pathway aqueous humor takes in the eye. The author of the image is José Ignacio Orlando, and the image was made available under the Creative Commons CC0 1.0 Universal Public Domain Dedication.

2/9/23, 11:20 AM

File:Aqueous humor pathway.svg - Wikimedia Commons

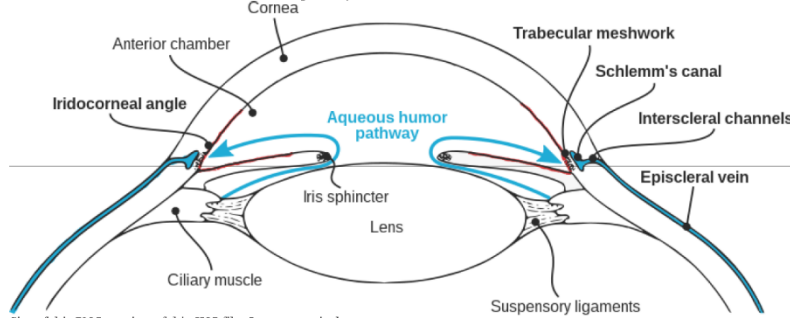
**WIKIMEDIA  
COMMONS**

## File:Aqueous humor pathway.svg



Download  
all sizes

From Wikimedia Commons, the free media repository



Size of this PNG preview of this SVG file: 800 × 320 pixels.

Original file (SVG file, nominally 859 × 344 pixels, file size: 289 KB)

[Open in Media Viewer](#)

[File information](#)

[Structured data](#)

Captions

[Edit](#)

English

Add a one-line explanation of what this file represents

### Summary

Description	English: Anatomical parts from the anterior and posterior chambers and aqueous humor pathway in English.
Date	29 March 2017
Source	Openclipart ( <a href="https://openclipart.org/detail/276637/aqueous-humor-pathway">https://openclipart.org/detail/276637/aqueous-humor-pathway</a> )
Author	ignaciorlando ( <a href="https://openclipart.org/artist/ignaciorlando">https://openclipart.org/artist/ignaciorlando</a> )

### Licensing



This file is from the *Open Clip Art Library*, which released it explicitly into the **public domain** (see [here \(https://openclipart.org/share\)](https://openclipart.org/share)).

To the uploader: Please provide as parameter the link to the page where this image appears.



This file is made available under the [Creative Commons CC0 1.0 Universal Public Domain Dedication \(https://creativecommons.org/publicdomain/zero/1.0/deed.en\)](https://creativecommons.org/publicdomain/zero/1.0/deed.en).



The person who associated a work with this deed has dedicated the work to the public domain by waiving all of their rights to the work worldwide under copyright law, including all related and neighboring rights, to the extent allowed by law. You can copy, modify, distribute and perform the work, even for commercial purposes, all without asking permission.

([https://commons.wikimedia.org/wiki/File:Aqueous\\_humor\\_pathway.svg](https://commons.wikimedia.org/wiki/File:Aqueous_humor_pathway.svg))

The following permission is for the “Depiction of vision for a Glaucoma patient” image used in Chapter 1: Background, Section 1.2: Glaucoma and Common Treatments. The image illustrates the vision loss associated with glaucomatous damage. The author of the image is MyUpchar.com, and the image is licensed under the Creative Commons Attribution-Share Alike 4.0 International license.

2/9/23, 11:45 AM

File:Depiction of vision for a Glaucoma patient.png - Wikimedia Commons

**WIKIMEDIA COMMONS**

**File:Depiction of vision for a Glaucoma patient.png** [Download all sizes](#)

From Wikimedia Commons, the free media repository

[Use this file on the web](#)

[Use this file on a wiki](#)

[Email a link to this file](#)

[Information about reusing](#)

Size of this preview: 800 × 514 pixels.

Original file (2,605 × 1,667 pixels, file size: 2.28 MB, MIME type: image/png)

[Open in Media Viewer](#)

<b>File information</b>	Structured data
<b>Captions</b>	<a href="#">Edit</a>
English	Depiction of vision for a Glaucoma patient

**Summary**

<b>Description</b>	English: Depiction of vision for a Glaucoma patient. The typical pathophysiology associated with Glaucoma has been shown as well (blocked drainage channel in the eye and changes in the optic nerve).
<b>Date</b>	26 December 2019
<b>Source</b>	<a href="https://www.myupchar.com/en/disease/glaucoma">https://www.myupchar.com/en/disease/glaucoma</a>
<b>Author</b>	<a href="https://www.myupchar.com/en">https://www.myupchar.com/en</a>
<b>Permission (Reusing this file)</b>	<p>This work is free and may be used by anyone for any purpose. If you wish to <b>use this content</b>, you do not need to request permission as long as you follow any licensing requirements mentioned on this page.</p> <p>The Wikimedia Foundation has received an e-mail confirming that the copyright holder has approved publication under the terms mentioned on this page. This correspondence has been reviewed by a Volunteer Response Team (VRT) member and stored in our permission archive. The correspondence is available to trusted volunteers as <b>ticket #2019081910003902</b> (<a href="https://ticket.wikimedia.org/otrs/index.php?Action=AgentTicketZoom&amp;TicketNumber=2019081910003902">https://ticket.wikimedia.org/otrs/index.php?Action=AgentTicketZoom&amp;TicketNumber=2019081910003902</a>).</p> <p>If you have questions about the archived correspondence, please use the <b>VRT noticeboard</b>. Ticket link: <a href="https://ticket.wikimedia.org/otrs/index.php?Action=AgentTicketZoom&amp;TicketNumber=2019081910003902">https://ticket.wikimedia.org/otrs/index.php?Action=AgentTicketZoom&amp;TicketNumber=2019081910003902</a></p> <p>Find other files from the same ticket: <a href="#">🔍</a></p>

**Licensing**

I, the copyright holder of this work, hereby publish it under the following license:

This file is licensed under the **Creative Commons Attribution-Share Alike 4.0 International** (<https://creativecommons.org/licenses/by-sa/4.0/deed.en>) license.

You are free:

- to **share** – to copy, distribute and transmit the work
- to **remix** – to adapt the work

Under the following conditions:

- attribution** – You must give appropriate credit, provide a link to the license, and indicate if changes were made. You may do so in any reasonable manner, but not in any way that suggests the licensor endorses you or your use.
- share alike** – If you remix, transform, or build upon the material, you must distribute your contributions under the same or compatible license (<https://creativecommons.org/licenses/by-sa/4.0/deed.en#cc-by-sa>) as the original.

[https://commons.wikimedia.org/wiki/File:Depiction of vision for a Glaucoma patient.png](https://commons.wikimedia.org/wiki/File:Depiction_of_vision_for_a_Glaucoma_patient.png)